Characterization and optimization of the non-viral gene transfer vehicle “Artificial viral particles” (AVP)

Dissertation

zur Erlangung des akademischen Grades doctor rerum naturalium

(Dr. rer. nat.)

vorgelegt dem Rat der Biologisch-Pharmazeutischen Fakultät

der Friedrich-Schiller- Universität Jena

von Roman Egle

geboren am 03.08.1975 in München

Gutachter:

1. Prof Dr. Udo Bakowsky, Philipps-Universität Marburg

2. Prof. Dr. Alfred Fahr, Friedrich-Schiller-Universität Jena

3. Prof. Julijana Kristl, PhD, University of Ljubljana, Slowenien

Öffentliche Disputation am 17. März 2008

“Science may set limits to knowledge, but should not set limits to imagination”

Bertrand Russell (1872 – 1970)

For my parents

Acknowledgments

The completion of this thesis would not have been possible without many people's support. First and foremost, I would like to thank my mentor Prof. Dr. Alfred Fahr for giving me the possibility to do research in this exciting field and for supporting and guiding me throughout the course of my Ph.D. project.

I would like to extend my gratitude to my friends, colleagues and former colleagues at the department. They accompanied and helped me throughout the sometimes turbulent years. I am grateful for Angela Herre's help in cell culture, Ina Lehmann's help with confocal laser scanning microscopy, Steffi Richter's help in all fields of electron microscopy and for Dr. Xiangli Liu's proofreading. I am especially grateful to Christian Rothkopf who guided my first steps as freshman in the field of nanotechnology and cell culture.

I appreciate the co-operation with the team of Prof. Dr. Karl-Jürgen Halbhuber at the Institut für Anatomie II in Jena. I am indebted to Dr. Oehring and Alida Braunschweig for the preparation and examination of ultrathin sections of cells and to Frank Steiniger for Cryo-TEM preparations.

I am also indebted to Prof. Dr. Michael Köhler, Jörg Wagner and Frances Möller from the TU Ilmenau for providing me with a static micromixer, know-how and advice.

Furthermore, I would like to thank Dr. Lars Tönges from the University of Göttingen for performing siRNA experiments together with me.

Spending one year of my research abroad constituted a highlight in my professional and private life. For making this experience possible I am thankful to my host supervisors in Slovenia: Prof. Dr. Julijana Kristl and Prof. Dr. Irena Mlinaric-Rascan and again to my home supervisor Prof. Dr. Alfred Fahr. My warm thanks goes to the whole team in Ljubljana for making me feel welcome. Especially to my office colleagues Andrej Dolenc and Matej Pavli and to Miha Milek who introduced me into the mysteries of biochemistry without loosing patience. This research year abroad has been supported by a Marie Curie Early Stage Research Training Fellowship of the European Community's Sixth Framework Programme under contract number MEST-CT-2004-504992.

I want to thank all my friends who encouraged and supported me. Special thanks go to Dr. René Korn and to Franz Nagl for always being there to help or just to listen, for motivating me when necessary and for proofreading.

Finally, I would like to express my deepest thanks to my family, especially to my parents.

Table of contents

Table of contents

1. Introduction

1.1 Gene therapy and used vectors

Gene therapy is one of the big issues in medicine and biotechnology. The vast theoretical possibilities and the partially disillusioning experience in clinical trials raise hopes and fears and form a controversial topic. The basic principle of gene therapy, treating diseases by inserting or modifying genes also implicates the possibility to cure hereditary diseases such as cystic fibrosis or muscular dystrophy.

After a promising start, the successful treatment of severe combined immunodeficiency of a four year old girl in 1990 (Blaese et al., 1995), also unexpected dangers became apparent and resulted in the death of an 18 year old man in a clinical trial that was intended to treat his metabolic disease in 1999 (Teichler Zallen, 2000). This sad event resulted in a more cautious and restricted handling of gene therapy trials (Smith, Byers, 2002; Thompson, 2000). Also recent promising trials that improved hereditary immunodeficiency in three patients (Ott et al., 2006) got a bitter aftertaste by the tragic death of one of the patients (Zinkant, 2006). Up to now “Gendicine”, approved 2004 in China (Pearson et al., 2004; Peng, 2005), is the only gene therapy “drug” that has been approved for commercial use worldwide and its approval is also subject to critical discussion (Guo, Xin, 2006). In summary this promising field is still at the beginning and further research is needed.

Gene therapy can be divided into the areas germline therapy and somatic therapy. In germline therapy germ cells, ovum and sperm cells or their precursors, would be manipulated and the changed genetic information would not only be incorporated into the manipulated cells, but also inherited to future generations descending from those cells. This lasting engineering of the germline is highly controversial and mainly rejected for human beings from an ethical point of view (Rabino, 2003). Medical trials in humans are performed, at least up to now, only in the field of somatic gene therapy. In somatic gene therapy target cells not involved in the reproduction of the organism are genetically modified to heal an individual or improve its condition. Somatic gene therapy can be subdivided into *ex vivo* therapy and *in vivo* therapy. In *ex vivo* therapy target cells are taken from the body of the patient, genetically changed, and reinserted. In *in vivo* gene therapy cells are modified in the body of the patient. This demands specific targeting of the modification to its target cells.

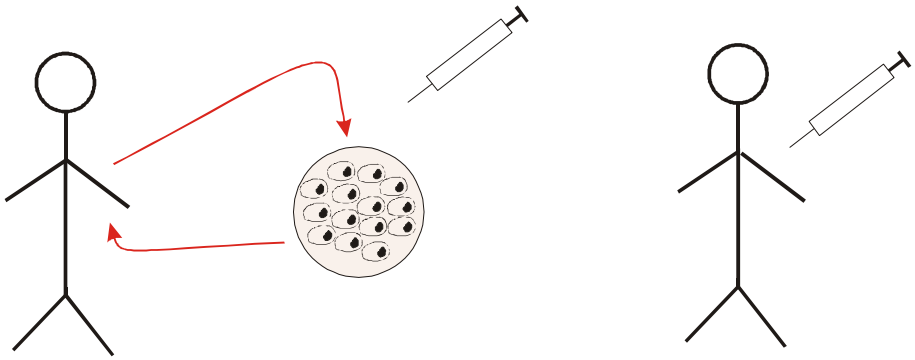

Ex vivo therapy:
Cells are taken from the body, transfected ex vivo and reinserted

In vivo therapy:
The transfection vector is brought directly into the body to transfect target cells

Fig 1.1 *Ex vivo* and *in vivo* somatic gene therapy

To bring genetic material successfully into cells, in other words to transfect them, either physical methods or a transporter construct can be used. Examples for physical methods are direct injection of naked DNA into muscle tissue (Davis et al., 1993) electroporation (Gehl, 2003), sonoporation and the "gene gun" where gold-nanoparticles coated with genetic material are shot into cells (Mehier-Humbert, Guy, 2005).

Using a transporter construct, a so called vector, to ferry the genetic material into the cell, seems a more elegant way. Nature developed very successful vectors: the viruses. They have to bring their own genetic material into host cells in order to replicate. As they were optimized by evolution over many millions of years they are extremely successful. Viruses that are genetically modified to be unable to replicate and cause disease can be used to bring therapeutic genetic material as payload into cells. This method is very efficient (Gardlik et al., 2005) and is therefore used frequently. 67.4 % of the ongoing or completed clinical gene therapy trials are using viral vectors (Adenovirus, Adeno-associated virus, Retrovirus, Vaccinia virus, Poxvirus, Herpes simplex virus, …) according to an online overview (The Journal of Gene Medicine, 2007). The above mentioned first approved gene therapy drug "Gendicine" is also based on an adenovirus.
But the use of viral vectors derived from pathogens poses the possible danger of recombination to a pathogen virus (Fischer, 2001) and even malignant disorders (Baum et al., 2003). As the host organisms have developed counter mechanism against viral infections, also unwanted immune reactions can be triggered (Lehrman, 1999).

Therefore, there is intensive research to develop, characterize and optimize non-viral gene transfer vectors as an alternative (Brown et al., 2001). As non-viral vectors are not derived from pathogens they lack risks of viral vectors and promise to be safer (Nabel et al., 1993).

To result in good transfection, the successful introduction of foreign DNA into the cell, such a vector has to overcome several obstacles (Wiethoff, Middaugh, 2003):

- The genetic material has to be compacted to be protected from degrading enzymes and allow transportation.
- The vector needs to bring its payload across the cell membrane.
- The material has to be freed from endosomes, before being digested.
- DNA as payload has to be brought to the nucleus to be transcripted (copied into mRNA).

For a possible *in vivo* use the vector also should:

- Be non-toxic
- Show low immunogeneticity
- Be stable in serum and blood
- Allow modifications to target it on specific organs or types of cells

And for routine use an easy, cost effective and reproducible manufacturing method is needed.

Genetic material such as DNA is charged negatively at physiological pH because of its phosphate groups. Therefore, it can be sized down and protected by complexing it with a cationic reagent. An early direct approach in this direction is the formation of co-precipitates of DNA with Calcium phosphate (Chen, Okayama, 1987). Other reagents of the first generation of gene transfer vehicles were pure cationic reagents like liposomes and polymers. Liposomes containing cationic lipids such as DOTAP (1,2-dioleoyl-3-trimethylammonium-propane), DOTMA (N-[1-(2,3,-dioleyloxy)propyl]-N,N,N-trimethylammonium), or DOSPA (2,3-dioleyloxy-*N*-[2(sperminecarboxamido)-ethyl]-*N*,*N*-dimethyl-1-propanaminium trifluoro acetate) form complexes with DNA, so called lipoplexes. Those lipoplexes were used to transfect cells in cell culture (Behr, 1989; Torchilin, Weissig, 2003; Felgner et al., 1987), and were especially effective when combined with helper lipids like DOPE (1,2-Dioleoyl-*sn*-Glycero-3-Phosphoethanolamine) (Hirsch-Lerner et al., 2005). 7.6 % of the ongoing or completed clinical gene therapy trials involved lipofection according to an online overview (The Journal of Gene Medicine, 2007). This number is small compared to the number of virus

related trials but it shows that transfection with non-viral vectors is seriously considered for human use.

The polymers used for complexation of nucleic acids, resulting in polyplexes, are polycations such as protamine sulfate, poly-l-lysin, chitosan, and polyethylenimin (PEI) (Park et al., 2006; Thomas, Klibanov, 2003). The polyamine PEI (Boussif et al., 1995) is of special interest as it shows superior transfection efficiency. Different molecular weights were tested (Godbey et al., 1999b; Kunath et al., 2003), and modifications like pegylation to achieve longer blood stream circulation and coupling to targeting motifs have been realized (Germershaus et al., 2006).

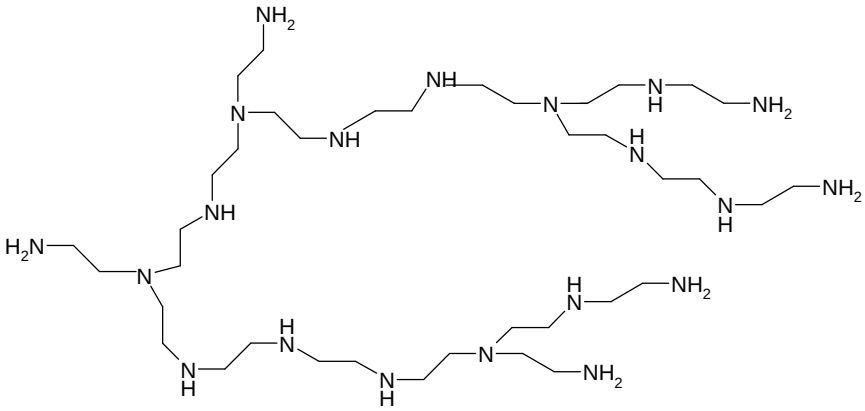

Fig 1.2 Polyethylenimine (PEI). In the polyamine PEI every third atom is a nitrogen in an amino group.

As possible reason for the superior transfection efficiency the “proton sponge” hypothesis was postulated by Behr in 1997 (Behr, 1997). It explains the high transfection rates of PEI by an escape of the nucleic acids and vectors from endosomes, in which cells take up foreign material, by a proposed mechanism of osmotic endosomal swelling: As PEI contains amine groups that remain unprotonated at physiological pH it possesses buffer capacity. Endosomes that turn to lysosomes get acidified by a proton pump (D'Souza et al., 1987). If now this acidification is buffered by the unprotonated nitrogens of PEI more and more protons will be pumped into the cell and chloride ions will flow into the cell to balance charge. The inflowing ions lead to an osmotic gradient and consequently osmotic swelling that might damage or rupture the endosomal membrane thus allowing the escape of the gene transfer vector and nucleic acids.

In conclusion, there are huge advances in the development of non-viral vectors but still transfection efficiency of lipo- and polyplexes is low compared to viral vectors (Sakurai et al., 2007) and there are also toxicity issues (Lv et al., 2006; Filion, Phillips, 1998).

So there are efforts to construct more advanced gene transfer vehicles that consist of a cationic reagent to condense DNA or RNA and a neutral or negatively charged second reagent that improves the resulting particle. For example by wrapping the cationic particle in neutral lipids (Yamauchi et al., 2006), by producing the so-called SPLP (Zhang et al., 1999) or by constructing virosomes from reconstituted viral membranes (de Jonge et al., 2007). Some of those complex particles try to copy nature's long evolving success by mimicking natural viruses (Belguise-Valladier, Behr, 2001; Tagawa et al., 2002).

1.2 Artificial viral particles (AVP)

Artificial viral particles are such an advanced gene transfer system. Their design was driven by the intention to combine the advantages of viral and non-viral vectors by mimicking an enveloped virus with a core of condensed DNA and a lipid envelope.

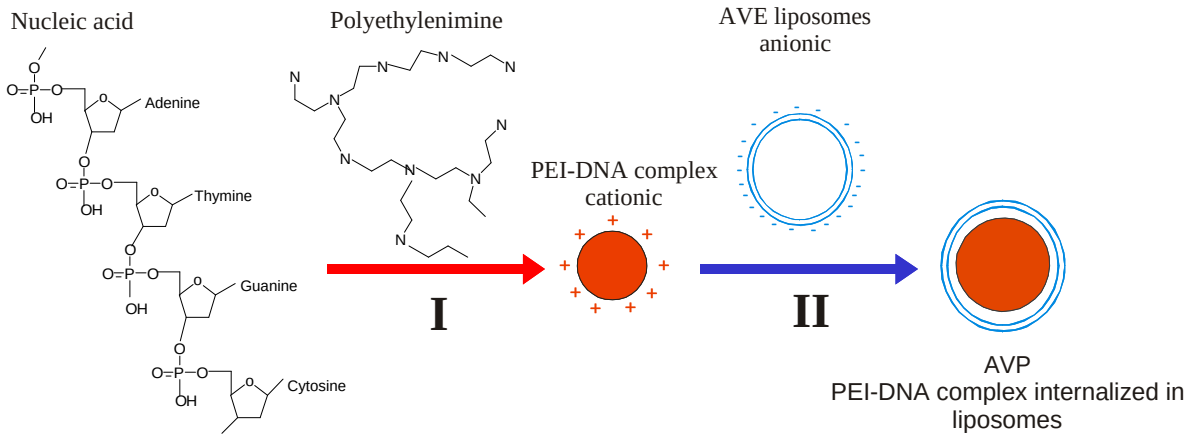

Fig. 1.3 Idealized AVP design

I Complexation of the negative charged nucleic acids with an excess of the positive charged polymer polyethylenimine, resulting in small cationic complexes

II Anionic AVE liposomes are brought into interaction with the cationic PEI-DNA complexes

DNA was condensed with the polymer polyethylenimine, whose advantages were described above. Also protamine sulfate, a polycation that condenses DNA in sperm was used as natural

alternative (Van Meel, Pearson, 1979). As lipid component liposomes with a lipid composition adopted from one of the most successful enveloped virus the HI-Virus were used (Chander, Schreier, 1992). Those liposomes were charged negative and called “Artificial viral envelope” (AVE) as their composition imitated the lipid envelope of some viruses. First step of the practical preparation of AVP was mixing a nucleic acid solution with an adjusted PEI solution followed by an equilibration time for the PEI-DNA complexes.
In the second step pre-fabricated anionic AVE liposomes were added to the PEI-DNA complexes and mixed including high shear force steps. After further equilibration the AVP were characterized and used in cell culture.

Application of AVP in experiments showed promising results:

- They were able to transfect different cell lines with a plasmid coding for a reporter protein (see chapter 1.4), and displayed low toxicity (Muller et al., 2001).
- Targeting them to the $a_v ß_3$ integrin receptor, expressed on melanoma cells, by introducing a cyclic RGD (Arginine-Glycine-Aspartic acid) peptid as targeting device into the AVP was realized and was proven successful by increased transfection rates on $a_v ß_3$ expressing cells (Nahde et al., 2001).
- Early physical characterization by size measurements and visualization in transmission electron microscopy (Cryo-TEM) showed small particles, sized ~180 nm that appeared to be filled with DNA (A.Fahr, K.Müller, 2001).
- The successful transfer of fluorescence marked oligonucleotides into cells by AVP was shown and traced by their fluorescence (Welz et al., 2000).
- Application of AVP containing antisense–oligonucleotides, designed to suppress synthesis of a B-Raf kinase, led to a downregulation of this kinase in cell culture (Bucké, 2001).

So AVP successfully transferred plasmids and oligonucleotides in cell culture and promised to be a highly interesting non-viral gene transfer vector. Especially the coating with negatively charged liposomes, that would likely reduce unwanted interactions with blood ingredients (Roerdink et al., 1983) and the possibility to integrate targeting motifs made them a candidate for later *in vivo* gene therapy and led to the filing of a patent (Bruesselbach et al., 2000).

But more intense studies and optimization of these particles are necessary. There are several possibilities to characterize a gene transfer vector physically and biologically. Selected important approaches will be introduced in the following section for better understanding.

1.3 Physical characterization of gene transfer vehicles

Non-viral gene transfer vehicles are normally dispersed in a buffer system. So from a physical point of view a water based dispersion of nanoparticles has to be characterized.
Size of the nanoparticles is below the limits of optical methods, such as light microscopy, that are defined by the wavelength of light. So particle size and morphology have to be determined with more sophisticated methods.

Particle size and size distribution of dispersions in the nano-range can be estimated using Photon Correlation Spectroscopy (PCS), also called Dynamic light scattering (DLS). Here fluctuations of stray light intensity of laser light strayed by dispersed particles are monitored. Intensity of the stray light fluctuates as the particles in dispersion show Brownian motion. The speed of the Brownian motion corresponds to particle size according to the Stokes-Einstein equation. Therefore, the hydrodynamic diameter of the particles can be deduced. Result of this calculation are two parameters: the Z-average as mean calculated hydrodynamic diameter describing the size of particles and the polydispersity index PDI describing the particle size distribution width (Müller et al., 1996). PCS is regularly used to determine and compare size of nanoparticles, including gene delivery vectors (Tabatt et al., 2004). Their size is important, as it is one factor that decides about the uptake of the vector into cells (Ogris et al., 1998; Wagner et al., 1991). Also for a possible *in vivo* use small size has to be insured to avoid complications like clotting of blood vessels.

But size measurements do not give any information about the morphology of the vehicles. Here electron microscopy can give further insights, as electrons are used to visualize structures down to the atomic level. In Transmission Electron Microscopy (TEM) an electron beam passes through a thin sample specimen, gets partially scattered and forms an image of the sample.

Biological samples have to undergo a special preparation before being examined by TEM.

- Negative staining, the embedding of samples in uranylacetate, is a fast preparation and contrasting technique. Picture quality is limited by uranylacetate salt grains and artefacts can be caused by the osmotic activity of the salt. Nevertheless, it is used regularly and successfully to examine gene transfer vehicles e.g. the characterization of completely and incompletely complexed PEI-DNA particles (Pollard et al., 1998), virosomes (de Jonge et al., 2007; Shoji et al., 2004) and complex gene transfer vehicles (Lee, Huang, 1996).
- After freeze fracture preparation a platinum replica of the surface of a fractured frozen sample can be examined in TEM. This way information about the morphology of surfaces and the interior of broken open gene transfer vesicles can be gathered. Here especially the work of Brigitte Sternberg on complexation of DNA, liposomes and artificial gene transfer vehicles is important (Sternberg et al., 1998; Jaaskelainen et al., 1998).
- Cryofixation, the ultra-fast freezing of a thin layer of the sample on a grid, which results in vitreous ice, allows direct examination of the frozen sample. This technique, also called Cryo-TEM results in high resolution pictures of gene carrier vesicles in their normal media, without artefacts from staining. As the beam passes through the sample also insights into the interior of the particles can be gained. This allows concluding if drug delivery systems like liposomes are filled or empty. But as the sample is not stained, contrast of biological samples can be low. Also the requirements for the electron microscope are high, as the sample has to stay frozen during examination and transport into the electron microscope. Nevertheless, this technique is successfully used to characterize filled liposomes (Fritze et al., 2006) and gene transfer vehicles (Alfredsson, 2005; Clement et al., 2005).

Another method to visualize the three-dimensional surface of non viral gene transfer vehicles is Atomic Force Microscopy (AFM). Here a sharp tip on a micro cantilever is used to scan the surface of the sample and deflection of the cantilever is monitored. This method was successfully used to probe the surface of poly- and lipoplexes (Tabatt et al., 2004; Neu et al., 2006).

Surface charge of the particles in dispersion is an important parameter. It strongly influences dispersion stability by inhibition of aggregation by repulsion of equal charges (Voigt, Fahr, 2007). It is expressed as zeta potential which is calculated from the measured electrophoretic mobility of dispersed particles in an electric field. Zeta potential is strongly dependent from the pH of the dispersant and also influenced by its ionic strength.
Charge interactions play an important role in the preparation and further fate of non-viral gene transfer vectors. They are the basic principle behind the complexation of anionic DNA with cationic polymers or lipids and they influence interactions between vectors and biological materials such as plasma ingredients and cell surfaces. These interactions can be an advantage as they increases particle uptake by interaction with the negatively charged cell membranes (Duguid et al., 1998; De Smedt et al., 2000). But they can also be a drawback as unspecific interaction with extracellular material and consequently inactivation of particles occurs (Ruponen et al., 2001).

1.4 Biological characterization of gene carrier vehicles

To determine if the “drug” nucleic acid is successfully delivered to its target, to test its efficiency, models are needed. Physical models can not imitate the complex machinery of uptake of particles and processing of genetic material in a cell. Therefore, biological systems are needed as models.

Either *in vivo* studies in animals, or *in vitro* experiments can be performed. *In vivo* the vector is subject to all the factors and influences in a living being like: distribution in different tissues, contact with and possible inactivation by blood components, a functioning immune system and cells in their natural environment. This results in a realistic model for a possible later medical application of the vector. But ethical reasons and also high costs and efforts vote against standard use in basic research on vectors.

In vitro experiments in cell culture represent an important alternative to minimize animal experiments. Prokaryotic and eukaryotic cells are kept and multiplied in culture media under suitable conditions (e.g. 37 °C, 5 % CO_2) in an incubator. They grow either attached to surfaces in petri dishes and culture flasks or freely dispersed in flasks. In research on vectors for gene therapy mainly eukaryotic cells derived from mammals in general or even from human sources are used.

Mammalian cells can be isolated from tissue, kept alive and propagated as primary cells. But those primary cells can be multiplied only for a limited number of generations before they enter a replicative senescence state and stop doubling (Rubin, 2002). Another, more convenient, approach is the use of immortalized cell lines that can be cultivated unlimited. Those cells are either derived from cancer cells, that are immortalized by an accidental mutation, or from cells that were artificially immortalized, e.g. by the Simian virus 40 (SV 40) (Hahn, 2002).
Still, cultured cells are not a perfect replica of a living eukaryotic organism. During cultivation in artificial conditions cells can change properties such as the expression of surface structures. Also their culture media environment can not imitate an embedding into a living organism with different tissues, distribution of foreign materials to organs, influence of blood components, and a functioning immune system. So a direct comparison between *in vitro* and *in vivo* results is hard (Li, Huang, 2000). But if it is kept in mind that cell culture is a model and not a perfect replica of natural conditions, they allow important insights. As those cultured cells can be propagated with low effort they are also a convenient tool.

As well for *in vivo* as for *in vitro* experiments genetic material coding for a reporter protein is often used to determine success of the transfection process. If these reporter genes are successfully brought into the cell and processed there they trigger the synthesis of a reporter protein that can be easily assayed. It can function as a degree of transfection success and also to localize the distribution of transfected cells e.g. in different organs in an animal experiment. These reporter proteins are either enzymes that can be detected by the conversion of an substrate or proteins that can be detected directly.

Luciferase, an enzyme that is responsible for the bioluminescence of fireflies and also occurs in marine organisms (Markova et al., 2004), is a prominent example of enzymes used as reporter proteins. It catalyses the oxidation of luciferin to oxyluciferin. In this reaction also light is emitted as luminescence. So enzyme activity as a degree of transfection success can be quantitated in the lysate of transfected cells from cell culture or from a specific organ of a transfected animal. Other examples of enzymes used as reporter proteins are ß-galactosidase and chloramphenicol acetyltransferase (CAT).

The “green fluorescent protein” GFP and its variants are the most prominent examples of reporter proteins that can be detected directly by its UV light induced fluorescence (Tsien, 1998). Naturally it occurs in the bioluminescent jellyfish Aequorea victoria. It has been used as reporter protein and also variated to new species that fluorescence more brightly and have shifted excitation maxima, e.g. the red shifted “enhanced green fluorescent protein” EGFP (Cormack et al., 1996).

This protein can be used to detect and localize transfection in dead and living cells by fluorescence microscopy or flow cytometry.

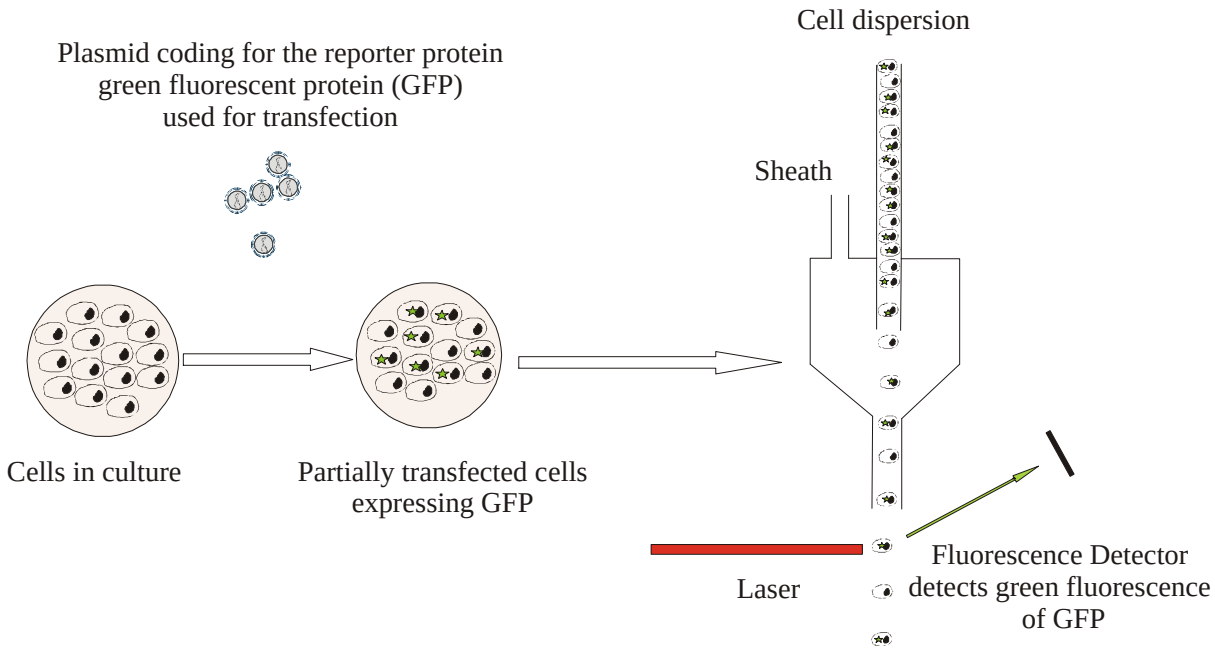

Fig 1.4. Detection of the reporter protein green fluorescent protein (GFP) in transfected cells by flow cytometry

In flow cytometry a cell suspension is moved in a sheath stream of buffer that separates the suspension into single cells (Rieseberg et al., 2001). They pass a laser beam and forward (FS) and sideward scattered light (SS) and emitted fluorescence of individual cells are detected. Cell populations can be identified by the forward scattered light that describes their size and the sideward scattered light that describes their granularity. Expression of a fluorescent reporter protein or fluorescence marking of cell allows further differentiation. So flow cytometry can be used to quantify the number of transfected cells and also the degree of expression in the transfected cells after a transfection experiment using GFP.

For gene transfer experiments the information for those reporter proteins is often encoded in a plasmid, a ring of double-stranded DNA occurring in bacteria. Normally they also contain antibiotic resistance genes for prokaryotes. This allows easy amplification in bacteria such as Escherichia coli (E.coli) to obtain sufficient amounts for gene therapy experiments.

1.5 Tracing gene carrier particles in cells

As explained before (see chapter 1.1) a gene transfer vector has to overcome several obstacles to bring its payload genetic material unharmed to its intracellular target. Tracing gene transfer vehicles on their way into the cell can not only give more profound knowledge about intracellular processes and handling of foreign material, but can also help to understand why some gene transfer vehicles are more successful than others. The gained insights into the mechanisms and possible manipulation of cellular uptake and processing can be used to further improve the gene carriers.

Following the gene carriers into the cell is not trivial, as they are in the nano-range and thereby hard to detect by light microscopy. Using reporter genes allows seeing the final result of a successful transfection experiment relatively easy as described above. But in order to trace the particles on their stations into the cell and in the cell, marking them is necessary.
This can be done by marking of the genetic material (Welz et al., 2000) or other components of the vector (e.g. the polymer used for complexation) with fluorescence markers. Fluorescence marked vectors were traced by fluorescence microscopy or confocal laser scanning microscopy in dead, fixed cells and also in living cells (Merdan et al., 2002; Godbey et al., 1999a). Also transmission electron microscopy was successfully used to trace gene transfer vectors in ultrathin slices of transfected cells (Labat-Moleur et al., 1996; Pitard et al., 1999; Zabner et al., 1995). For this purpose electron dense gold sol particles were used as markers (Zabner et al., 1995).

These examinations have been performed for a variety of different vectors and led to controversial results. Most researchers agree on endocytosis, uptake of extracellular material by invagination (Conner, Schmid, 2003), as uptake mechanism for gene transfer vehicles (Wiethoff and Middaugh, 2003). Fluorescence marked PEI-DNA complexes were found in endosomes, intracellular vesicles containing the taken up material (Godbey et al., 1999a; Merdan et al., 2002). Also Zabner and colleagues, found gold-marked lipoplexes in

endosomes in electron microscopic examinations (Zabner et al., 1995). But other possible uptake mechanism for gene transfer vehicles such as membrane fusion were also discussed (Zhang et al., 2007; Escriou et al., 1998).

Natural viruses are able to escape from endosomes (Cotten et al., 1992). As possible explanation for the escape of non-viral vehicles into cytoplasma the proton sponge theory (see chapter 1.1) (Behr, 1997) and other possibilities such as mimicking the fusogenic proteins of viruses have been postulated and tested in experiments (Cho et al., 2003; Funhoff et al., 2004).

The transfer of genetic material into the nucleus across the nuclear membrane is vital when DNA (e.g. plasmid) is transferred, as here transcription in the nucleus is necessary. During mitosis the nuclear membrane is opened (Bally et al., 1999) which allows direct access and can explain increased transfection rates in dividing cells (Mortimer et al., 1999). Another possible entry pathway for DNA or the whole vector are the nuclear membrane pores (Liu et al., 2003).

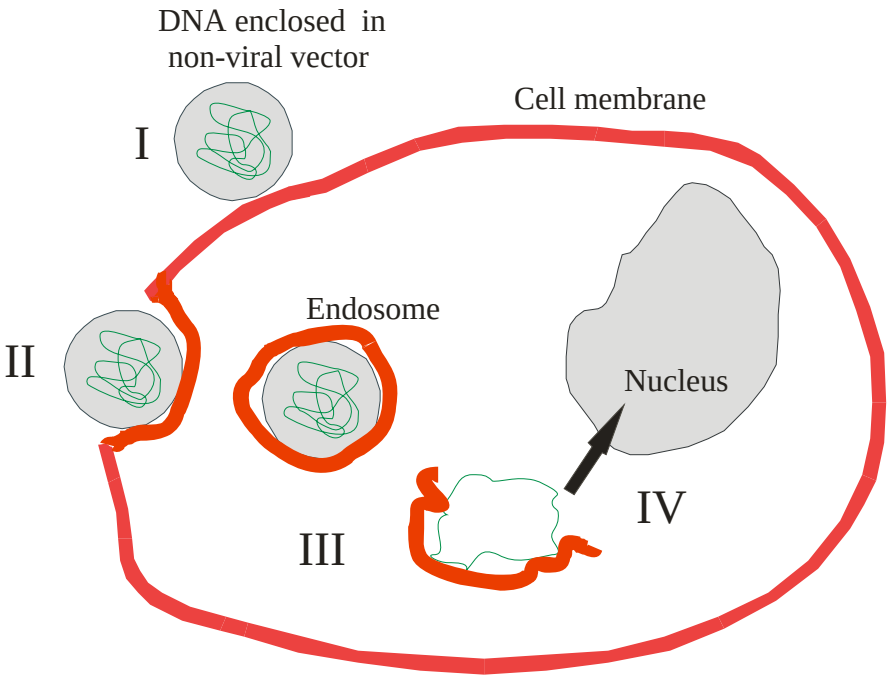

Figure 1.5 Proposed pathway of DNA in non-viral vectors into a cell

I **Attachement of the gene transfer vector to the cell surface**

II **Uptake into the cell by endocytosis**

III **Escape from endosomes and release into cytoplasma**

IV **Transfer to the nucleus for transcription**

1.6 Aim of the work

Gene therapy is a controversial topic. Despite drawbacks and failures it still is a field full of promises for novel possibilities of medical treatment in the future. Construction of dosage forms for genetic material is a new technological challenge. Different non-viral vectors were and are developed and investigated as possible alternatives to the use of viral vectors. Composition and layout of those vectors is crucial for efficiency and tolerance in biological systems.

A promising approach for non-viral gene delivery are artificial viral particles (AVP). They mimic principally the design of enveloped viruses with a condensed core and a lipid envelope. They are composed of the cationic polymer polyethylenimine (PEI) in order to condense the genetic material in combination with anionic liposomes to imitate the viral envelope. Despite initial works that were done when the system was established, questions regarding the AVP themselves and their suitability for tasks in medical and basic research applications remained open.

Aim of this work was thus the detailed characterization of artificial viral particles and optimization of their composition and manufacturing. Furthermore, they should be adapted and used for new applications.

Consequently several tasks were addressed during this work:

- Characterization of the structure of AVP using electron microscopy and size and charge measurements. Relating biological activity to structure after separation of particle species in ultracentrifugation.
- Following uptake of AVP into cells and their fate in cells using fluorescence marking techniques and electron microscopic examinations of ultrathin slices of transfected cells.
- Transfer of AVP preparation from manual pipetting to an operator independent, easy to scale up production in a static mixer.
- Investigation of influences of changed AVP composition and of forces applied during AVP production on structure and biological efficiency of AVP. Usage of the gained insights to optimize AVP.

In co-operations AVP were also tested as innovative reagent for the transfer of siRNA and for stable expression of a recombinant protein consisting of GFP coupled to an enzyme.

2. Materials and Methods

2.1 Methods:

2.1.1 Preparation of artificial viral envelope (AVE) liposomes

The phospholipids 1,2 Dilauroyl-sn-glycero-3-phosphoethanolamine (DLPE) (Sygena, Liestal, Switzerland), 1,2-Dioleoyl-sn-Glycero-3-Phosphoethanolamine (DOPE) (Avanti Polar Lipids Inc., Alabaster, USA), 1,2 Dioleoyl-sn-glycero-3-phospho-l-serine (DOPS) (Avanti Polar Lipids), 1,2-Dioleoyl-sn-glycero-3-phosphoethanolamine-N(glutaryl) (N-glut-DOPE) (Avanti Polar lipids) and cholesterol (Chol) (Genzyme, Cambridge, UK) were used as stock solutions in chloroform and stored at –20 °C.

	Composition	Molar ratio
AVE	DOPS : DLPE : Chol	1 : 1 : 1
AVE-DOPE	DOPS : DOPE : Chol	1 : 1 : 1
AVE-act	DOPS : DLPE : Chol : N-glut-DOPE	3 : 3 : 3: 1

Table 2.1 Composition of the three used types of AVE liposomes

Lipids (see table 2.1 for lipid composition) were mixed and diluted in 1 ml chloroform and dried into a thin film in a rotating 100 ml glass vessel warmed by a water bath at 40° C, applying gentle vacuum. Residuary chloroform was removed by vacuum desiccation for one hour. The lipid film was hydrated by addition of 1 ml sterile Tris buffer at 40 °C (10 mM pH 7.4) resulting in a total lipid concentration of 10 µmol per ml. The multilamellar liposome suspension was shortly ultrasonicated in an ultrasonic bath (Bender Hobein, Zürich, Switzerland) and allowed to swell for another hour. Final preparation of the small unilamellar liposomes was done by extruding the suspension through polycarbonate membrane filters with a pore size of 50 nm in a Liposofast mini-extruder (Avestin, Ottowa, Canada) 21 times.
Liposome size and size distribution were checked by photon correlation spectroscopy.
AVE-act liposomes, containing N-glutaryl-DOPE, were additionally incubated with the carbodiimide EDC (N(-3-dimethyl-aminopropyl)-N´-ethylcarbodiimide hydrochloride, Merck, Darmstadt, Germany) for eight hours at 37 °C to activate the carboxyl group of the N-glutaryl anchor. Residual EDC was removed by column gel chromatography using Sepharose G25 (Pharmacia).

All liposomes were stored at 4 °C after filtration through Millex-GV-0.22 µm filters (Millipore, Schwalbach, Germany) under aseptic conditions.

Fluorescence marked liposomes:

For special purposes, like visualizing liposomes in ultracentrifugation or tracing per fluorescence microscopy, liposomes were marked with lipophilic fluorescent dyes.

The red lipophilic dye DiI (1,1′-Dioctadecyl-3,3,3′,3′-tetramethylindocarbocyanine perchlorate) (Sigma-Aldrich, München, Germany) was added as ethanolic solution to the phospholipids dissolved in chloroform before forming an lipid film.

The phosphatidylethanolamin coupled Rhodamin (Rh-PE) (1,2-Dioleoyl-*sn*-Glycero-3-Phosphoethanolamine-N-(Lissamine Rhodamine B Sulfonyl) (Ammonium Salt) (Avanti Polar Lipids) was added as chloroform solution to the phospholipids in chloroform before forming an lipid film.

The amount of dye corresponded to 0.025 µmol DiI or 0.05 µmol Rh-PE per 10 µmol total lipid.

2.1.2 DNA complexation agents (Polyethylenimine (PEI), Protamine sulfate (PS), Poly-L-lysin (PLL) and preparation of fluorescence marked PEI)

Every third atom in the polymer polyethylenimine is a nitrogen atom in an amino group that can be protonated (Choosakoonkriang et al., 2003), which results in a high positive charge under physiological conditions. Besides the possible application in gene therapy mentioned in the introduction, PEI is widely used for technical applications, e.g. as additive for coatings (BASF, 1996).

The PEI used as standard DNA condensation reagent in this work was Lupasol® G100. It is a technical grade branched polyethylenimine in a 50 % watery solution and was a friendly gift of BASF (Ludwigshafen, Germany).

Before being used for transfection experiments, PEI was diluted to 0.9 mg/ml, pH was adjusted to 7.4 and the solution was sterile filtered and aliquoted.

In some experiments also jetPEI® (Polyplus, San Marco, Ca, USA), a commercial “linear polyethylenimine derivative” (Polyplus, 2002) was used to condense DNA.

As alternatives for PEI in artificial viral particle (AVP) preparation also protamine sulfate (Ely Lilly, Indianapolis, USA) a natural polycation that condenses DNA in sperm (Van Meel

and Pearson, 1979), and Poly-L-lysine MW 15.000 and 150.000 g/mol (Sigma) were tested. Both are reagents that were used to complex DNA for gene transfer before (Farrell et al., 2007; Tsuchiya et al., 2006).

Fluorescence marked PEI

To be able to trace the path of the AVP component PEI into cells by fluorescence microscopy, PEI was marked with the green fluorescent marker oregon green.

Alternatively to standard AVP preparation PEI with a molecular weight of 25.000 g/mol (Lupasol HF) (BASF) was used instead of the normally used PEI MW 5000 g/mol to facilitate separation of unbound marker by dialysis.

The marking procedure was adapted from the work of Merdan (Merdan et al., 2002).10 mg PEI was dissolved in 1 ml 0.1 M sodium hydrogencarbonate pH 9. 1 mg Oregon Green 488 carboxylic acid succinimidyl ester 5 isomer (Molecular probes, Invitrogen, Carlsbad, CA, USA) dissolved in 200 µl DMSO was added dropwise under stirring. The reaction batch was left to incubate for three hours in the dark at room temperature to allow coupling. Unbound marker was separated by dialysis (membrane cut off 10.000 g/mol) first against phosphate buffered saline (PBS) and finally against purified water until no more traces of oregon green were detectable by Vis-absorption (488 nm).

2.1.3 Preparation of Artificial viral particles (AVP)

AVP gene transfer vectors were prepared freshly prior to each transfection. Unless stated otherwise, preparation was done following the previously described procedure (Nahde et al., 2001).

First DNA (e.g. plasmid coding for EGFP) and polyethylenimine (PEI) were mixed in Tris buffer 10 mM pH 7.4 to complex the DNA, resulting in a nitrogen / phosphate ratio of 20.7 / 1 and a positive / negative charge ratio of ~ 4.5 / 1 for standard AVP.

After allowing the PEI-DNA complexes to ripen for 15 min, AVE liposomes were added and mixed by vigorous pipetting. After incubation for 20 min, the resulting AVP were used directly for characterization or transfection.

In later preparations in a chipmixer (described in detail in chapter 3.3) a syringe pump (World Precision Instruments, Sarasota, USA) and glass syringes (Hamilton, Bonaduz, Switzerland) were used. In this case equal volumes containing either PEI and DNA or in the second step PEI-DNA and AVE liposomes were mixed.

2.1.4 Photon correlation spectroscopy

Photon correlation spectroscopy (PCS) or dynamic light scattering (DLS) is a method that allows evaluation of size and size distribution of particles in the nano-range.

Here fluctuations of stray light intensity of laser light strayed by dispersed particles are monitored. Intensity of the stray light fluctuates as the particles in dispersion show Brownian motion. The speed of the Brownian motion corresponds to particle size according to the Stokes-Einstein equation. Therefore, the hydrodynamic diameter of the particles can be deducted. Result of this calculation are two parameters: the Z-average as mean calculated hydrodynamic diameter describing size of particles and the polydispersity index PDI describing particle size distribution breadth (Rainer H.Müller et al., 1996).

Particles were measured after dilution in filtered (Sterifix 0.2 µm filter, Braun Melsungen AG, Melsungen, Germany) 10 mM Tris buffer pH 7.4 on a Zetasizer Nano ZS (Malvern Instruments, Worcestershire, UK) in a detection angle of 173°. Unless stated otherwise three measurements at measurement position 7.65 using run time and attenuator (intensity adjustment) recommended by the analysis software were performed. Data was evaluated with the general purpose analysis model of the Dispersion Technology Software version 4.10 (Malvern Instruments)

Some of the early measurements were also done on a Zetaplus (Brookhaven Instruments, Holtsville, USA) in an angle of 90°.

2.1.5 Zetapotential measurements

One possibility to evaluate surface charges of particles in dispersion is applying voltage to the dispersion and measuring the velocity of the electrophoretic movement of charged particles. The resulting parameter describing the surface charge is called zetapotential (Rainer H.Müller, 1996).

Zetapotential of samples was determined after dilution in filtered 10 mM Tris buffer pH 7.4 in a disposable Zeta cell (Malvern Instruments) on a Zetasizer Nano ZS (Malvern Instruments) or in a glass capillary on a Zetasizer 3000 in three consecutive measurements. Zetapotential was calculated according to the Smoluchowski model (Müller, 1996) using the general purpose analysis model.

2.1.6 Transmission electron microscopy

All electron microscopic examinations were done by transmission electron microscopy. Samples were prepared using the following techniques. Negative staining and freeze fracture were done with the friendly help of Steffi Richter and Cryo-TEM preparation with the friendly help of Frank Steiniger.

A) Negative staining:

5 µl of sample were pipetted on a Formvar-coal coated copper grid (200 mesh BAL-TEC GmbH, Witten, Germany) and allowed to attach for 60 seconds after which excess liquid was sucked off with a piece of filter paper. Next 5 µl of a saturated uranyl acetate solution were pipetted on the sample and also allowed to attach for 60 seconds before being sucked off. After drying at room temperature samples were examined in a CEM 902a transmission electron microscope (Carl Zeiss NTS GmbH, Oberkochen, Germany).

B) Freeze fracture:

A perforated gold grid (mesh 400, BAL-TEC) was wetted with sample and placed between two copper platelets. A surplus of sample was sucked off with a piece of filter paper before the "platelet-grid" sandwich was shock frozen at –150 °C by plunging in liquid propane (Jet Freezer JFD-030, BAL-TEC). The frozen sandwich was transferred in frozen state into the freeze fracture unit (BAF 060, BAL-TEC) and broken apart at –150 °C at 10^{-7} to 10^{-6} mbar.
The newly generated surfaces were shadowed with 2 nm of a platinum-carbon mixture (95:5 V:V) under 45 °. Carbon was coated 20 nm thick on top of the platinum replica to stabilize it.
The platinum replicas of the freeze fracture surfaces were detached from the sample using purified water and washed 3 times using a 1 / 1 Chloroform / Methanol mixture (v/v). Replicas were transferred on a grid and examined in a CEM 902a transmission electron microscope.

C) Cryo-TEM:

A drop of sample was pipetted on a coated copper grid (Quantifoil R1.2/1.3, Quantifoil, Jena, Germany) and excess of sample sucked off with a piece of filter paper. To avoid the formation of crystals the grid was plunged rapidly into liquid ethane in a cryobox (Carl Zeiss NTS GmbH) and thereby shock-frosted at -175 °C. After transfer in frozen state in a Gatan 626 cryotransfer system (Gatan GmbH, München, Germany) into the precooled transmission

electron microscope Philips CM 120 (Philips, Eindhoven, NL) the sample was examined at 120 kV.

2.1.7 Preparation of ultrathin sections of transfected cells for electron microscopy

To trace AVP into cells, gold-marked plasmid (see chapter 2.1.11) was processed to AVP as described using standard manual preparation (see chapter 2.1.3). HepG2 cells were grown and transfected as described in chapter 2.1.12 and 2.1.13.

Cells were handed over 24 h after transfection to Prof. Oehring for fixation, preparation of ultrathin sections and examination in transmission electron microscopy as described before (Kettering et al., 2007).

Cells were fixed for 30 minutes at 20 °C in a 2 % (v/v) solution of glutaraldehyde in a 0.1 M cacodylate buffer pH 7.4 containing 5 % glucose, followed by a washing step with 0.1 M cacodylate buffer pH 7.4 containing 6.8 % glucose. In the next step cells were treated for two hours at 4 °C with an equivoluminar mixture of a 2 % solution of OsO_4 in distilled water and a 3 % $K_4[Fe(CN)_6]$ solution in 0.2 M cacodylate buffer 0.2 M, pH 7.4. Cells were rinsed with 0.1 M cacodylate buffer pH 7.4 containing 6.8 % glucose until the solution remained clear and dehydrated in graded series of ethanol before being embedded in Epon 812 via hydroxypropylmethacrylate as intermedium. Finally samples were cured in an oven at 60 °C for six days.

For examination in a transmission electron microscope ultrathin (~70 nm) sections were cut with an Ultracut S ultramicrotome (Leica, Wetzlar, Germany) and stained with uranyl acetate and lead citrate.

2.1.8 Ultracentrifugation

To separate samples by ultracentrifugation a sucrose (Merck, Darmstadt, Germany) gradient was constructed layer by layer in an ultracentrifugation tube. Therefore, the sterile filtered sucrose solutions were carefully placed into the centrifugation tube using a flexible tube pump (Pharmacia, Uppsala, Sweden). To avoid turbulences the nozzle was always kept to the surface of the gradient. Directly before the centrifugation started the sample was pumped onto the gradient as last layer. Samples were ultracentrifuged in a SW 55 TI swinging bucket rotor (Beckmann Coulter, Krefeld, Germany) in the preparative ultracentrifuge XL-80 (Beckmann Coulter). After centrifugation the bottom of the centrifugation tube was pierced with a ∅ 0.90 x 40 mm needle (B.Braun Melsungen AG, Melsungen, Germany) and the successive fractions were carefully collected.

2.1.9 Escherichia coli transformation and plasmid amplification and purification

Escherichia coli (E.coli) "XL-Blue MRF´ supercompetent cells" (Stratagene, La Jolla, USA) were transformed with the plasmid EGFP-C3 (Clontech, Mountain View, USA). Therefore, 0.4 µl sterile filtered ß-mercaptoethanol (Merck) (diluted 1:10 (m:m) in water) was added to 20 µl thawed E.coli cells to permeabilize their cell walls. Cells were incubated 10 minutes on ice, followed by the addition of 500 ng plasmid and another incubation for 30 minutes on ice. After a heat shock treatment (40 s in 42 °C water bath, followed by 2 minutes on ice), cells were taken up in 225 µl antibiotic free Luria Bertani low salt media (International Diagnostics Group, Lancashire, UK) and allowed to grow for 1.5 hours at 37°C on a shaker.

This seed was used to inoculate 150 ml Luria Bertani media that contained 30 µg of the selective aminoglycoside antibiotic kanamycin (Carl-Roth GmbH, Karlsruhe, Germany). The plasmid used contains besides the code for EGFP also information that allows E.coli to withstand kanamycin. Consequently only transformed E.coli that contain the plasmid proliferate, whereas untransformed E.coli die or at least can not multiply. After overnight growth at 37 °C on a shaker, stocks of the transformed E.coli were frozen with 50 % sterile glycerol (Caesar & Loretz, Hilden, Germany) as cryoprotecant.

For plasmid amplification 200 ml sterile Luria Bertani media containing 30 µg of the selection antibiotic kanamycin per ml was inoculated with transformed E.coli from the frozen stock. E.coli were allowed to proliferate overnight at 37°C in a shaking Erlmeyer flask.

The plasmid coding for EGFP was extracted from E.coli cells using the HP Genelute Maxi Kit (Sigma) or its replacement product GenElute Endotoxin-free Plasmid Maxiprep Kit (Sigma) following manufacturer´s instruction. Shortly: E.coli cells were destroyed by alkaline SDS (Sodiumdodecylsulfate) lysis, proteins were aggregated and removed and the desired plasmid was bound in a column, washed and eluted. Plasmid concentration was measured by UV-absorption at 260 nm in a Bio photometer (Eppendorf, Hamburg, Germany) and purity of the plasmid was assessed by checking the ratio of absorption at 260/280 nm. Here the purified plasmids resulted in ratios between 1.8 and 2.0 indicating high purity of plasmid.

In early experiments herring-DNA (Sigma) was used as model DNA for physical characterisation experiments.

2.1.10 Agarose gel electrophoresis

Plasmid purification and later plasmid biotinylation was monitored by gel electrophoresis in agarose gels. Here nucleic acids migrate in an electric field through a gel because of their negative charge. Their size in basepairs and their structure (open or supercoiled) determine

their speed and thereby allow separation. After separation nucleic acids were visualized on a UV transilluminator with ethidiumbromid which forms a strong fluorescent complex by intercalation with nucleic acids.

A 1 % agarose gel (peq Gold Universal Agarose, Peqlab, Erlangen, Germany) was prepared in TAE buffer and supplemented with 10 µl 0.2 % ethidiumbromid solution (Carl-Roth) before being poured. After allowing the gel to solidify for 1 h, samples were supplemented with loading buffer (Peqlab) and loaded into the gel. Samples were separated for 1 hour at 70 V in a Biometra Agagel Standard (Biometra, Göttingen, Germany) horizontal gel electrophoresis chamber. A DNA ladder sample (Peqlab) was included to allow quantification of DNA size. Examination on the UV-transilluminator (Intas, Göttingen, Germany) was documented with a digital camera (Intas).

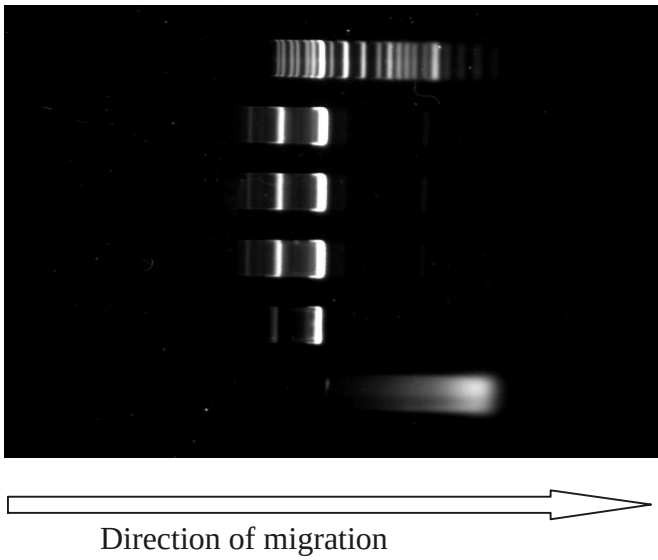

Figure: 2.1 Agarose gel electrophoresis.
Samples from top to bottom: DNA-ladder, 3 times plasmid, plasmid from another purification, small fragments of herring DNA

2.1.11 Marking plasmids with gold nanoparticles

The procedure to mark plasmids with gold nanoparticles was adapted from the work of Zabner et. al (Zabner et al., 1995).

First plasmid DNA was biotinylated. Therefore, 100 µl of a 1 µg/µl plasmid solution in water was mixed with 100 µl of a 1 µg/µl watery solution of EZ-Link photoactivatable Biotin (Pierce, Rockford, USA). This commercial reagent consists of biotin coupled by a linker to a photoactivatable nitrophenyl azide group.

The reaction batch was cooled with ice and exposed to UV-light (312 nm) in a quartz cuvette on a UV-transilluminator (Biometra) for 15 minutes. Upon this activation the photoactivatable

group forms a covalent stable unspecific bond to the plasmid. Reaction was stopped by addition of 100 µl 0.1 M Tris buffer pH 9.0.

For purification 200 µl 2-butanol was added, mixed with the sample and centrifuged. After phase separation the upper now orange coloured butanol phase containing excess reagent was discarded.

After repetition of this step the biotinylated plasmid was purified further by precipitation. Therefore, 20 µl of a 3M sodium acetate solution pH 5.2 and 600 µl ice cold ethanol were added and the sample was frozen at –20°C over night. The next day the precipitated plasmid was purified by washing with ice cold ethanol, dried, rehydrated in water and stored at -20 °C. Directly before use the biotinylated plasmid was mixed with 6 µl undiluted Streptavidin-gold dilution (Streptavidin /Gold Em Grade 10 nm, Electron Microscopy Services, Washington, USA) per µg plasmid and allowed to couple for 30 minutes before it was processed further. During this time the stable streptavidin – biotin complex is formed that marks the plasmid with the 10 nm gold particles.

2.1.12 Cell culture

HEK (human embryonic kidney) 293 kidney cells (friendly gift of Ronny Rüger, Jena), HepG2 hepatocellular carcinoma cells (DSMZ, Braunschweig, Germany) and L929 mouse connective tissue fibroblast (DSMZ) cells were grown to 60 to 90 % confluency in RPMI 1640 (PAA, Pasching, Austria) supplemented with 10 % fetal calf serum (Sigma), 2mM L-glutamine (BioWhitaker, Verviers, Belgium). HUVEC (Human umbilical vein endothelial cells) were grown in ECGM (PromoCell, Heidelberg, Germany) supplemented with 2 % fetal calf serum, 1 ng/ml basic fibroblast growth factor (recombinant), endothelial cell growth supplement/ heparin, 0.1 ng/ml epidermal growth factor (human, recombinant), 1.0 µg/ml hydrocortisone. All cells were grown in a humidified atmosphere at 37 °C and 5 % CO_2.

In initial experiments media was supplemented with 100 U/ml penicillin, 100 µg/ml streptomycin (both BioWhitaker), while later experiments were performed in antibiotic free cell culture.

2.1.13 Transfection procedure

Transfection, meaning the introduction of foreign genetic material into a cell, is the main task of gene carrier vehicles such as AVP. Their ability to do this was evaluated by transfecting cells in cell culture with a plasmid coding for an easy to detect green fluorescenting reporter protein.

The day before transfection cells were trypsinated and $50*10^3$ cells per well for HEK293/ HepG2 /L929 or $25*10^3$ cells per well for HUVEC cells were seeded in 24 well plates in their normal growth media. Cells reached 70 to 90 % confluency on the day of transfection. Prior to transfection media was changed to Medium 199 (Sigma) containing 10 % fetal calf serum (FCS) for HepG2 and HUVEC, while HEK293 were left in their growth medium RPMI 1640. Cells were transfected with gene transfer vectors, e.g. AVP, corresponding to 2 µg plasmid per well unless stated otherwise.
Six hours after transfection media was changed to fresh growth medium.

2.1.14 Flow cytometry

Flow cytometry was mainly used as a tool to evaluate biological efficiency or ability to transfect cells of AVP or other gene transfer vectors. As a plasmid coding for green fluorescent protein (EGFP) was used as model DNA, cells that were successfully transfected expressed EGFP and could be differentiated from untransfected cells because of their green fluorescence.
In flow cytometry a suspension of cells is diluted. Single cells are brought in a stream of buffer into a laser beam and forward and sideward scattered light is detected. Parallel emitted fluorescence is registered. The percentage of cells expressing the green fluorescent protein was assessed 24 h after transfection on an Epics XL-MCL flow cytometer (Beckmann Coulter, Krefeld, Germany).
Cells were rinsed with phosphate buffered saline and detached with trypsin (PAA) (0.25 % in PBS). After detachment of cells, residual trypsin was neutralized with serum containing media and cells were analysed by flow cytometry.
For data analysis the software Expo 32 v1.2 (Beckmann Coulter) was used. Forward and sideward light scattering of $10 *10^3$ events were plotted and used to gate cells in the resulting dot blot and exclude small waste particles and remnants of destroyed cells from analysis. From those gated cells a dot blot of red and green fluorescence was created and a gate was set up to differentiate between transfected green fluorescent cells and untransfected cells that just showed weak autofluorescence. Transfected cells showing more green fluorescence than untransfected cells were counted as positive and percentage of transfected cells calculated as final result.

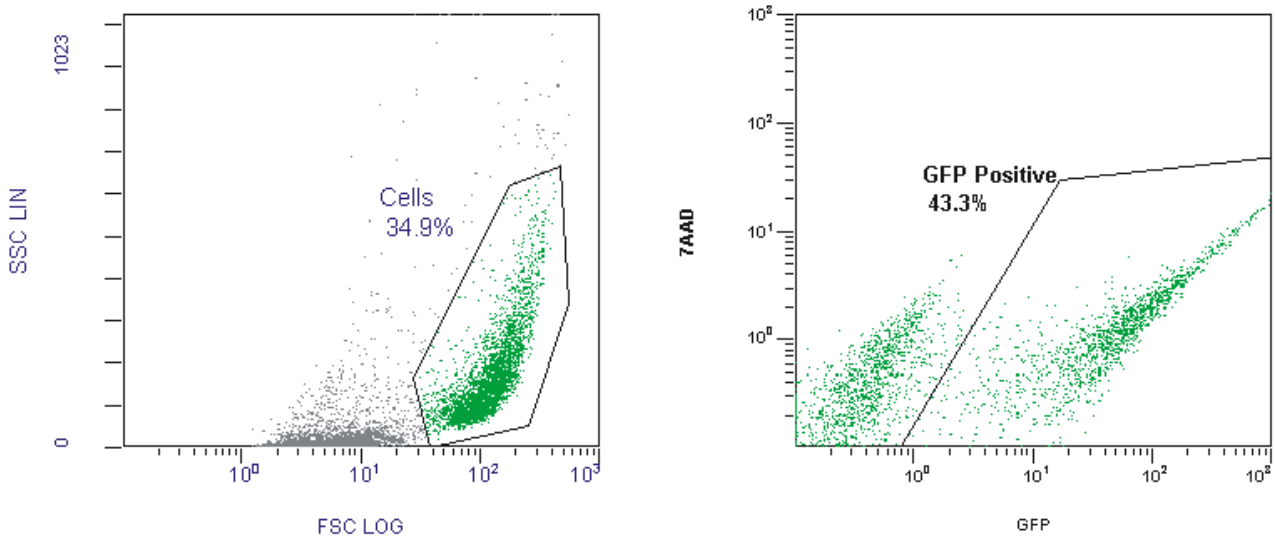

Figure: 2.2 Dot blot of forward and sideward scattering (A) with gated cells and of green fluorescence (B) with gated transfected cells that show green fluorescence because of expressed green fluorescent protein.

2.1.15 Sulforhodamine B (SRB) Toxicity assay

The Sulforhodamine B (SRB) toxicity assay is a colorimetric assay (Papazisis et al., 1997). Here living and still attached cells are coloured by the protein stain sulforhodamine B, while dead non-attached cells are washed away before staining.

Cells were grown in 24 well plates and treated with samples e.g. AVP according to standard transfection procedures. Media was carefully removed 24 h after treatment before the cells were fixed by an one hour incubation with 500 µl of a 10 % trichloroacetic acid (Merck) solution in the fridge. Afterwards cells were washed five times in purified water and dried overnight in a fridge.

The dried cells were stained with 300 µl of a 0.4 % (m/V) Sulforhodamine B (Fluka, Buchs, Switzerland) solution in 1 % acetic acid for 20 minutes and washed five times with 1 % acetic acid.

Finally the protein bound dye was dissolved in 1 ml of 10 mM Tris base and absorbtion was measured at a wavelength of 557 nm in a DU 640 Spectrophotometer (Beckman Coulter).

2.1.16 Confocal laser scanning microscopy

Confocal imaging was performed with the friendly help of Ina Lehmann. Cells grown on sterile cover slips were washed twice with phosphate buffered saline (PBS) and fixed for 10 minutes in a 3.7 % formaldehyde solution. After fixation they were washed again with PBS

and finally embedded in mowiol 4-88 (Calbiochem, Bad Soden, Germany) containing n-propylgallate (Sigma) as antifading reagent and fixed to microscopic slides.
The fixed slides were examined on a LSM 510 inverted confocal laser scanning microscope (Carl Zeiss AG, Jena, Germany) in z-stacks of 0.39 µm.

2.1.17 DNA quantitation with Picogreen ® and modifications to decomplex DNA from PEI-DNA or AVP samples

In samples with pure highly concentrated DNA, DNA content can be measured by UV-absorbance at 260 nm (A_{260}). For samples with low DNA content Picogreen® (Invitrogen, Carlsbad, USA), a specific fluorescent probe for detection of double stranded DNA was used. Together with DNA it forms a highly fluorescent product that was detected using a Fluostar Optima plate reader (BMG Labtech Offenburg, Germany) (excitation 485 nm, emission 520 nm).
DNA in AVP is condensed with PEI and therefore not accessible to the fluorescent probe. To de-complex AVP and PEI-DNA samples, pH was raised to decrease the number of protonated N of the polyethylenimine and thereby its positive charge. This procedure was adapted from a procedure published by Moret et al (Moret et al., 2001).
3 µl sample were added to 100 µl Hepes buffer pH 11.6. 100 µl of Picogreen® diluted in a ratio of 1 : 200 in Hepes buffer pH 11.6 were added. After mixing by pipetting the fluorescence was measured. Samples were measured in triplicate. The contained DNA was calculated from a standard curve of AVP measured in duplicate on the same plate and parallel to the samples.

2.2 Buffer and Solvents

Buffer

Tris buffer 10 mM

Trizma® Pre-set crystals pH 7.4 (Sigma-aldrich)	1.516 g
Purified water (Direct-Q® S, Millipore, Billerica, USA)	to 1000 ml

If necessary, pH was adjusted to 7.4 using a pH Meter 761 Calimatic (Knick, Berlin, Germany) with an Inlab 423 electrode (Mettler Toledo, Giessen, Germany). Buffer was sterile

filtered using Sterifix 0.2 µm filters (Braun Melsungen AG) and aliquoted under laminar air flow conditions.

Phosphate buffered saline (PBS)

10 X concentrate:

di-Sodium hydrogen phosphate dihydrate (Merck)	14.6 g
Potassium dihydrogen phosphate (Merck)	2.0 g
Sodium chloride (AppliChem, Darmstadt, Germany)	80 g
Potassium chloride (Merck)	2.0 g
Purified water	to 1000 ml

The buffer concentrate was autoclaved. Before use the concentrate was diluted using purified water, pH was adjusted to 7.3 to 7.4 and the buffer was autoclaved again.

Tris-acetate-EDTA buffer (TAE buffer)

50 X concentrate

Tris base (ICN Biomedical Inc, Aurora, USA)	24.2 g
Acetic acid (100 %) (Merck)	5.71 ml
EDTA (Sigma-aldrich)	3.725 g
Purified water	To 100 ml

Before use the 50 fold concentrate was diluted using purified water, resulting in pH 8 to 8.5.

Hepes buffer 0.05 mol pH 11.6

Hepes (Biowest, Miami, USA)	520.6 mg
Sodium chloride (AppliChem, Darmstadt, Germany)	644 mg
Purified water	to 100 ml

After preparation pH was adjusted to 11.6.

Solvents:

Chloroform (p.A.)	Merck
DMSO	Sigma
Ethanol (p.A)	Merck
Formaldehyde 37 %	Carl-Roth
Methanol (p.A)	Merck

3. Results and Discussion

3.1 Characterization of AVP structure and structure activity relations

3.1.1 AVP characterization by Dynamic Light Scattering and Zetapotential measurements

AVP and their components are colloidal particles in the nano-range of less than 1 µm and thereby can not be detected by particle sizing methods intended for macroscale particles such as sedimentation or sieving techniques. Therefore, dynamic light scattering (DLS) also called photon correlation spectroscopy (PCS) was used. This resulting Z-average is a calculated hydrodynamic diameter that describes the average size of particles and the polydispersity index (PDI) specifies particle size distribution breadth (see chapter 2.1.4). Additionally, zeta potential, characterising surface charge of the investigated particles was measured. (See chapter 2.1.5 for details).

	Z.average [nm]	PDI	Zetapotential [mV]
PEI-DNA	103 (+/- 0.954)	0.227 (+/- 0.002)	+ 36.8 (+/- 2.9)
Liposomes (AVEact)	88.7 (+/-0.693)	0.087 (+/- 0.019)	- 67.3 (+/- 1.2)
AVP (AVPact)	118 (+/- 0.738)	0.175 (+/- 0.014)	+ 46.0 (+/-1.23)

Table 3.1: Size and Zetapotential of AVP and their educts

The final AVP are prepared from two components, pre-complexed PEI-DNA and AVE liposomes. As seen in Table 3.1 their properties differed greatly.

PEI-DNA complexes are derived from a self aggregation process of negatively charged DNA and a surplus of positively charged PEI. Measurements showed particles of about 100 nm with a broad particle size distribution (PDI 0.227) and a positive (+ 36.8 mV) zeta potential.

AVE liposomes are derived from a lipid film hydration followed by an extrusion through a 50 nm membrane. Here measurements showed small defined particles of about 90 nm with a

very narrow size distribution (PDI 0.087). The liposomes were charged negatively (- 67.3 mV), which can be explained by their component phosphatidylserine. Here the carboxylic acid of serine led to a negative charge.

The AVP, as a combination of positively charged PEI-DNA complexes and negatively charged AVE liposomes, showed a Z-average of about 120 nm, and a moderate particle size distribution (PDI 0.175). Their zetapotential was positive (+ 46 mV) and even slightly higher than that of the PEI/DNA complexes, which is consistent with the observations made in earlier experiments on AVP (Bucké, 2001).

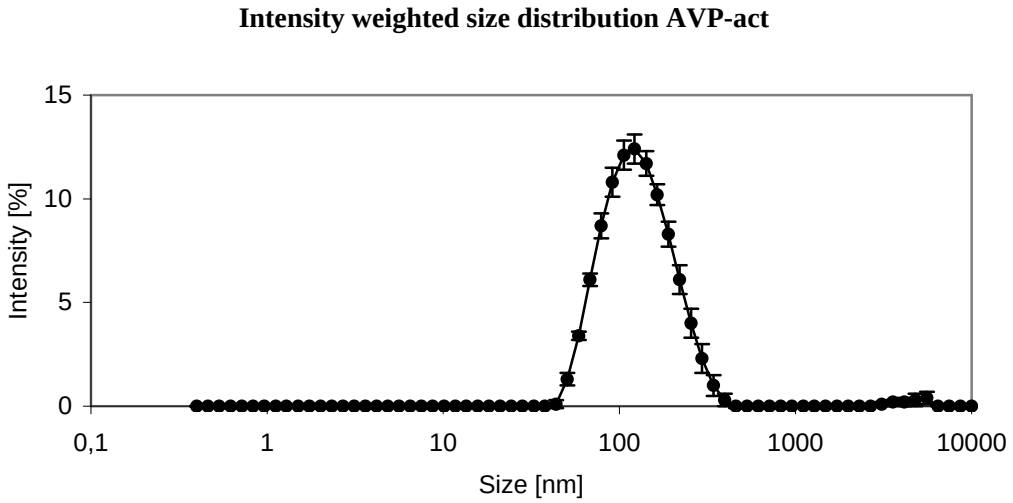

Figure 3.1: Graphical depiction of intensity weighted size distribution of AVP-act

A graphical depiction of their intensity weighted size distribution showed a main peak between 100 and 200 nm and also a small peak in the area of 3000 to 6000 nm, sign of bigger aggregates that are beyond the operational range of the PCS.

Summary:

Size of AVP and its components was in the nano-range of particles and below 300 nm as described before (Muller et al., 2001; Nahde et al., 2001; A.Fahr and K.Müller, 2001; Bucké, 2001). Zetapotential of PEI derived AVP was positive, which is consistent with the results of Sabine Bucké but interferes with the hypothesis, that AVP consist exclusively of particles covered by anionic liposomes (Muller et al., 2001).

3.1.2 Structure of AVP in transmission electron microscopy

To characterize the structure of AVP beyond estimating particle size by photon correlation spectroscopy, electron microscopy was used, as particle size is below the limits of visualization in light microscopy. In light microscopy a sample can be examined nearly without initial arrangements. But in electron microscopy the sample has to undergo special preparation before examination. Different sample preparation techniques lead to different perspectives on the same sample and can also alter the sample. As each technique has its individual advantages and disadvantages a combination of different preparations leads to the most subjective view and judgement.

Negative staining

For negative staining preparation the sample is embedded in electron dense uranyl acetate. So the embedded sample displaces some uranyl acetate, leading to lower interaction with the electron beam at its location and consequently to a picture with good contrast.

A **B**

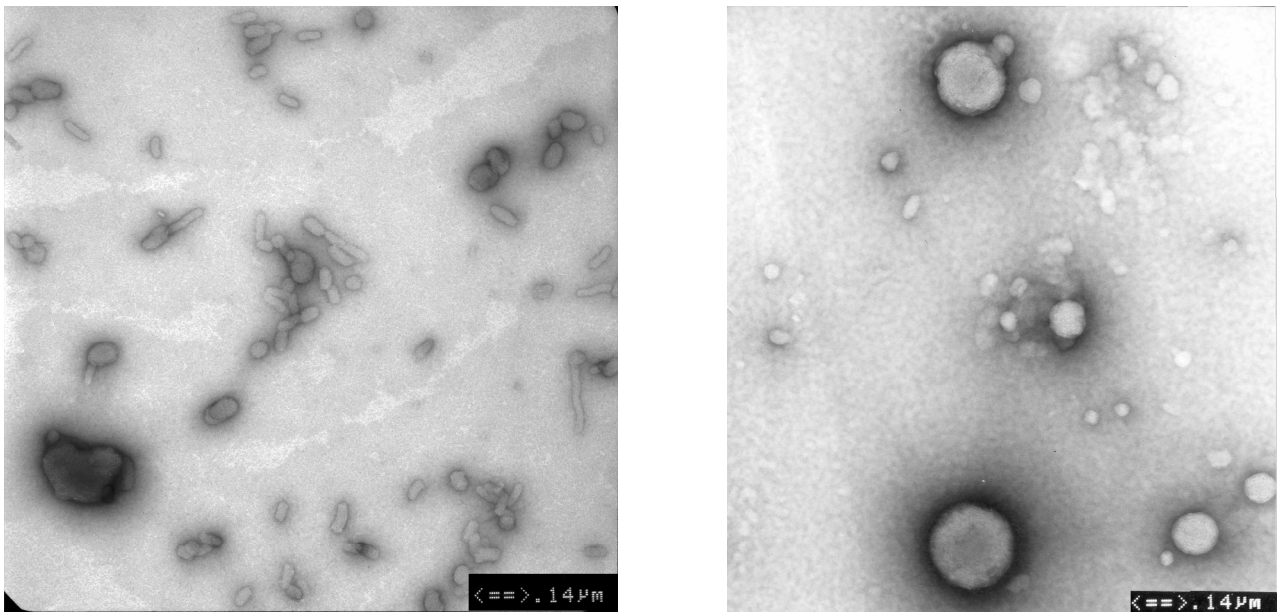

Figure 3.2: TEM pictures of PEI-DNA complexes (A) and AVP (B) after negative staining.

The core of AVP - the PEI-DNA complexes - were characterized by negative staining (figure 3.2 A). In these studies round, oval and zylindric particles sized in a range of 40 to 100 nm could be seen and confirmed the results of the size measurements in PCS (see chapter 3.1.1). The observed defined round to oval structures are consistent with the spherical complexes

seen by Pollard et al. (Pollard et al., 1998) in negative stained PEI-DNA complexes with an excess of PEI. Free sticking out filamentous DNA as seen by Pollard et al. in PEI-DNA samples with incomplete condensation or in DNA-poly-L-lysin complexes by Gershon et al. (Gershon et al., 1993) was not found. So electron microscopy confirms that the DNA in the DNA-PEI complexes used as basis for AVP is completely complexed as expected and shown by dye exclusion before (Muller et al., 2001). Despite those defined small particles also bigger aggregates could be identified in lower magnifications (not shown).

The final AVP, derived from the PEI-DNA complexes combined with liposomes, are expected to be more sensitive to the hygroscopic properties of uranyl acetate because of their content of liposomes that are sensitive to osmotic dehydration. This could lead to artefacts. Therefore, the results have to be regarded with care and compared to the results from other preparation techniques.

The examination of an AVP sample after negative staining (figure 3.2 B) showed a mixture of round particles in the range of 100 to 200 nm that appeared solid and structured and can be assigned to the expected filled particles. Additionally smaller particles similar to those seen in the examination of pure PEI-DNA complexes (figure 3.2 A) were observed. According to our judgement those small particles are PEI-DNA condensates. They were partially distributed freely, partially attached to the bigger round particles and partially aggregated to bigger formations.

Freeze fracture:

Using the freeze fracture technique avoids possible uranyl acetate derived artefacts. After freeze fracture preparation a platinum replica of the surface of a freshly broken frozen sample is examined in electron microscopy. Hereby the three-dimensional structure of the nanoparticles can be visualized.

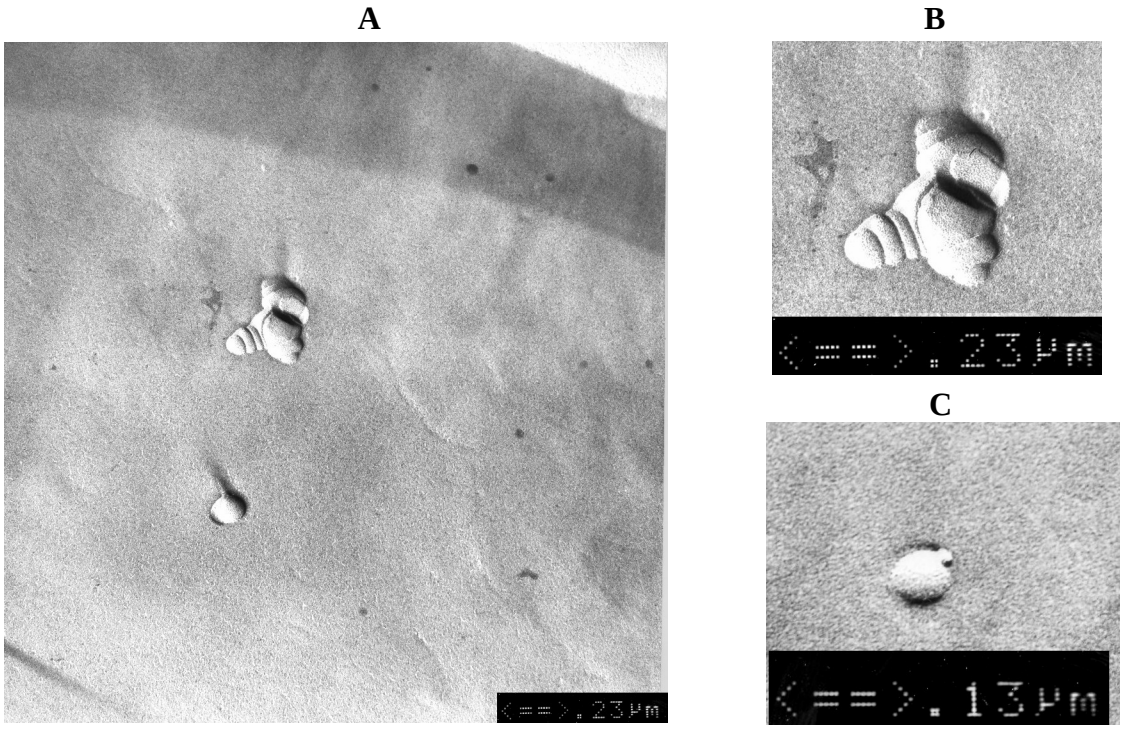

Figure 3.3: Freeze fracture preparation of AVP, overview (A) and takeouts of deformed aggregated particles (B) and small particles with wart-like attachments (C)

In freeze fracture preparations of AVP again defined round particles were found. In an overview (figure 3.3 A) small worm-like clusters of those particles can be seen next to free separated ones. In magnification (Figure 3.3 B) it becomes obvious that those clusters were composed of several small round particles. The innermost particles of those chains or clusters did not appear round, but deformed, as if squeezed by forces from the neighbouring particles. Those clusters show vague resemblance to lipoplexes of cationic liposomes and DNA examined in freeze fracture by Jääskeläinen et al. (Jaaskelainen et al., 1998). As only their round surface can be seen they could be filled AVP but also just empty liposomes. On some of the smooth appearing surfaces small wart-like attachments were found (figure 3.3 C). It can be hypothesized that they consist of free positively charged PEI-DNA complexes attached to the anionic liposome surface.

Besides those defined particles and small clusters of particles also huge aggregates of an amorphous mass with embedded liposomes were found (not shown).
In rare occasions ruptures through one of the round particle were seen. Here in magnification a structured interior became visible that indicates a filling inside of the complex particle. Other particles had part of their surface ripped away and showed an onion-like structure (for both see chapter 3.3.2 in the freeze fracture preparations of AVP from a static chipmixer)

Cryo TEM:

With Cryo-TEM the interior of the sample can be explored, as the electron beam passes through the particles and allows conclusion on the interior of particles. In Cryo-TEM examinations of AVP different structures already known from negative staining and freeze fracture were found again and thereby confirmed.

A **B**

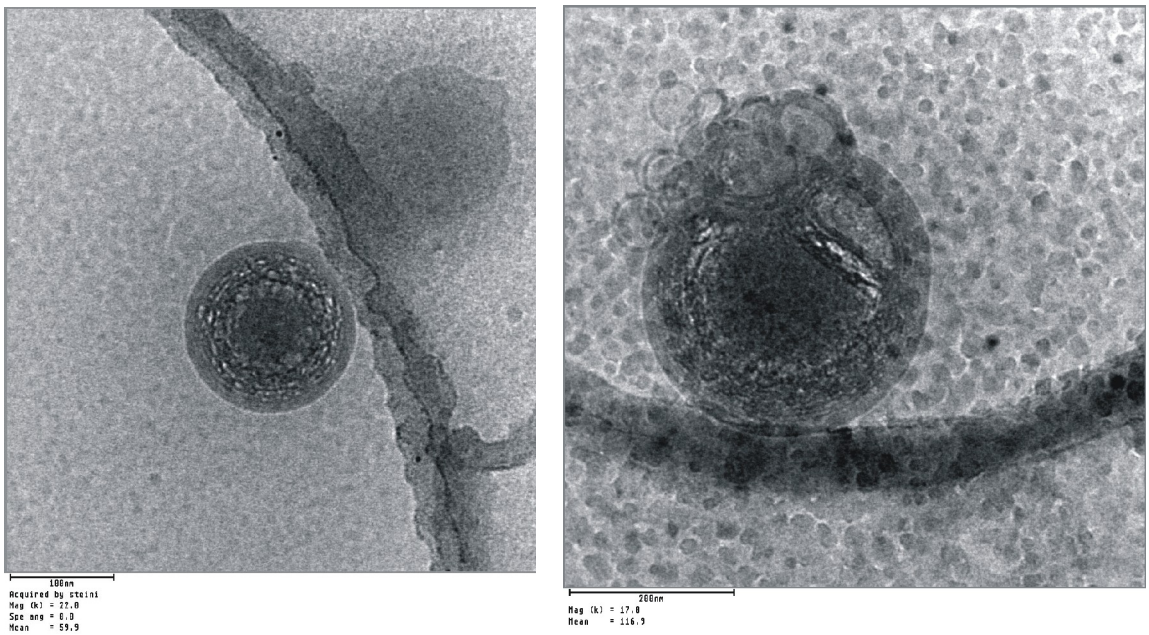

Figure 3.4: AVP in Cryo-TEM, particles appear filled with a smooth liposomal surface

AVP were found in their previously described (Muller et al., 2001; Nahde et al., 2001) form of filled particles. They appeared as particles defined by a smooth membrane and were completely or partially filled with dark material (figure 3.4 A, B). This filling material began to boil when exposed to the electron beam, thereby showing its sensitivity to the energy input from the electron beam. The whole sample consisted of DNA, polyethylenimine and liposomes in the embedding Tris buffer. The surface of the liposomes is charged negatively,

so the attached structures are likely to be positive charged. This supports the notion that the filling consists of either the cationic complexes of DNA and PEI or pure cationic PEI.
Besides the filled AVP also other structures already seen in freeze fracture could be found again.

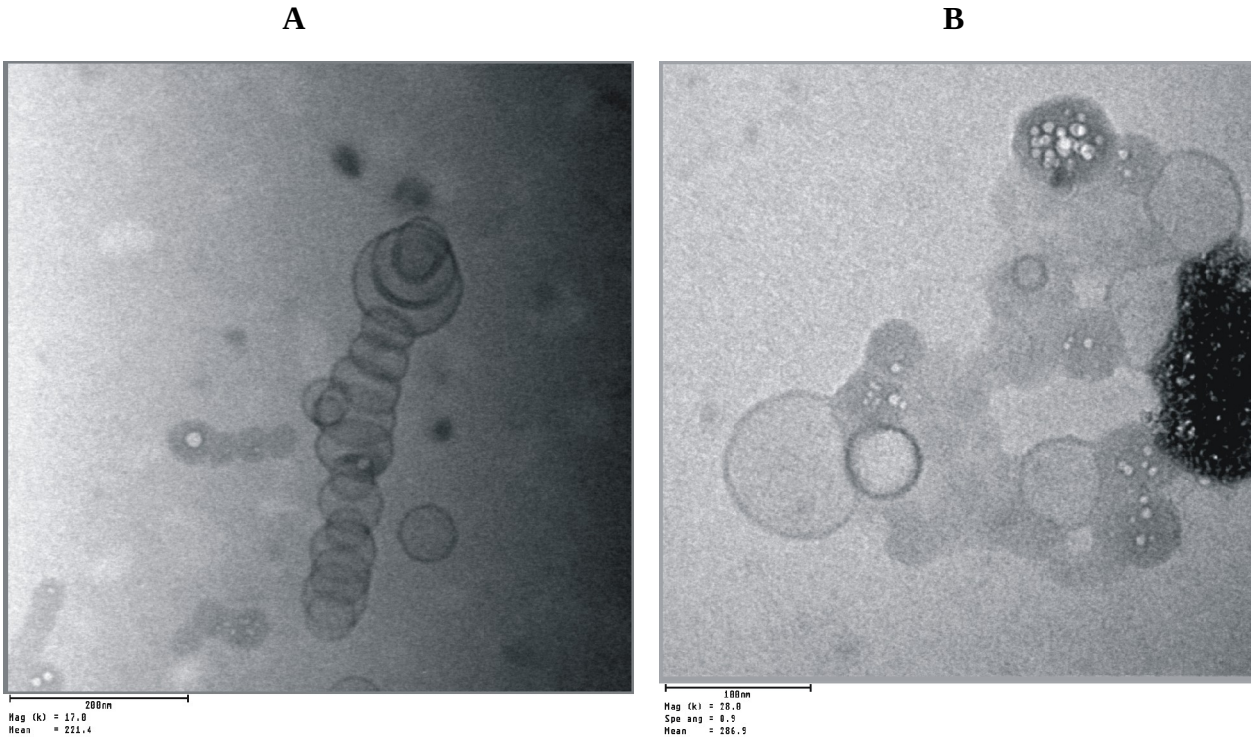

Figure 3.5: Cryo-TEM of AVP, Worm-like adhered empty liposomes (A) and mixed clusters (B)

The adhered structures consisting of round deformed particles that were already seen after freeze fracture preparation (see figure 3.3) appeared again (figure 3.5 A) in the form of worm-like structures. Cryo TEM revealed that they consist mainly of empty liposomes. Again these clusters showed resemblance to clusters of lipoplexes of cationic lipids with DNA, in this case examined in Cryo-TEM by Pitard et al. (Pitard et al., 1999).
Other aggregations consisting of small groups of clustered empty or partially filled liposomes, partially coated and glued together with compact material were found too (figure3.5 B). That coat appeared dark in Cryo-TEM and started to boil in the electron beam as seen before also for the filling in the AVP. In interpretation this coat can be attributed to PEI-DNA complexes

Mock AVP: Liposomes and PEI combined in the absence of DNA:

The examined AVP samples contained nothing but DNA, PEI and liposomes besides the embedding Tris buffer. Therefore, the filling observed in Cryo-TEM could either be DNA complexed by PEI, pure DNA or pure PEI.

To determine if the observed filled particles are a proof that AVP consist of liposomes with a filling of DNA complexed by PEI as the theory (Nahde et al., 2001) describes, a control experiment was performed.

PEI was mixed with anionic liposomes in the absence of DNA to produce mock AVP without DNA filling. Those mock particles consisting of liposomes and PEI in the absence of DNA were compared in Cryo-TEM to normal DNA containing AVP.

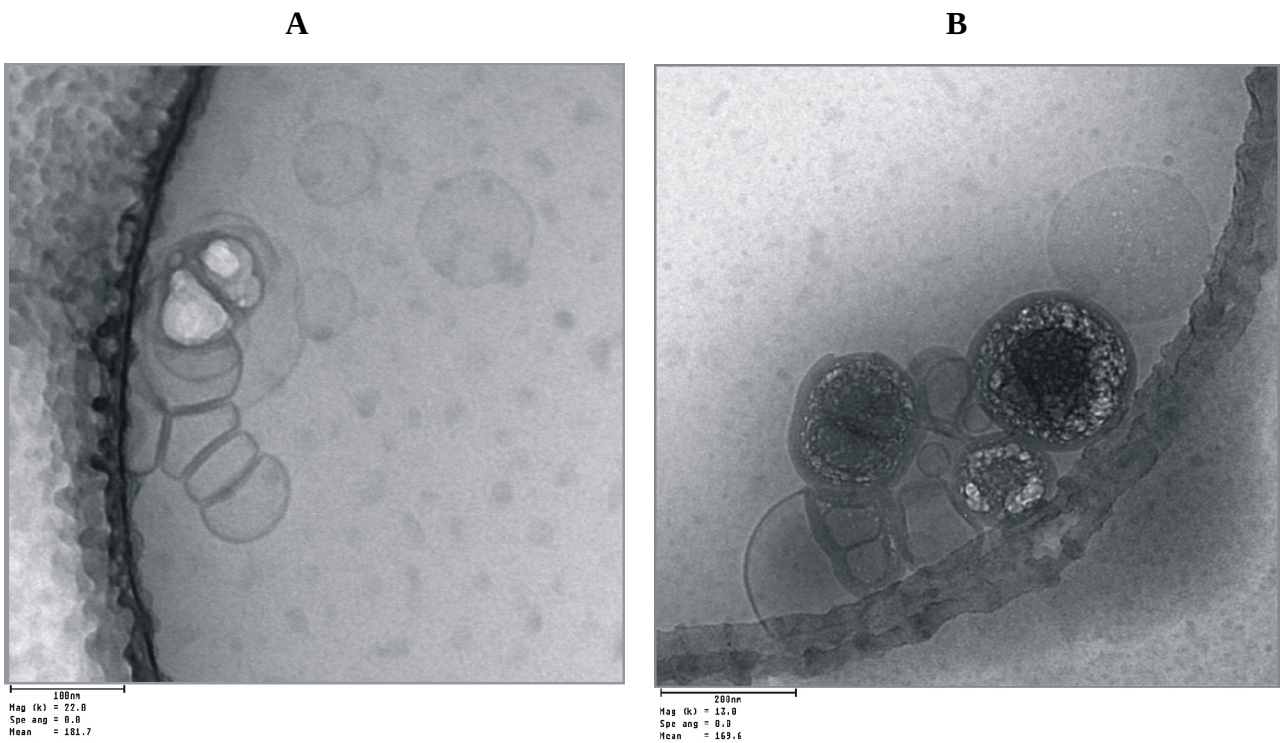

Figure 3.6: Cryo TEM of MOCK AVP, PEI combined with AVE liposomes in the absence of DNA

As expected, empty glued together liposomes (figure 3.6 A) and empty liposomes that seem to have a coat of PEI could be found. Surprisingly also particles with an outer liposomal membrane and a filling that started to boil when exposed to the electron beam were found (figure 3.6 B) that were similar to the previously observed AVP samples**.**

It was noticeable that the clusters of particles consisting of a mix of dark electron sensitive material and filled and empty liposomes that were seen in normal AVP samples (e.g. figure 3.5 B) could not be found in the MOCK sample.

Summary:

The insights won from PCS and different examinations in electron microscopy form a coherent picture and are consistent with previous descriptions (Bucké, 2001; Muller et al., 2001; Nahde et al., 2001; A.Fahr and K.Müller, 2001).

AVP contain particles defined by an outer liposomal membrane and an inner filling. The positive total zetapotential and the observed coat-like substance are hinting towards a surplus of the positively charged polymer PEI, the only positive reagent in the mixture, maybe attached to the surface. Besides those filled particles also empty liposomes and compact particles, interpreted as PEI-DNA complexes could be found. They appeared separately or joined together to differently sized aggregates. The sample containing mock AVP without DNA showed that particles appearing filled in electron microscopy can also derive from liposomes interacting with the cationic polymer PEI. So it can not be concluded doubtlessly that the DNA in AVP is contained exclusively in the filling.

3.1.3 AVP separation by Ultracentrifugation

Separation and characterization of sample fractions:

Electron microscopy examinations brought the realization that AVP do not consist of only one species of particles, but of a mix of differently sized constructs. Now the question arose which of those particles were the responsible ones for the successful transfection of cells.

Therefore, a separation of the mix of particles in an AVP sample into different species and a characterization of their physical properties was aimed at. Furthermore, the different fractions should be tested in transfection experiments in cell culture.

Size of the particles in the nanosphere range inhibited easy separation by normal centrifugation. So ultracentrifugation in a sucrose gradient was chosen as separation method. This system already showed its suitability to separate and purify gene transfer systems in the works of Bartsch et al. and of Gao et al. (Bartsch et al., 2004; Gao, Huang, 1996). It was used and optimized to separate different particle fractions contained in AVP (see chapter 2.1.8 for a detailed description).

In order to be able to detect the sample visually in the sucrose gradient AVE liposomes stained with the red lipophilic fluorescence dye DiI (see chapter 2.1.1) were used. This resulted in red stained AVP and therefore easy visual detection in the sucrose gradient.

The AVP sample was layered on top of the sucrose gradient and separated by forced sedimentation in the ultracentrifuge. After initial orientation experiments with different sucrose concentrations and ultracentrifugation parameters that turned out to be either too effective thereby leading to sedimentation of the complete sample to the bottom of the tube, or too weak to achieve a separation, parameters were found that allowed to separate the mixture.

A gradient of 0.5 ml 50 %, 1.5 ml 20 %, 1.25 ml 15 % and 1.25 ml 12.5 % sucrose solution was used to separate 0.5 ml AVP sample. After a 13.5 hour centrifugation at 40.000 rpm (rounds per minute) (corresponding to an average radial centrifugal force (RCF) of 151.693 g) a red coloured band appeared in the gradient. The fraction of the gradient that contained the red band and the bottom fraction were examined in PCS and by electron microscopy.

The fraction of the red band possessed a Z-average of 144 nm (+/- 3.11) and a zetapotential of + 57.4 (+/-3,2 mV), a narrow size particle size distribution (PDI of 0.130 (+/-0.032)). PCS measurements of the bottom fraction showed bigger particles (Z-average 219 nm +/- 27.4 nm) with a wide particle size distribution (PDI 0.339 +/- 0.036).

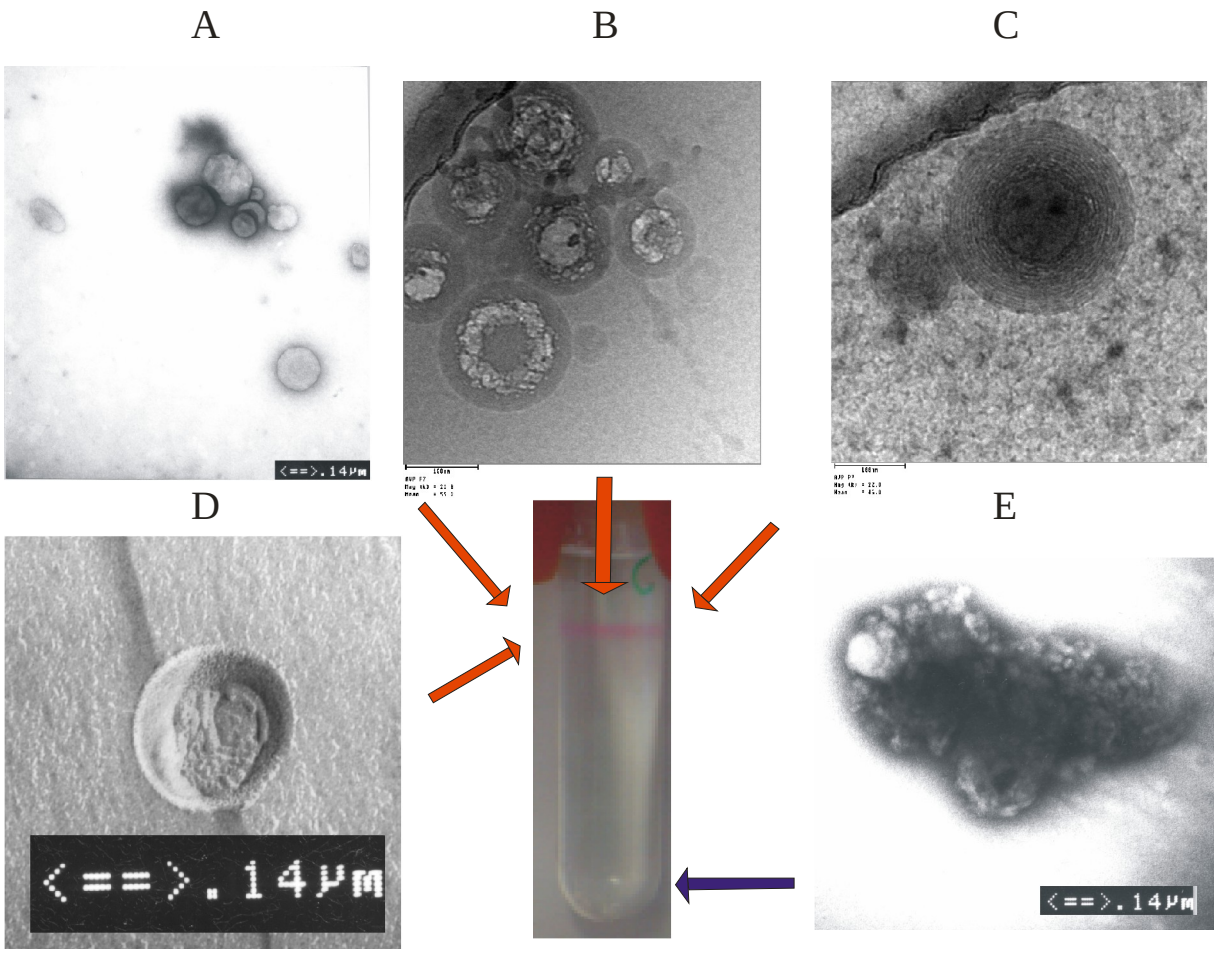

Figure 3.7: Band of red dyed AVP in the sucrose gradient after ultracentrifugation and its electron microscopic examination by negative staining (A), Cryo-TEM (B,C), freeze fracture (D) and a negative staining preparation of the bottom sediment (E)

In electron microscopy after negative staining the fraction of the red band showed solid appearing complex particles, besides empty liposomes as seen in figure 3.7 A. The bottom fraction showed large aggregates after negative staining as seen in figure 3.7 E. The defined particles of the fraction of the red band were visualized also in Cryo-TEM and appeared mainly as filled particles (figure 3.7 B; C). After freeze fracture of this fraction also defined particles were found. A part of them was even ruptured and showed an inner structure, indicating a filling (figure 3.7 D).

In summary the AVP sample was separated in large aggregates at the bottom of the tube and a fraction of small, well defined particles, partially appearing filled in electron microscopy.

Efficiency in cell culture:

The different fractions were also tested for their biological efficiency, their ability to transfect cells in cell culture. To be able to detect successful transfection, a plasmid coding for the green reporter protein EGFP was used as model DNA and expression of the protein monitored by flow cytometry (see chapter 2.1.14). But none of the fractions led to a display of the green reporter protein that would indicate transfection. Nevertheless, the cells treated with the fraction of the red band (derived from AVP marked with the red dye DiI) exhibited a shift towards red fluorescence showing that at least red dyed particles or liposomes got attached or were taken up by the cells.

This inability to transfect cells with the reporter plasmid was confirmed in repetitions. Also re-uniting the fraction of the red band and the bottom fraction did not lead to successful transfection. To exclude the possibility that the separation conditions were responsible for the loss of biological efficiency, an AVP sample was mixed with sucrose solution just as in the gradient and left over night at room temperature parallel to an ongoing ultracentrifugation separation. This control mixture of un-separated AVP mixed with sucrose solution was able to transfect cell though transfection efficiency was slightly lower (26.8 % transfected cells) compared to a freshly prepared AVP sample (40.13 % transfected cells).

Variation of centrifugation speed

As the general conditions were not responsible for the complete loss of biological efficiency, the separation conditions were varied further.

A shortening of the centrifugation time from 13 h to 2 h and finally to 1 h still resulted in the formation of a red band, similar to the one obtained after 13 h of centrifugation, but still no fraction was able to transfect.

Changing centrifugation time to 30 minutes and additionally centrifugation speed to 20.000 rpm (corresponding to average RCF 37.923 g) led to the formation of a red band that did not sediment deeply into the sucrose gradient, but accumulated at the border between sample layer and the beginning of the gradient with 12.5 % sucrose.

Characterization of this fraction in PCS resulted in a Z-average of 103 nm (+/- 0.64 nm) and a PDI of 0.111 (+/- 0.012) which did not differ much from the red particle containing fraction derived from a parallel centrifugation for 1 h at 40.000 rpm that showed a Z-average of 90.7 nm (+/-0.416) and a PDI of 0.113 (+/-0.019).

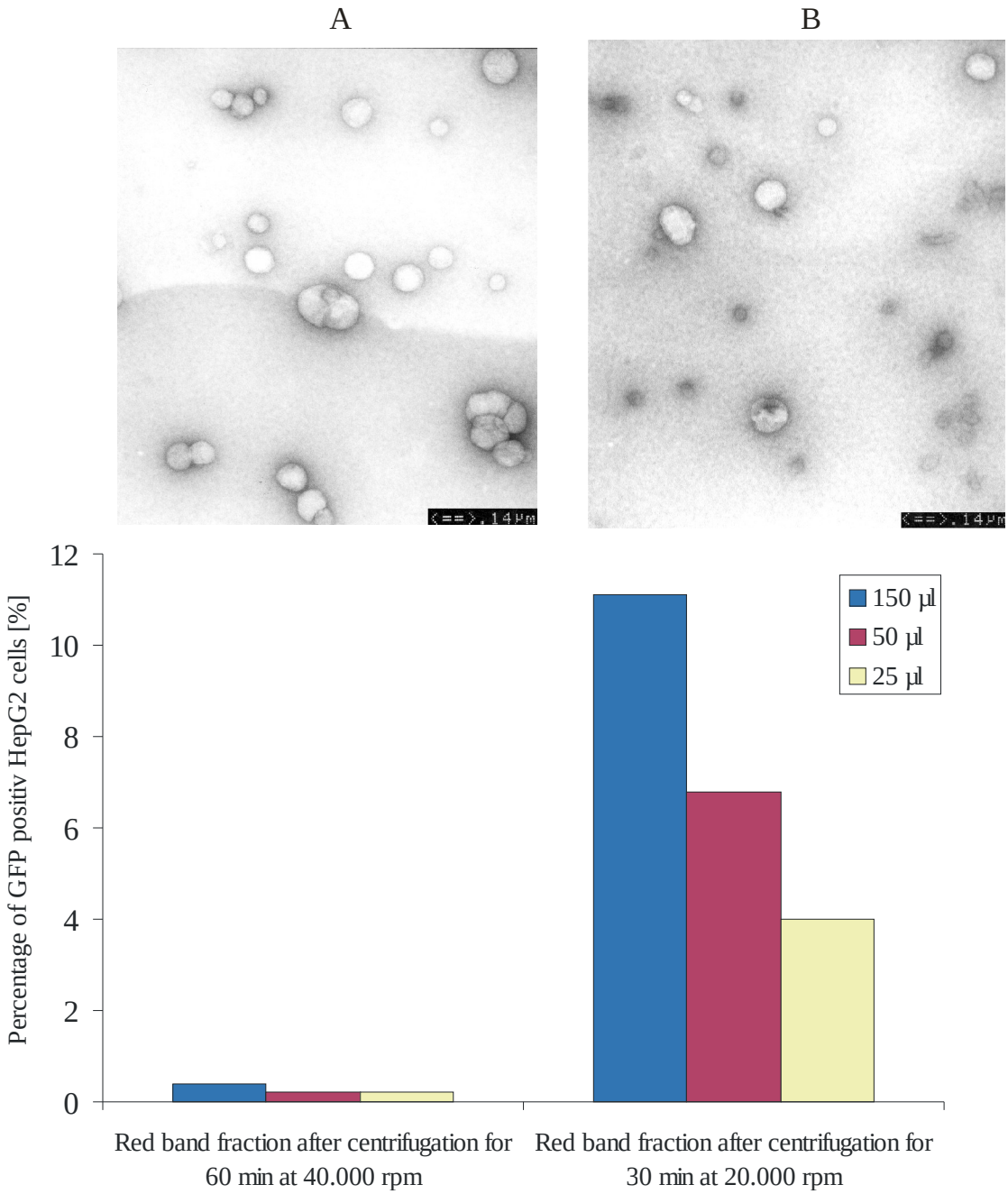

Figure 3.8: Dose dependent transfection success of red fraction of AVP separated by ultracentrifugation and corresponding electron microscopic visualisation after negative staining.

But in cell culture a huge difference became obvious. The particles of the fraction containing the red band resulting from the established centrifugation at 40.000 rpm again were not able to transfect cells. In contrast to that the particles of the red band resulting from the slower centrifugation were able to transfect cells in a dose dependant manner as seen in figure 3.8.
The differences between the fraction derived from slower centrifugation at 20.000 rpm (figure 3.8 B) that was able to transfect cells and the fraction derived from centrifugation at 40.000

rpm (figure 3.8 A) unable to transfect cells were investigated by electron microscopy after negative staining preparation. Here in both samples round defined particles, partially appearing solid could be found. They were similar to those seen already before in negative staining preparations of the red fraction after separated at 40.000 rpm (see figure 3.7 A). In the modestly centrifuged sample additionally smaller defined particles could be seen that looked similar to pure PEI-DNA complexes as examined after negative staining (see figure 3.2 A).

This differing ability to transfect cells depending on the centrifugation conditions was reproducible. A later control experiment showed that centrifugation at 20.000 rpm and unmodified centrifugation time 1 h also resulted in a fraction of particles able to transfect cells. So the critical parameter is rather centrifugation speed and derived from it force of centrifugation than duration.

Still, transfection efficiency of particles from the fraction derived from centrifugation was lower than that of the untreated fresh AVP mixture. This could be caused by efficiency lowering conditions as seen in the decrease of transfection efficiency of a sample stored overnight mixed with sucrose solution. But also an uneven distribution of free PEI in the gradient might play a role, as after a centrifugation of AVP derived from dyed PEI we observed the colour of the dye after the centrifugation mainly in the upper part of the centrifuge tube. Also adsorption of the AVP to the wall of the ultracentrifugation tube or to the teflon tubings of the pump, used to layer the AVP sample on the sucrose gradient, might have occurred.

Summary:

The AVP sample was successfully separated into small defined particles showing a filling in electron microscopy and big aggregates by ultracentrifugation in a sucrose gradient. The defined particles resulting from a centrifugation with strong forces were not able to transfect cells, while lowered centrifugation forces led to a fraction that was able to transfect cells *in vitro*. Electron microscopy of the successful fraction showed smaller particles that looked similar to the pure PEI-DNA complexes observed in figure 3.2 A additional to the big filled particles. As transfection efficiency of AVP is higher than that of the pure PEI-DNA complexes, the success of this fraction can not be derived only from the PEI-DNA complexes. Our results suggest that the mixture of those small free particles with the bigger AVP is essential for transfection success.

3.2 Tracking AVP into cells

3.2.1 Marking AVP with gold nanoparticles and tracing them with electron microscopy

Marking the plasmid with gold

The genetic material (DNA or RNA), representing the "drug" load of the AVP shows only low contrast to the electron beam. So it would be very hard to detect it in ultramicrotome slices from cells that contain a variety of intracellular organelles showing similar contrast in electron microscopy. Therefore, the genetic material was marked with gold nanoparticles that show high contrast to the electron beam. This marking allows tracing the particles on their way into cells, as demonstrated previously (Pitard et al., 1999; Zabner et al., 1995).

The procedure of marking the plasmid with gold nanoparticles via a streptavidin-biotin bond was adapted from the protocol of Zabner (Zabner et al., 1995) (see chapter 2.1.11 for details)

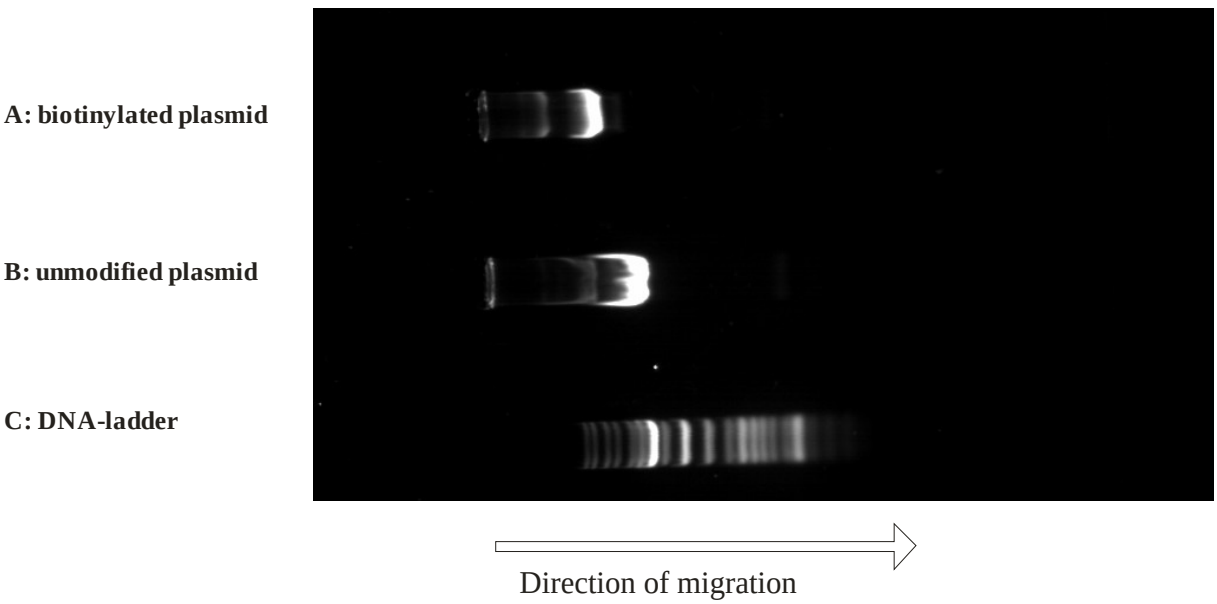

Figure 3.9 Gel electrophoresis of biotinylated plasmid (A), unmodified plasmid (B) and (C) a DNA ladder for comparision

A biotin link was attached to the plasmid via an azo reaction and the biotinylated plasmid purified by DNA precipitation. The biotinylated plasmid was compared to unbiotinylated plasmid in agarose gel electrophoresis. Here the biotinylated plasmid migrated slower than the unbiotinylated plasmid (figure 3.9). This sign of increased size is consistent with the enlargement of the plasmid as a consequence of successful attachment of biotin.

The plasmid was stored in this biotinylated form and marked with gold directly prior to use. Therefore, Streptavidin-gold nanoparticles (10 nm) were added to the biotin coupled plasmid. They formed the stable streptavidin-biotin complex and coupled thereby the gold nanoparticles to the biotinylated plasmid.

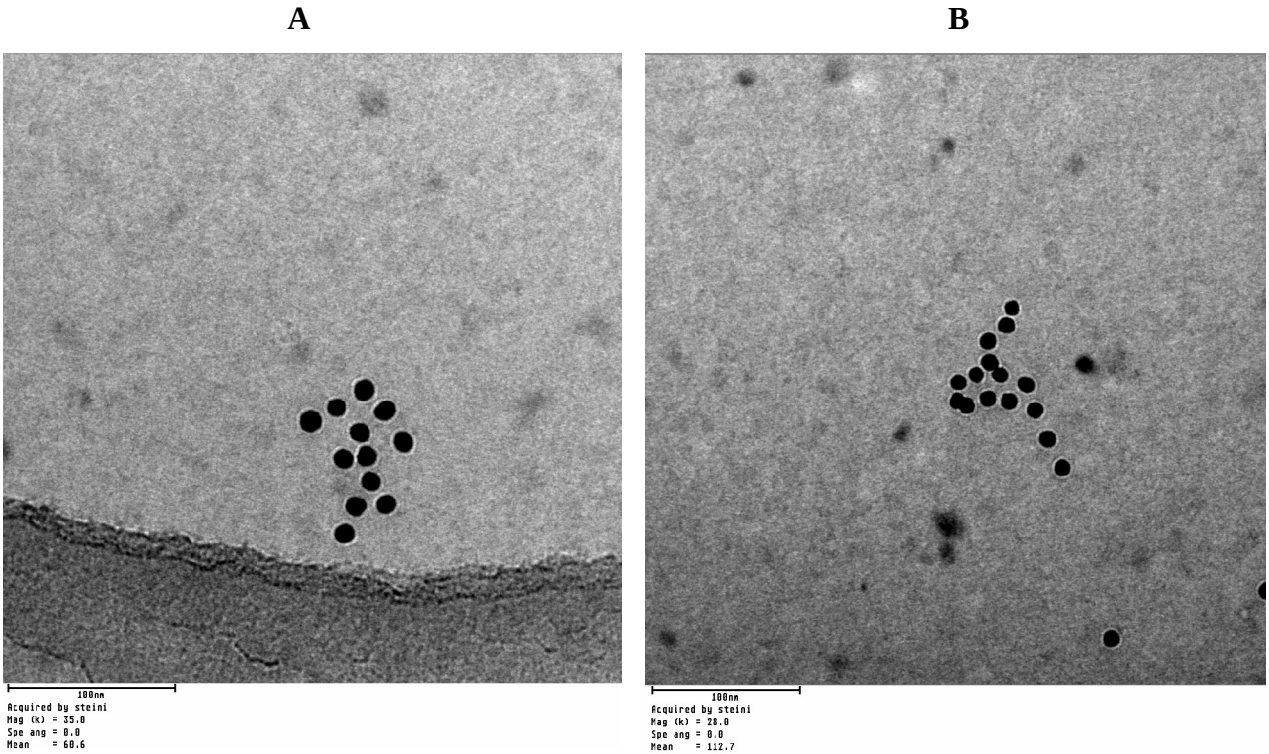

Figure 3.10 Gold-marked plasmid in Cryo-TEM. The plasmid is outlined by its marking with 10 nm gold nanoparticles

The marked plasmid was examined dispersed in Tris buffer in Cryo-TEM.
The plasmids themselves were still not detectable by the electron beam, but their outline could be traced by the 10 nm gold particles appearing as black dots because of their high contrast to the electron beam (figure 3.10).

Complexing the gold-marked plasmid with PEI

These gold-marked plasmids were processed further according to the standard AVP preparation method (see chapter 2.1.3) to PEI-DNA particles by complexation with the cationic polymer PEI.

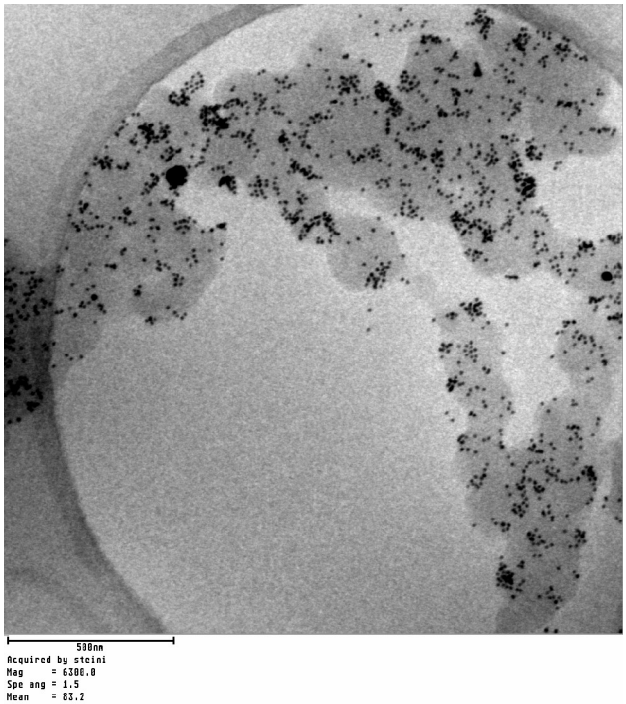

Figure 3.11: Gold-marked plasmid complexed with PEI

In Cryo-TEM these PEI-DNA particles clearly showed marking with gold nanoparticles (figure 3.11). But these gold-marked condensates were mainly aggregated to bigger particles. It seems that the gold-marked plasmid showed a larger tendency to form big aggregates with PEI than the untreated plasmid. Repetitions using different amounts of streptavidin-gold nanoparticles to mark the plasmid all led to the same aggregated particles.

Processing the gold-marked PEI-DNA complexes to AVP

Despite a higher tendency to form aggregates the gold-marked PEI-DNA complexes went through the final processing step with AVE liposomes to gold-marked AVP.

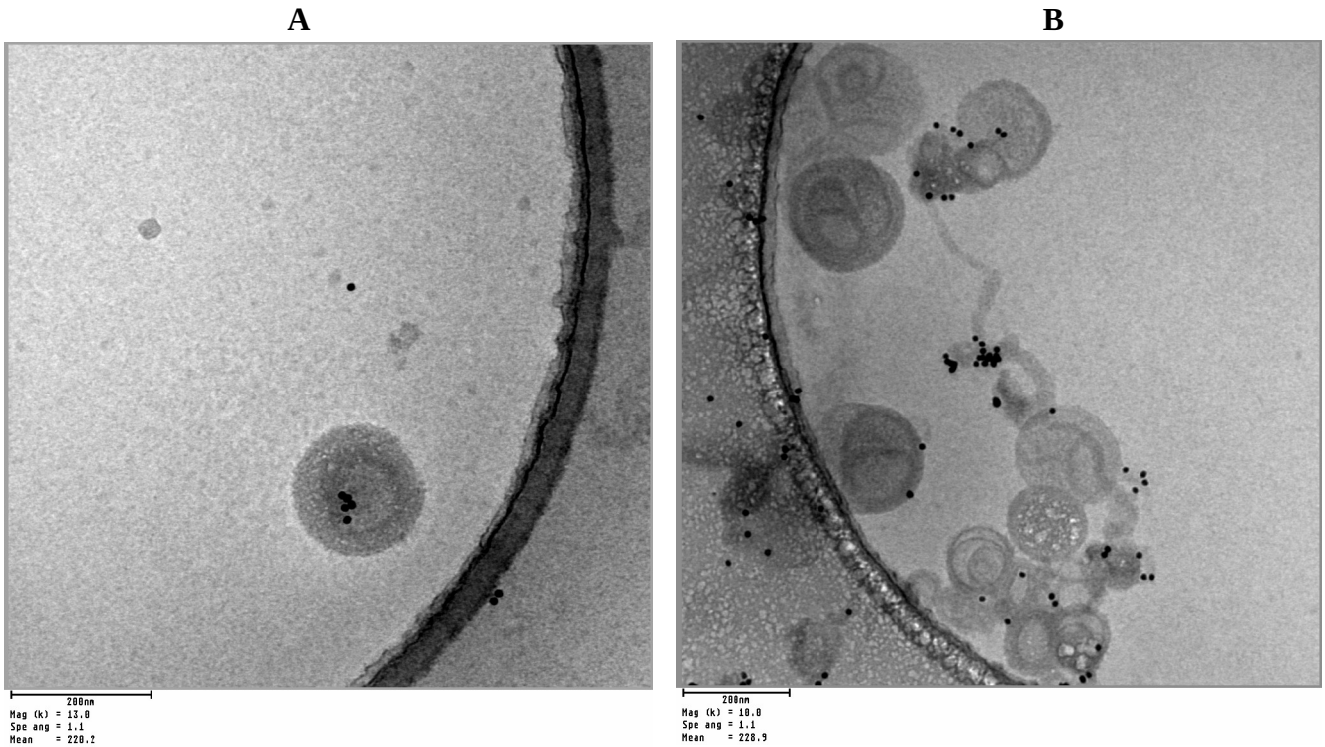

Figure 3.12: Gold-marked AVP in Cryo TEM. In A the 10 nm gold nanoparticles appear to be in the interior of the filled particle. In B the gold-marking is mainly distributed at its surface

Examination of those AVP containing gold-marked plasmids in Cryo-TEM showed particles with a gold-marking that appeared to be in the filling (figure 3.12 A) thereby complying with the concept of filled particles.

But the gold-marked DNA could also be on the outside of the liposome, facing the viewer. The majority of the observed particles showed a marking on the outside of the liposomal hull as seen in figure 3.12 B**.** This marking was mostly in the dark material between aggregated liposomes. So it can be concluded that the modified gold-marked plasmid is situated mainly at the outside of the AVP particle.

Tracing gold-marked plasmid into cells

Despite these artefacts, four µg of the just described gold-marked plasmid were processed to AVP and used to transfect a well (24 well plate) of HepG2 cells. 24 h after transfection, the living cells were fixed and stained with heavy metals for examination by electron microscopy in a co-operation with Dr. Oehring (see chapter 2.1.7 for details). After embedding in synthetic resin and hardening of the resin, the cells were cut into ultra-microtome slices (~70 nm thin). Examination of those slices in transmission electron microscopy showed gold-marked AVP in different stages of their way into and in the cell. For interpretation pictures were sorted into a logical chronological order:

Uptake

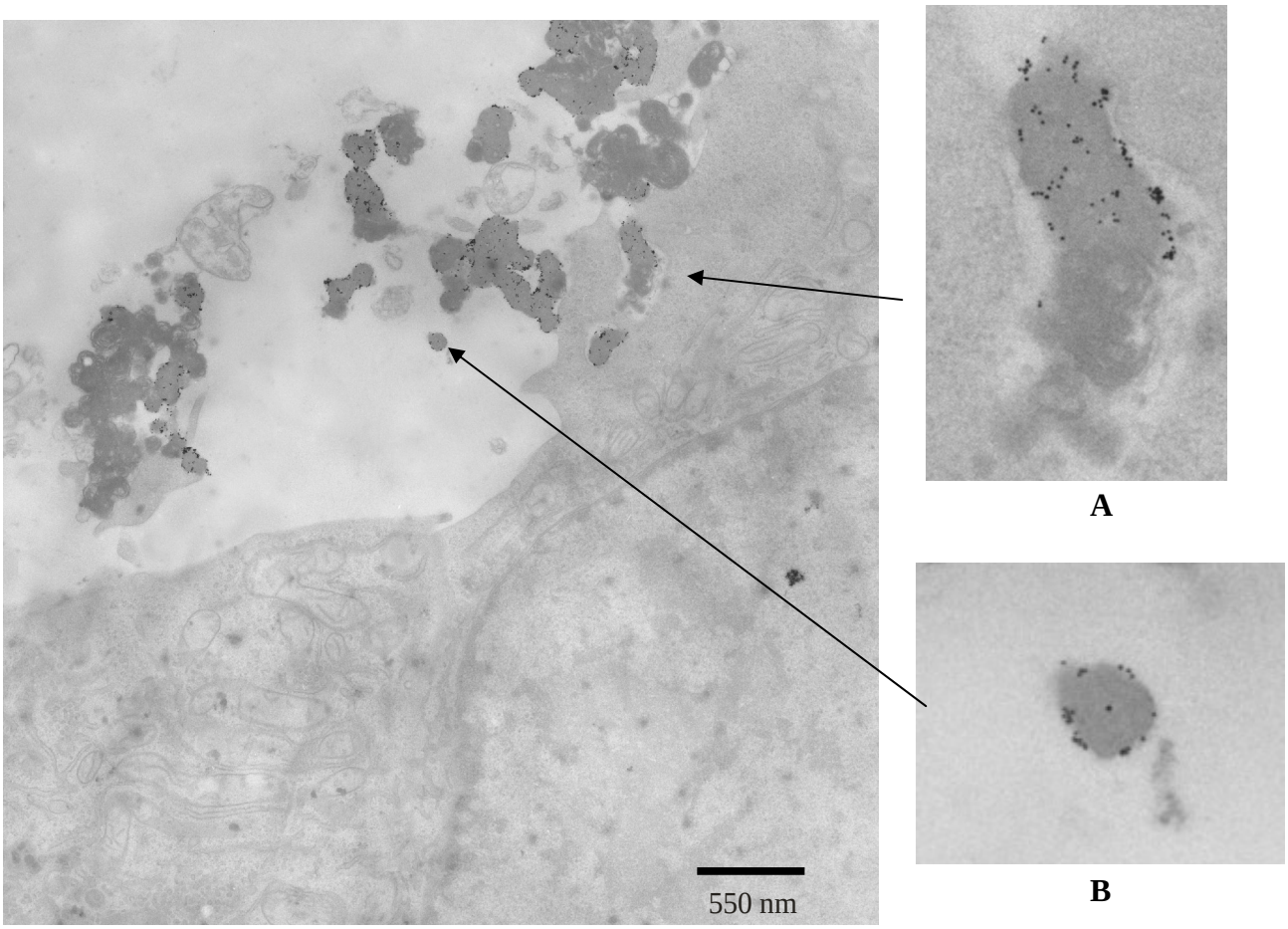

Figure 3.13: Uptake of gold-marked AVP into cells, gold-marked AVP can be found just taken up (close-up A) and still outside of the cell (B)

Firstly uptake of gold-marked AVP into the cell could be observed (figure 3.13). Here gold-marked AVP were seen on the outside of the cell next to the cell membrane and also in the process of being taken up by the cell in smaller or bigger clusters. Gold-marked AVP were

taken up in well defined, bordered structures, most likely endosomes. The close-up (figure 3.13 A) shows particles that have already been taken up and are clustered in an organelle separated from cytosol, while close-up B shows an extracellular unaggregated gold-marked AVP particle

Intracellular organelle

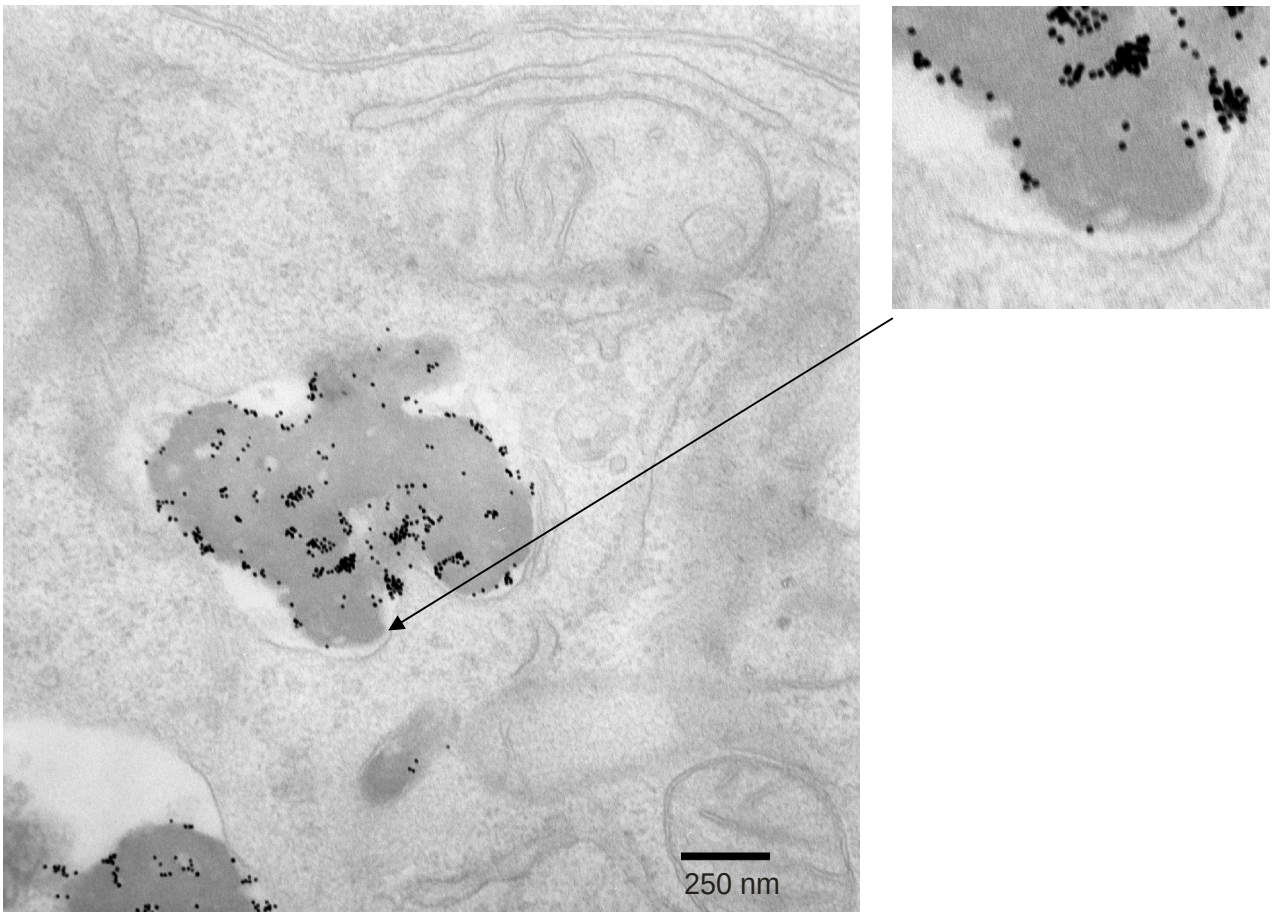

Figure 3.14 Gold-marked AVP in intracellular department. Close-up shows clear separation from neighbouring cytosol.

Those defined organelles containing bulks of AVP were also found deeper in the cell, still clearly separated from the cytosol as seen in figure 3.14. In close-up a clear separation of gold-marked AVP and cytosol and a separating membrane is visible.

Free in Cytosol I

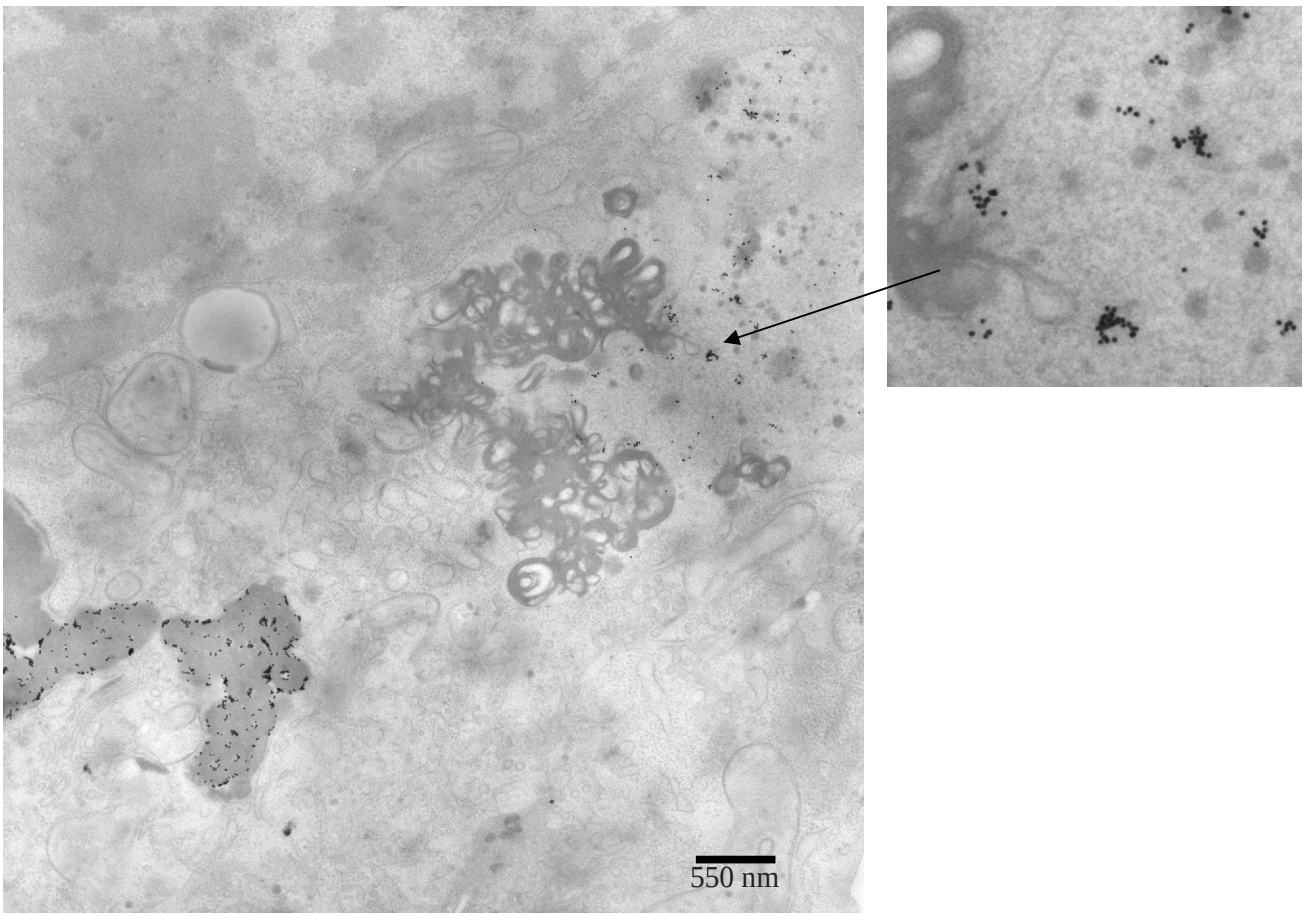

Figure 3.15 AVP still in cell organelle (left hand) and free in cytosol (right hand). Magnification shows free gold-marked AVP in cytosol next to a membrane-like structure

On the left hand of figure 3.15 AVP still clustered in an organelle could be seen, but on the right hand of the picture gold-marked particles spread freely in the cytosol without enclosing membrane were found. In magnification as well AVP marked with gold nanoparticles, as unmarked AVP and seemingly free marked plasmid could be found directly in cytosol. Interestingly those free particles appeared next to structures that looked like reformed membranes and are untypical for cells. Here in magnification a myelin-like appearing structure of membranes could be recognized.

Free in Cytosol II

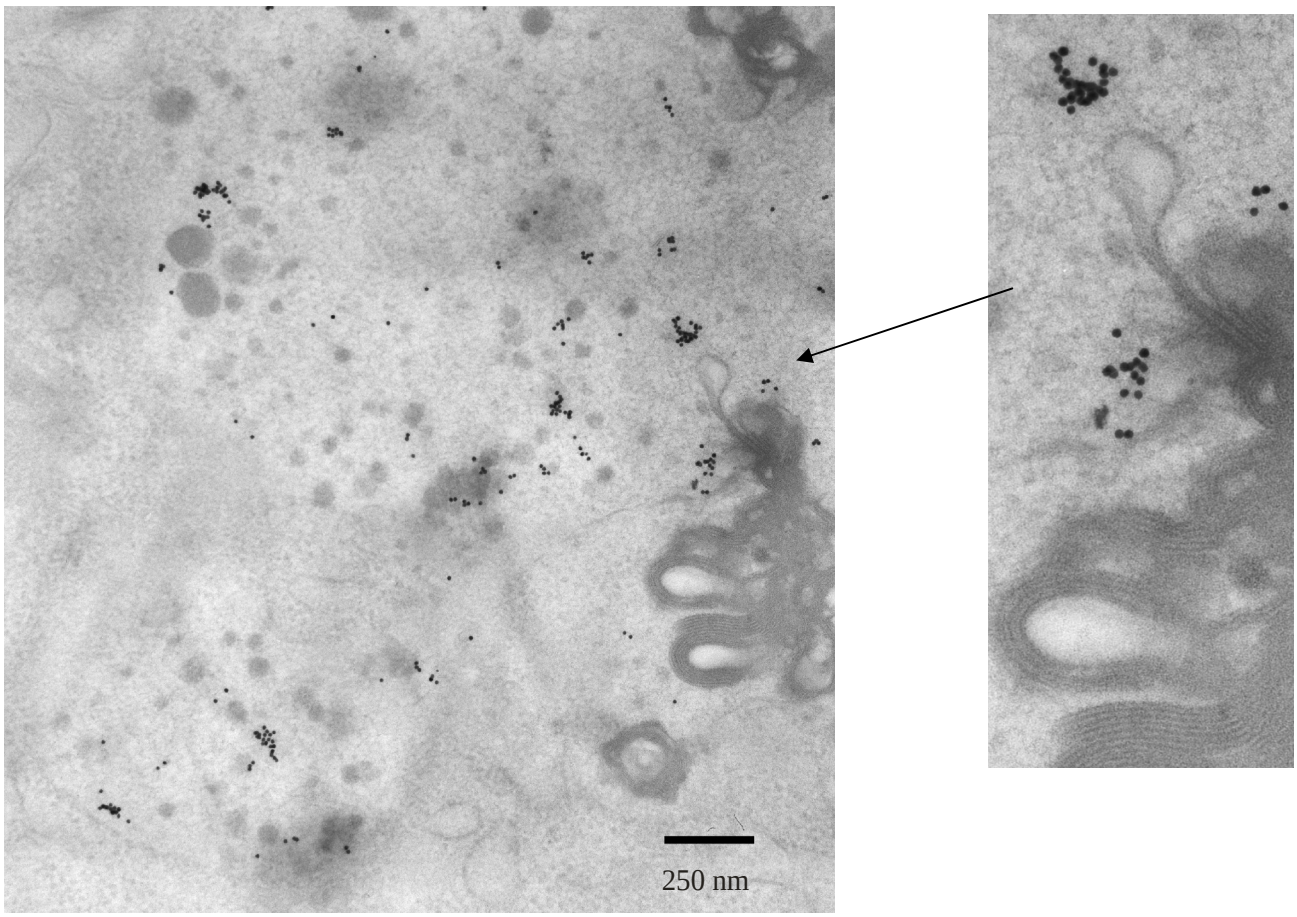

Figure 3.16 AVP with and without gold-marking free in cytosol next to membrane-like structures

In figure 3.16 a similar situation was found. AVP with and without gold-marking were spread freely in the cytosol, again close to the described membrane structures.

Near nuclear membrane

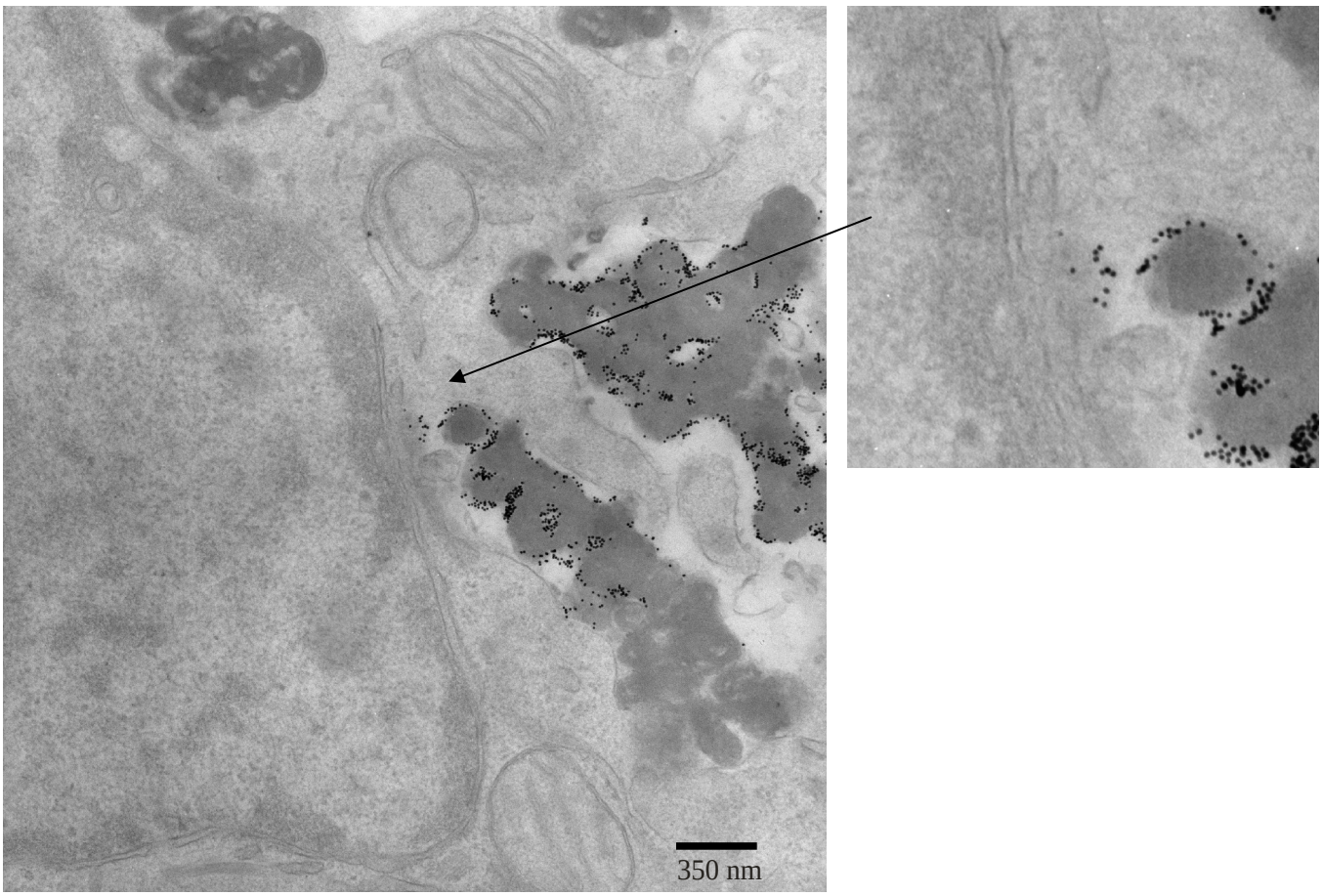

Figure 3.17 AVP near nuclear membrane. In magnification gold-marked AVP can be seen next to an abnormality in the nuclear membrane that might be a pore.

The drug plasmid finally has to get into the nucleus to be transcripted into mRNA and finally initiate the expression of foreign proteins. We did not detect gold-marked plasmid in the nucleus, but free gold-marked plasmid directly next to the nuclear membrane. In figure 3.17 gold-marked AVP can be seen next to the nuclear membrane. In magnification an anormality of the membrane was seen next to gold-marked plasmid that could be interpreted as a nuclear pore. It can be speculated that gold-marked plasmids can not pass the membrane in the way unmodified plasmid could, as they are sterically changed by the gold-marking itself as discussed earlier.

Summary:

The procedure of marking the plasmid with gold to visualize it in TEM succeeded and Cryo TEM showed gold nanoparticles outlining the marked plasmids. However, condensation of these gold-marked plasmids with PEI led to large aggregated PEI-DNA complexes that prove to be a suboptimal educt for the formation of AVP. Most of the gold-marked plasmid did not get included into the liposomes. It can be concluded that the modified marked plasmid derivate was not included into the liposomes. Conclusions on the inclusion of normal, unmarked plasmid can not be drawn from these investigations, as the plasmid was changed by the marking itself. Adding a construct of streptavidin, biotin, a linker chain and the goldparticles themselves sterically changes the normally easy to deform DNA string and could thereby lead to changed behaviour in the process of AVP preparation.

Despite this disadvantages the gold-marked AVP, even when modified by marking, turned out to be a valuable tool to track the way of AVP into the cell.

We observed that the gold-marked gene transfer vector AVP was taken up and present in the cell clustered together in intracellular organs, sharply separated from the cytosol. Those intracellular vesicles can be interpreted as endosomes in electron microscope pictures.

The appearance of the gold-marked vectors in the intracellular compartments is similar to the results of Zabner et al.(Zabner et al., 1995) who traced a gold-marked gene transfer vector based on cationic lipids into African green monkey kidney COS-1 cells. Also Kettering et al. (Kettering et al., 2007) who followed the way of magnetic nanoparticles into the ductal breast carcinoma cell line BT-474 obtained similar pictures. Both of them identified these intracellular compartments as endosomes in TEM examinations of ultrathin cell slices.

In contrast to their results we also observed free gold-marked AVP in cytosol next to structures that look like the remnants of ripped apart membranes, and were not described by Zabner and Kettering. Those structures were found next to gold-marked AVP spread freely in cytosol in several photographs. In general AVP were not present widely distributed all over the cell. So it seems plausible that the membrane structures are the leftovers of destroyed endosomes that released the included gold-marked AVP into the cytosol.

This is in perfect agreement with the proton sponge theory for PEI postulated by Jean Paul Behr (Behr, 1997) and described by the same group already before (Boussif et al., 1995). This theory was strengthened for PEI by living cell confocal laser scanning microscopy examinations in the work of Merdan et al (Merdan et al., 2002). It explains the high transfection efficiency of PEI derived transfection vehicles by a proposed mechanism of

endosomal swelling caused by the buffering capacity of enclosed PEI, resulting in bursting endosomes and consequently liberation of the enclosed gene transfer vehicles into cytoplasma (see chapter 1.1).

Pitard et al (Pitard et al., 1999) followed a gold-marked gene transfer vector based on a cationic cholesterol derivate into human epithelial HeLa cells by TEM. He also described free gold-marked gene transfer vectors in the cytosol parallel to vector enclosed in intracytoplasmatic vesicles. He points out the possibility that tertiary amine groups contained in the used cationic cholesterol derivate have buffered pH in endosomes and thereby allowed endosomal escape.

Labat-Moleur (Labat-Moleur et al., 1996) used lipopolyamine to complex DNA and transfect several adherent cell lines with it. He also observed his unmarked vectors by characteristic patterns in TEM as well in endosomes as free in cytosol and sees the buffering abilities of free nitrogens in the polyamine as a possible explanation leading to endosomal release.

Our results are in agreement with the previously made observations regarding the uptake of other gene transfer vehicles. Furthermore, the finding of released gold-marked AVP, which contain PEI, strengthens the proton sponge theory for PEI on the base of electron microscopical examinations.

3.2.2 Tracing fluorescence marked AVP into the cell

Tracing AVP marked by DiI and Oregon Green after incubation for one hour

Parallel to tracing AVP by electron microscopy AVP were followed also by confocal laser scanning microscopy on their way into cells and on their stations in the cell. Here, not the plasmid was marked, but the components of the carrier: the liposomes and the PEI. Liposomes (AVE-act) were marked with a red lipophilic dye in the membrane. PEI molecular weight 25.000 g/mol was marked with green fluorescenting Oregon Green similar to a method used by Godbey et al (Godbey et al., 1999a) before.

In a first experiment AVP constructed of Oregon Green marked PEI and DiI stained liposomes (see chapter 2.1.1 and 2.1.2) were used to transfect HepG2 liver carcinoma cells, seeded on cover slips. Routine transfection procedure was followed but the amount of fluorescence marked transfection vector was doubled to obtain sufficient fluorescence. So 4 µg plasmid processed to double fluorescence marked AVP were applied per well. The cells were fixed and stained after 1 hour of incubation with AVP and examined in three-dimensional z-stacks with the friendly help of Ina Lehmann by confocal laser scanning microscopy.

A **B**

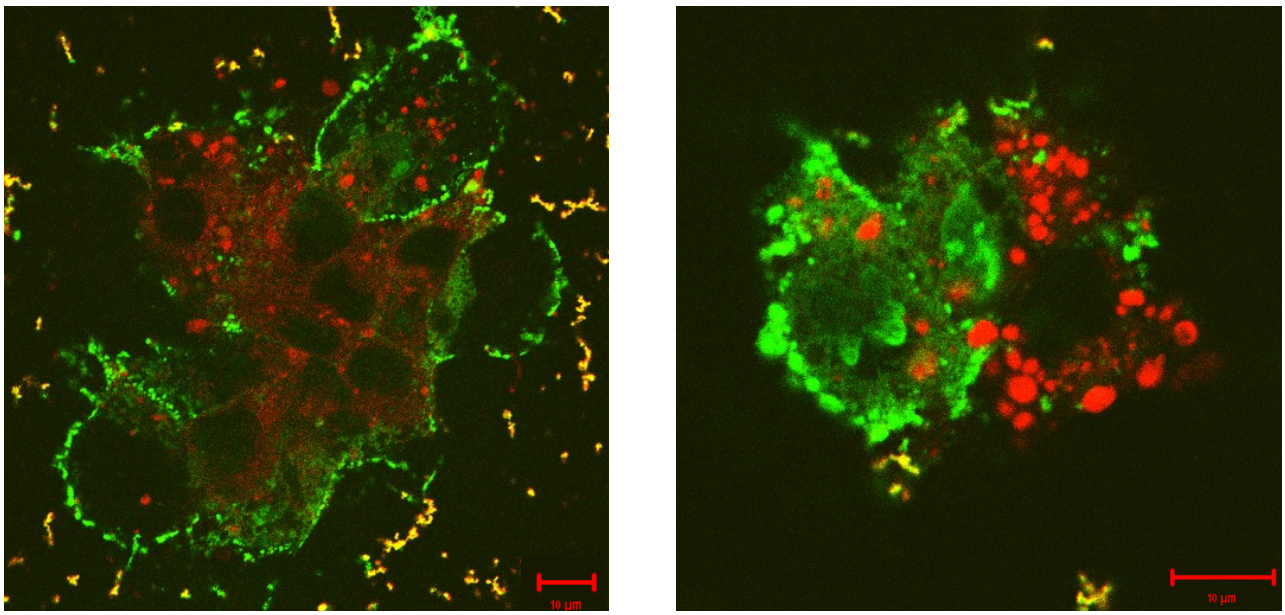

Figure 3.18 HepG2 cells transfected with double stained AVP (PEI=Oregon Green, liposomes=DiI red) after one hour of incubation. In A the optical plane cuts through a cluster of HepG2 cells, the left HepG2 cell in B is seen from above.

The AVP that were still outside of the cell were visible as small extracellular fluorescenting dots. They showed the green fluorescence of the marked PEI and the red fluorescence of the marked liposomes, resulting in yellow dots in the combined overlay pictures (figure 3.18).

Figure 3.18 A shows the fluorescence picture of an optical plain cut through the middle of a cluster of HepG2 cells. Here, at the surface of the cells and in the cells the red and green fluorescence were separated.. The red fluorescence of the DiI marked liposomes was found inside the cell already after 1 hour of incubation. It was accumulated in red stained vesicles and also distributed as red haze all over the cell.

In contrast to that the green fluorescence of the marked PEI was mainly located in particles attached to the cell surface that outlined the cell. Only few green dots at the interior of the cell, signs of taken up PEI, were found.

In a view on a cell from above (see left cell in figure 18 B), the layer of green marked PEI particles seemed like a coat on the surface of the cell. In optical cuts through the cell (see figure 18 A) it outlined the cell membrane in green.

This separation in two distinct fluorescences at the border of the cell was surprising. DiI is known to be a very lipophilic membrane marker, and is often used to stain liposomes. One explanation could be, that the DiI might switch from the membrane of the liposome to the cell membrane or cell and thereby falsely suggest uptake of the liposomes in advance of the PEIDNA core.

Six hour incubation with AVP marked by Rh-PE and Oregeon Green

Therefore, in the next setup the DiI was exchanged for another red marker, the membrane anchored Rhodamin-PE. After 6 h incubation with double marked AVP corresponding to a plasmid dose of 4 µg per well, a part of the cells was fixed after 1 hour as done before. Additionally another part of the cells was left to incubate for 6 h with the marked AVP before fixation.

A **B**

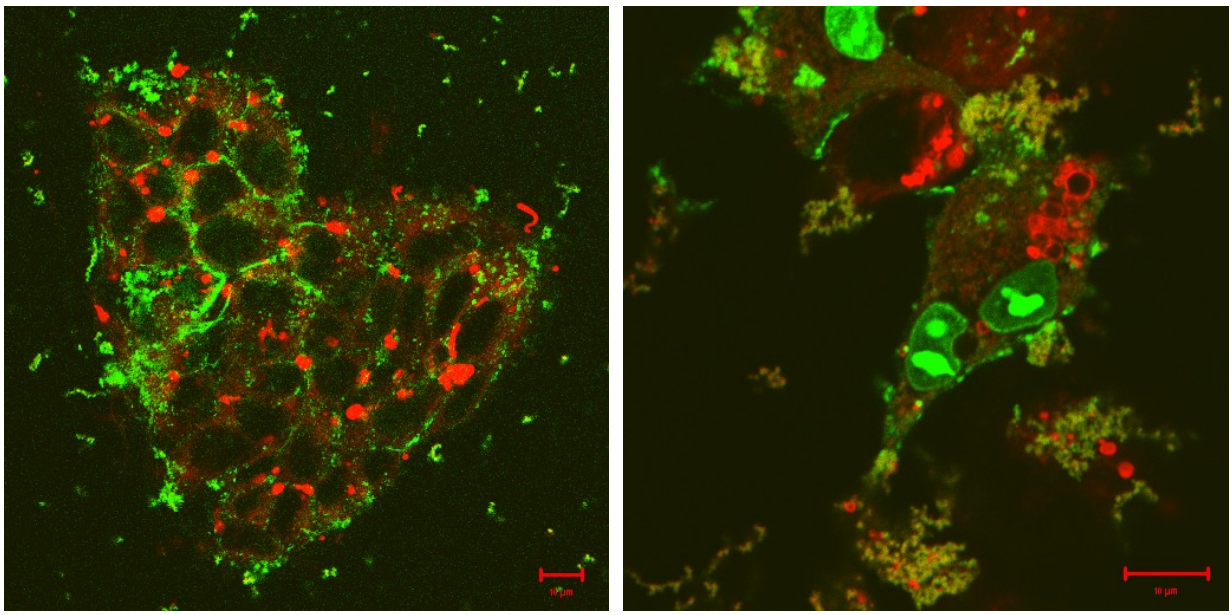

Figure 3.19 HepG2 fixed after 1 h (A) and 6 h (B) incubation with double marked AVP (PEI=Oregon Green, liposomes=Rhodamin PE red). After 6 h incubation the nuclei of cells appeared green stained.

The situation after 1 h as seen in figure 3.19 A was similar to the one seen when DiI was used as dye. Again red fluorescence was accumulated in round vesicles inside the cells. This time more green fluorescence in particles could be seen inside the cell, but the majority of the green fluorescent PEI derived particles was still sticking to the outside of the cells.

In the examination of cells fixed 6 h after transfection the picture changed from the previously seen. The red fluorescence was still located mainly in intracellular vesicles, but now some of the formerly dark appearing nuclei of the cell were fluorescenting green (figure 3.19 B). Also more green fluorescence was distributed all over the cell. But still a lot was sticking to the outside of the cells. This green staining of the nuclei demonstrated that after 6 hours the green stained PEI reached the nucleus, the target of the plasmid. Theoretically this newly appeared fluorescence could be caused by an early expression of EGFP, for which the used reporter

plasmid coded. Despite an unlikely strong expression of EGFP after 6 hours the experiment was repeated with a plasmid coding for the non-fluorescent luciferase instead of EGFP.

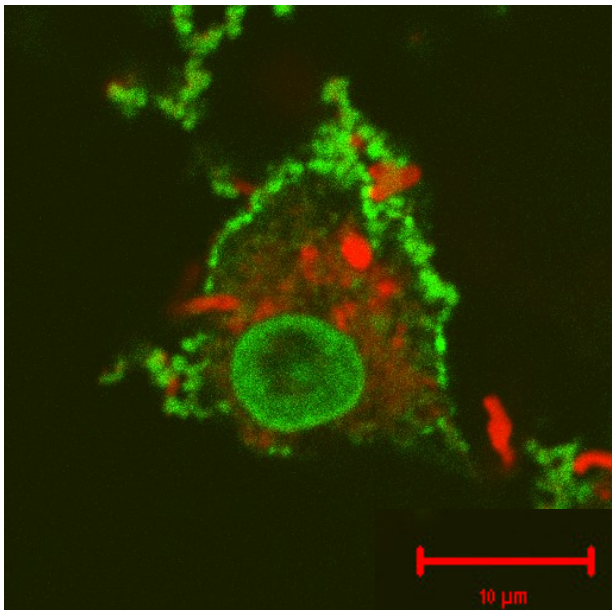

Figure 3.20 HepG2 cell with green stained nucleus after 6 h incubation with double marked (PEI=Oregon green, liposomes=Rhodamin PE red) AVP containing a plasmid coding for the non-fluorescent luciferase.

This resulted after 6 h incubation in a result similar to the one obtained using plasmid coding for EGFP. As seen in figure 3.20 again red fluorescence was located mainly in round vesicles inside the cell and green fluorescence was present in the nucleus of the cell and to a minor degree spread all over the cell. Bigger green particles were attached on the outer membrane of the cell.

Summary:

Confocal laser scanning microscopy showed that the PEI in AVP is able to reach the interior of the cell and the nucleus, where it accumulates. An observation which is in accordance with the findings of Godbey (Godbey et al., 1999a) and Merdan et al. (Merdan et al., 2002). Godbey tracked pure PEI-DNA complexes on their way into EA.hy 926 cells using fluorescence marked PEI and observed accumulation of particles at the outer membrane of cells at the beginning. After 3 hours he found PEI inside the nuclei of cells. Merdan et al used living cell laser scanning microscopy to track double fluorescence marked PEI-Ribozyme complexes live on their way into SW13 adrenal gland carcinoma cells. He observed initial

adherence of the marked complexes to cellular membranes within a few minutes, followed by a faint green fluorescence distributed all over the cell. Monitoring of the uptake process in living cells showed there bursting or rupturing endosomes / lysosomes filled with PEI derived complexes.

In our experiments the lipid part of AVP seemed to be separated from the PEI-DNA complexes when entering the cell and accumulated in vesicles. This gives room for several conclusions.

One obvious conclusion would be that the lipid or liposome part of AVP is not involved in the transfection process at all, but is bound and taken up independently of the PEI-DNA complexes. But as the AVP show a much higher transfection efficiency compared to pure PEI-DNA complexes and as modifying the AVE liposomes greatly influences transfection efficiency (seen chapter 3.4.2) this is unlikely. It might be that the free empty liposomes, which are contained in a normal AVP sample (see chapter 3.1.2) are taken up completely independently and thereby lead to the early appearance of intracellular red fluorescence.

Another more likely explanation would be that the complete AVP complex (liposome-PEI-DNA) is intact in dispersion, as also seen by the yellow colour of mixed fluorescence, but brakes up when reaching the cell membrane. This hypothesis would allow liposomes to play a role in binding and eventual uptake processes and PEI in endosomal escape processes. Another explanation could be a separation of the lipophilic dye and liposomes in contact with cells, leading to separate uptake as described for Rh-PE by Yan et al. (Yan et al., 2004)-

Welz et al traced protamine sulfate derived AVP that contained red marked liposomes and green marked oligonucleutides into HepG2 cells (Welz et al., 2000; Welz, 2000). He observed co-localization of fluorescence marked liposomes and oligonucleotides but only small intracellular fluorescence after 1 hour. Five hours after transfection they describe separation of liposomes and oligonucleotides and localization of oligonucleotides in the nucleus. So our studies on uptake and fate of polyethylenimine containing AVP are in general accordance with his results for protamine sulfate derived AVP.

In conclusion, tracking the PEI part of AVP showed uptake and intracellular behaviour well comparable to that observed before for pure PEI-DNA complexes. The results for fluorescence marked AVP are in accordance to the results of tracing the gold-marked plasmid in AVP into cells (see chapter 3.2.1). The role and fate of the liposomal component of AVP could not be clarified without doubt, but it seems to be taken up separately and prior to the PEI-DNA complexes.

3.3 Continuous production of AVP in a static mixer

3.3.1 Early mixers

In early preparations of AVP the role of the applied shear forces in the combination of the anionic liposomes with the cationic PEI-DNA condensates was not evident. Co-workers who worked on AVP production before gave the advice to use high shear forces as they were necessary for good particle formation according to their lab experience. In the standard manual preparation method those high shear forces were achieved by pressing a thin pipette tip to the base of an Eppendorf cup (1.5 ml) containing the sample and pipetting up and down several times. Thereby the particle dispersion was forced to pass through a narrow gap between pipette tip and tube wall.

This method was sufficient for small lab scale production, but not for scale up of AVP production. Also it was not suitable for systematic testing of the influence of the occurring forces on the resulting particles. Therefore, the search for an easy to scale up production method that allows controlling occurring forces independently from the operator and day to day performance started. It resulted in the design and use of different mixers. The overall idea (figure 3.2.1) was to replace the two separated manual pipetting steps by two controlled mixing steps in a mixer.

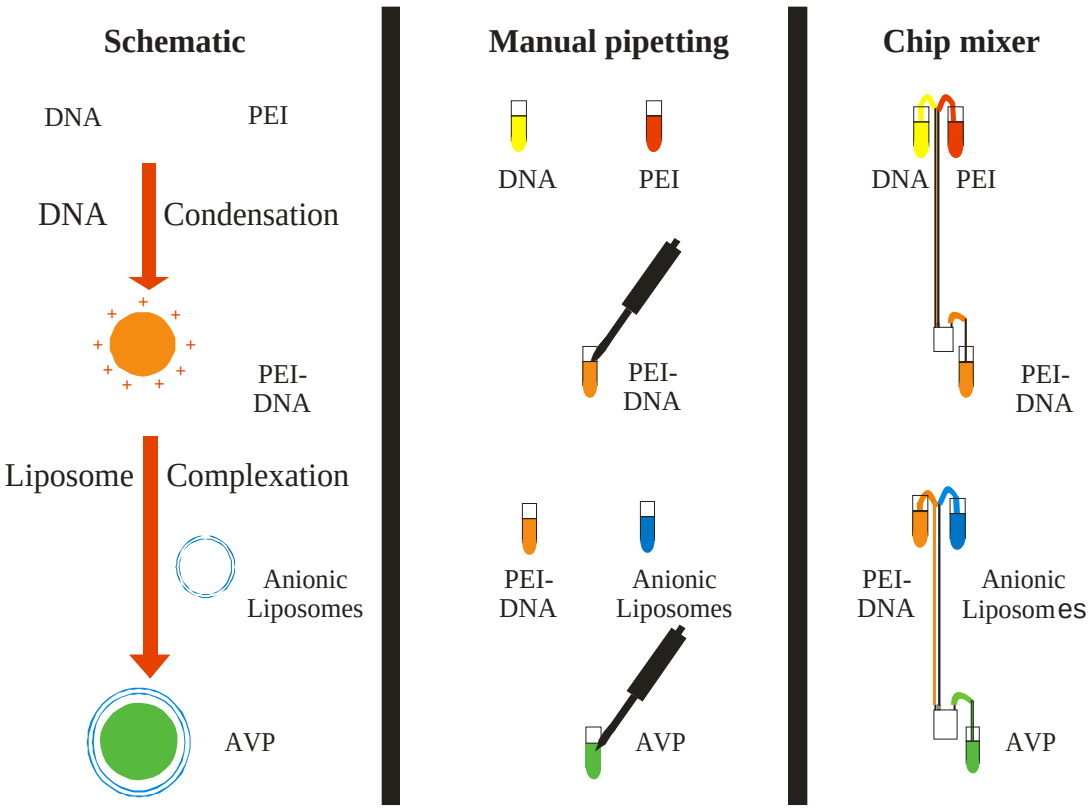

Figure 3.21 Overview: AVP production by manual pipetting or in a chip mixer

A prototype mixer “Mark I” existed from earlier experiments in Marburg. It consisted of a perspex mixing chamber, fuelled by two glass syringes that were driven by metallic weights moved by gravity. Trials to use this mixer showed that the forces on the two syringes were variable, depending on the friction of the metal weights in their guiding tubes. Furthermore, the chamber and its fittings tended to leak. So new alternatives were searched for.

The criteria were:

- Low dead volume, as the mixer should be usable for lab-scale experiments with less than 1 ml volume.
- Easy to scale up for later use with bigger volumes.
- Constant and adjustable mixing forces independent from the operator and its day to day performance to achieve reproducible results and allow determinination of the influence of shear forces on the process.
- If possible a see through mixing chamber, to be able to monitor the mixing process and detect deposits.

Dynamic HPLC mixer

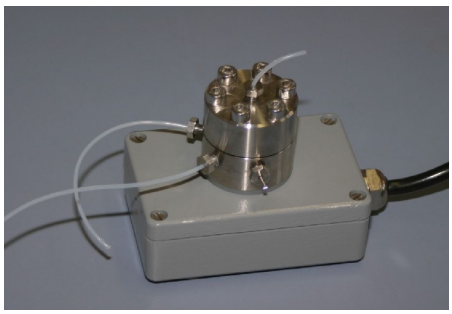

Figure 3.22 Dynamic HPLC mixing chamber, tested for AVP production

A micro fluid mixing chamber (figure 3.22) for HPLC eluents that consists of a mini magnetic stirrer in a low volume mixing chamber and can be connected by HPLC fittings was tested as successor of the Mark I mixer. PEI-DNA complexes were produced in this mixer and were in the nano-range (119.4 nm +/- 2.1) according to PCS measurements. But in this mixer the forces during mixing were hard to predict or calculate. Furthermore, the magnetic stirrer was not visible and not adjustable. Therefore, a better solution was searched for.

Static mixer Mark II

A new mixer with a static mixing concept was constructed. The new mixer called “Mark II” was planned with the friendly help of the local university repair shop and later constructed there. It consisted of two polyacrylate plates. One of them contained a T-shaped mixing structure while into the other one HPLC fittings were mounted.

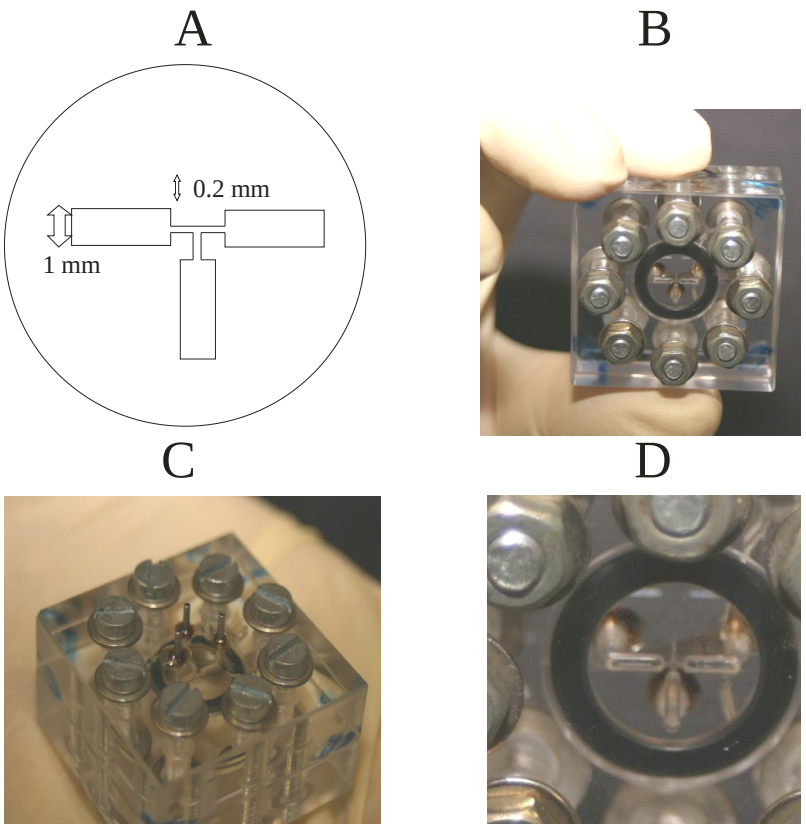

Figure 3.23 New prototype static mixer “Mark II”. The mixer consists of a T formed mixing chamber as seen schematically (A), cut and embedded in perspex plates (B), and is connectable by HPLC fittings (C). The last picture (D) shows a magnification of the mixing chamber.

The plates were tightened by a rubber fitting, screwed and additionally glued together and resulted in a mixer with a visible T-shaped mixing chamber, accessible by standard HPLC fittings (figure 3.23).

The T-shaped mixing chamber itself consisted of two influx channels and one efflux channel with a diameter of 1 mm and the mixing T with channel diameter 0.2 mm. Teflon tubes were fitted to the HPLC connections and connected by adaptors to Hamilton glass syringes.

This mixer proved to be tight and was used to prepare PEI-DNA condensates and also AVP.

Systematic PEI-DNA condensation in „Mark II“

This self-constructed mixer was used to perform a small test series that evaluated the influence of ionic strength of buffer and concentration of the reagents (PEI and DNA) on the size of the PEI-DNA complexes.

Therefore, model DNA (DNA from herring) was mixed with PEI in Tris buffer of low (5 mM) and high (20 mM) concentration adjusted to pH 7.4 resulting in different ionic strengths. For this preparation normal reagent concentrations (final concentration of PEI and DNA equals standard manual preparation) and high concentration (final conc. equals 4 fold standard concentration) was used. Size of the condensates was measured 5 and 30 minutes after condensation by PCS.

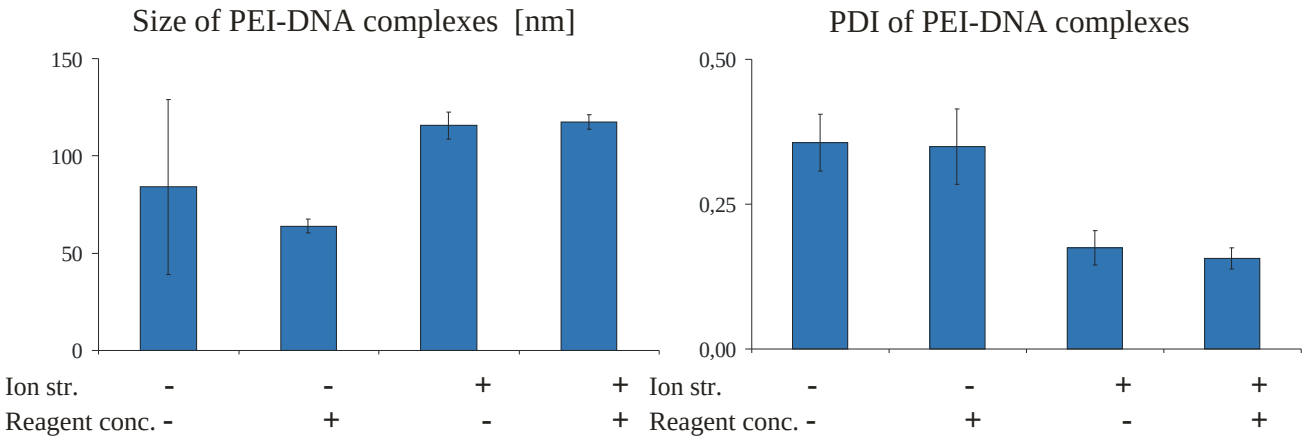

Figure 3.24 Size (Z-average) and PDI of PEI-DNA complexes and their dependence of Ionic strength of the buffer (concentration 5 vs. 20 mM) and reagent concentration (1 fold vs. 4 fold). High Ionic strength buffer (20 mM Tris) led to bigger particles with lower PDI. Error bars depict standard deviation of three independent mixing experiments.

The concentration of the reagents had no visible influence on particle size or size distribution as seen in figure 3.24 which depicts the situation after 30 minutes ripening time

In contrast to that, concentration and thereby the ionic strength of the Tris buffer had a strong influence on particle formation. Low concentrated buffer led to smaller condensates but a broad particle size distribution (high PDI), while high concentrated buffer led to bigger condensates with a narrow particle size distribution.

Directly (5 min) after mixing of PEI and DNA size of particles prepared at different ionic strength already varied, but the differences were not as pronounced as after 30 minutes. Interestingly the PEI-DNA complexes grew during the period between measurements in the high concentrated buffer, while they shrunk in the lower concentrated buffer. The PDI of all samples decreased slightly during particle ripening.

AVP from Mark II analysed by Cryo TEM

As already depicted PCS measurements alone can not describe particle shape, filling or the parallel existence of different species of particles (see chapter 3.1.1). As PEI-DNA complex preparation in the mixer Mark II was successful, also AVP were produced in it. Therefore, PEI-DNA complexes prepared in the mixer were allowed to ripen for 15 minutes as in manual preparation and processed with diluted liposomes in the mixer to AVP. Those AVP were examined in Cryo TEM to compare them to manually produced AVP. They showed (figure 3.25) the familiar mix of filled particles (figure 3.25 A), glued together particles (figure 3.25 B) and empty or coated liposomes (figure 3.25 C) already seen in AVP samples produced by manual pipetting (see chapter 3.1.2)

A

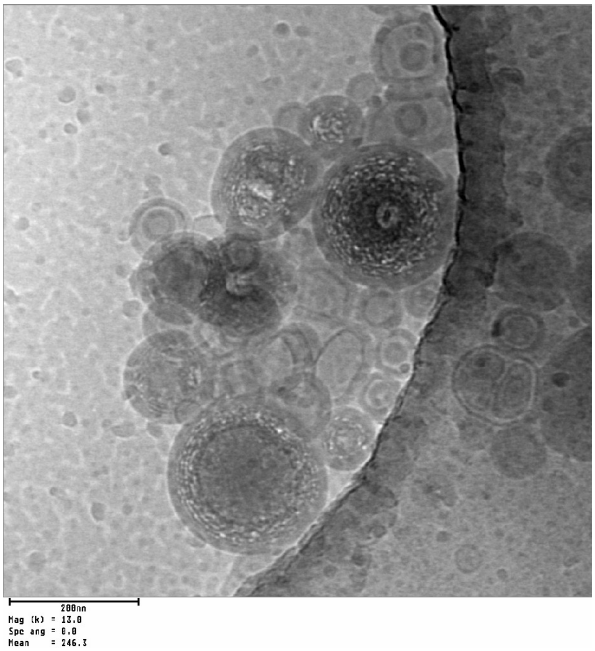

B

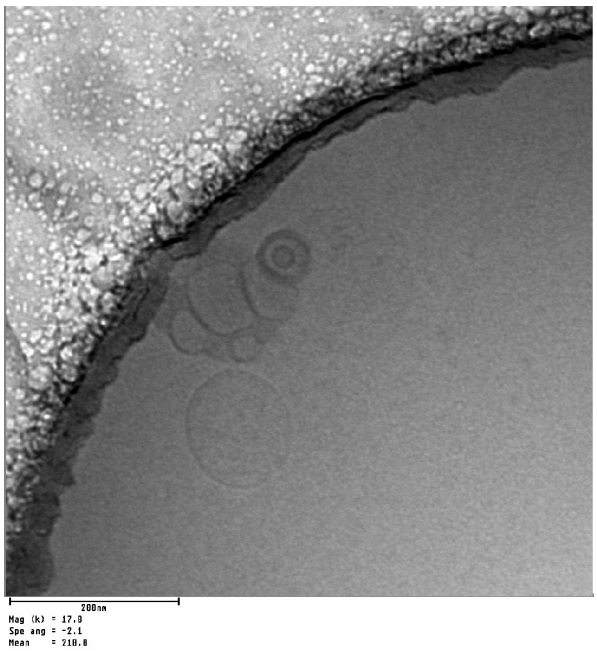

C

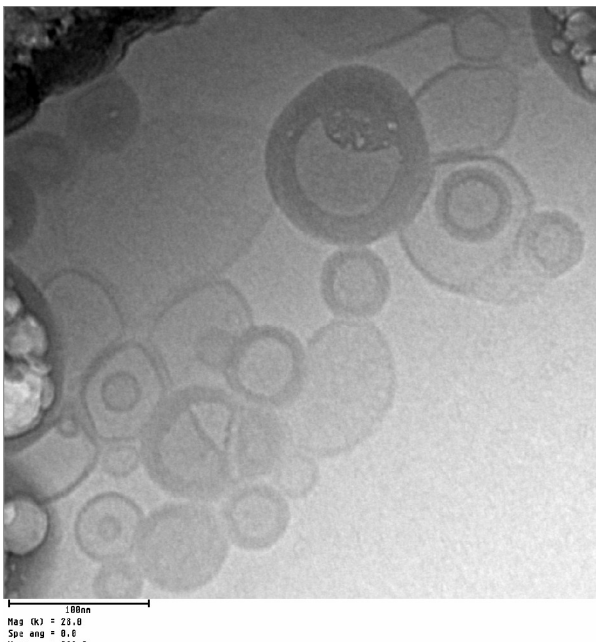

Figure 3.25 AVP produced in the self constructed static mixer Mark II examined in Cryo TEM contained filled particles (A), empty glued together (B) and coated liposomes (C).

Summary:

Formation of AVP and PEI-DNA complexes was possible in the home-made static mixer "Mark II" and resulted in PEI-DNA complexes similar to AVP produced by manual pipetting as seen by size measurements and electron microscopic examinations. It showed its suitability for a systematic exploration of DNA condensation processes that depend on reproducible conditions. But during first experiments with this prototype it became obvious that some specifications should be improved:

- The used material polyacrylate is sensitive to organic solvents and temperature, complicating intensive cleaning or disinfection which would be important for the production of samples with minimised germ content for cell culture.
- The pipes in the T mixing chamber itself were not scalable under 0.2 mm, as this was the lower limit of the involved CNC milling machine. Pressing the syringes manually to pass the reagents through the mixing chamber led only to low resistance. So application of sufficient forces and mixing could be doubted.
- The mixing efficiency in the mixer and its dependence on flow through speed were not described yet and its proper characterization would have gone beyond the scope of this work.

3.3.2 Use of the static chipmixer "Statmix 6" to produce AVP

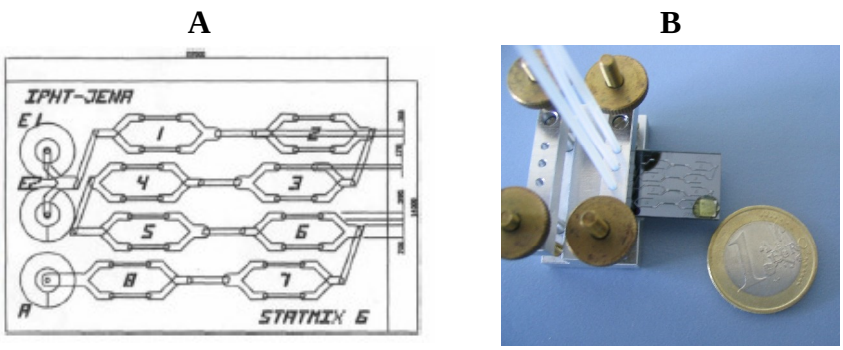

Figure 3.26 Chipmixer statmix 6 from the IPHT as construction scheme (Kirner et al., 2004) (A) and complete setup with connections (B).

By a, fortunate accident our group contacted the group of Prof. Dr. Köhler at the "Department of Physical Chemistry and Microreaction Technology" from the Institute of Physics in Ilmenau was made. They already had characterized the mixing process in a prototypical three layer glass-Si-glass micromixer (Kirner et al., 2004). This mixer called "Statmix 6" mixes fluid streams by separating and reuniting them 8 times in a chip mixer in the size of a thumbnail. This mixer was developed in the IPHT (Institut für photonische Technologien) in Jena. Prof. Köhler´s group kindly provided us with one of those mixers, suitable fittings and also with their know-how regarding its usage and possible problems.

Transmission electron microscopy of AVP produced in the Statmix 6

In a first set of tests the Statmix 6 was used to prepare PEI-DNA complexes and AVP from model DNA (herring). The resulting AVP were characterised by PCS (Z-average 135 nm (+/- 1.33), PDI 0.209 +/- 0.023) and examined in transmission electron microscopy after freeze fracture preparation.

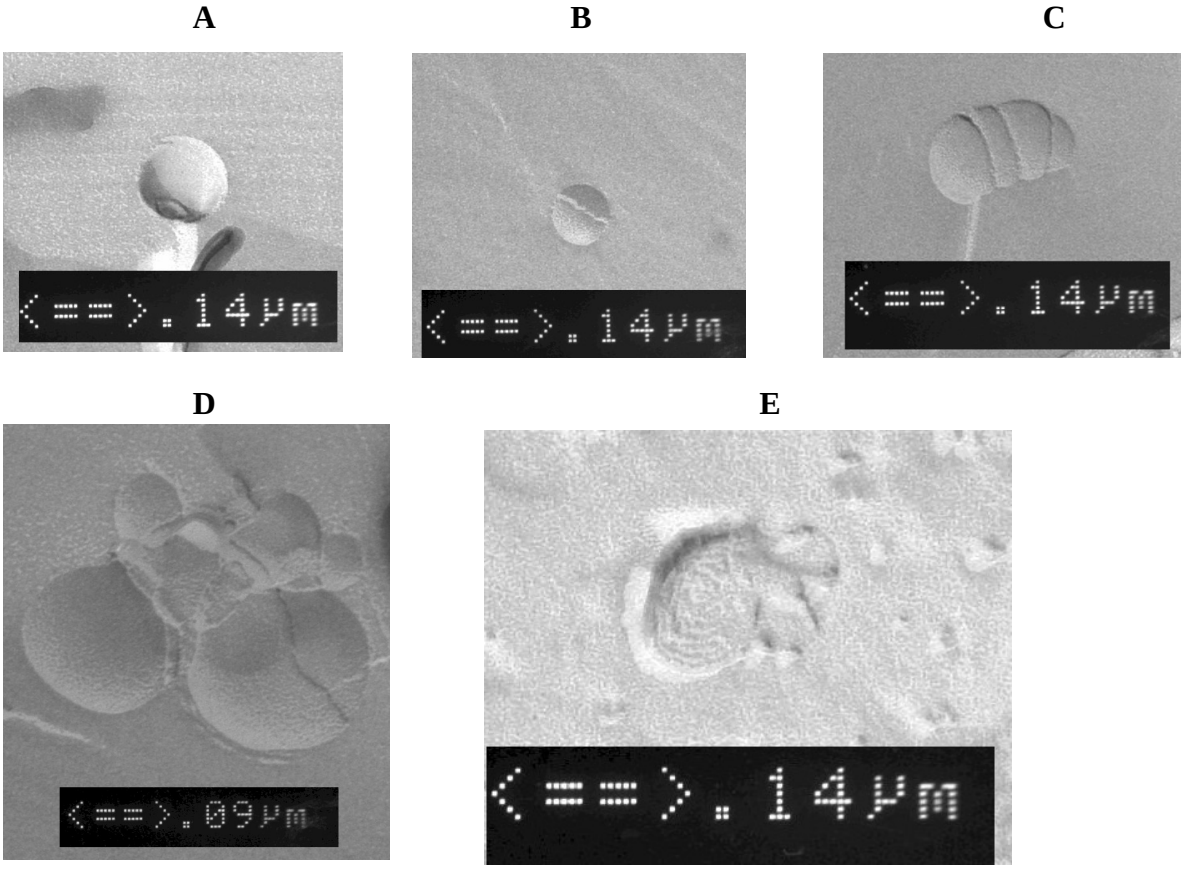

Figure 3.27 AVP produced in the chipmixer "Statmix 6" examined in TEM after freeze fracture preparation. A similar mix of different particle species as in manual preparation was observed.

The mix of particle species visible after this preparation (see figure 3.27) corresponded well to the AVP samples examined before (see chapter 3.1.2). Round particles with wart-like attachments of small particles (figure 3.27 A) were found. Also particles with partially ripped away outer layer (figure3.27 B) and aggregates of wormlike appearing deformed liposomes (figure 3.17 C) could be found again. In magnification of small aggregations an amorphous material could be seen that glued the liposomes or filled AVP together (figure 3.27 D). In this preparation the lucky incident happened that one of the filled particles was ripped apart when the frozen sample was broken apart and showed an inner structure, sign of a filling (figure 3.27 E).

Syringe pumps and low germ preparation

Up to that point the influx syringes were operated by hand as steady as manually possible. After principally showing that particles formed in the mixers physically correspond to particles derived from manual preparations, a better adjustable system was introduced. Syringe pumps that push the plunger by turning screw threads allowed to operate the syringes with a steady adjustable speed resulting in a steady pulsation-free liquid flow (figure 3.28 A). For experiments that tested the biological effectiveness of the produced AVP in cell culture the whole setup was disinfected using 70 % ethanol and used in a laminar air flow box to allow low germ preparation of AVP (figure 3.28 B).

A **B**

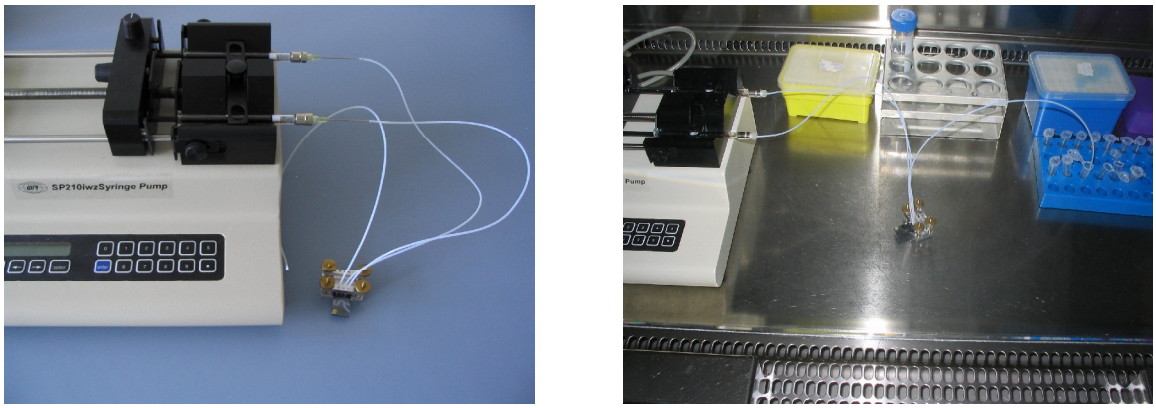

Figure 3.28: Syringe pump for steady liquid influx to the chipmixer (A) and setup under laminar air flow to avoid contamination (B).

Influence of mixing parameters on AVP properties

Using this new setup a follow up experiment to the experiments that had linked ionic strength of the buffer to the size of the PEI-DNA complexes in the "Mark II" mixer was performed. Now ionic strength, already detected as critical parameter in the preliminary experiment with the self-constructed static mixer in chapter 3.3.1, and additionally flow speed of the reagents were varied. The resulting particles were not only characterized by PCS but also their transfection efficiency in cell culture was evaluated.

Four sets of AVP and their starting material PEI-DNA complexes were prepared in the mixer under differing conditions:

- Concentration of the Tris buffer and thus ionic strength varied between low (5 mMol) and high (50 mMol).
- The tested flow speed was varied between low (0.05 ml/min) and high (0.25 ml/min) per syringe.

Parallel a control sample was prepared by manual pipetting using the established Tris buffer concentration of 10 mM. AVE-DOPE was used as liposome species suited for transfection. Particle size from three independent experiments was measured in triplicate, while transfection efficiency in cell culture was measured in two experiments in triplicate (3 wells).

Particle size of AVP mixed in Statmix 6 under differing conditions

Concentration and derived from it ionic strength of the used Tris buffer again had strong influence on the resulting particle size (figure 3.29).

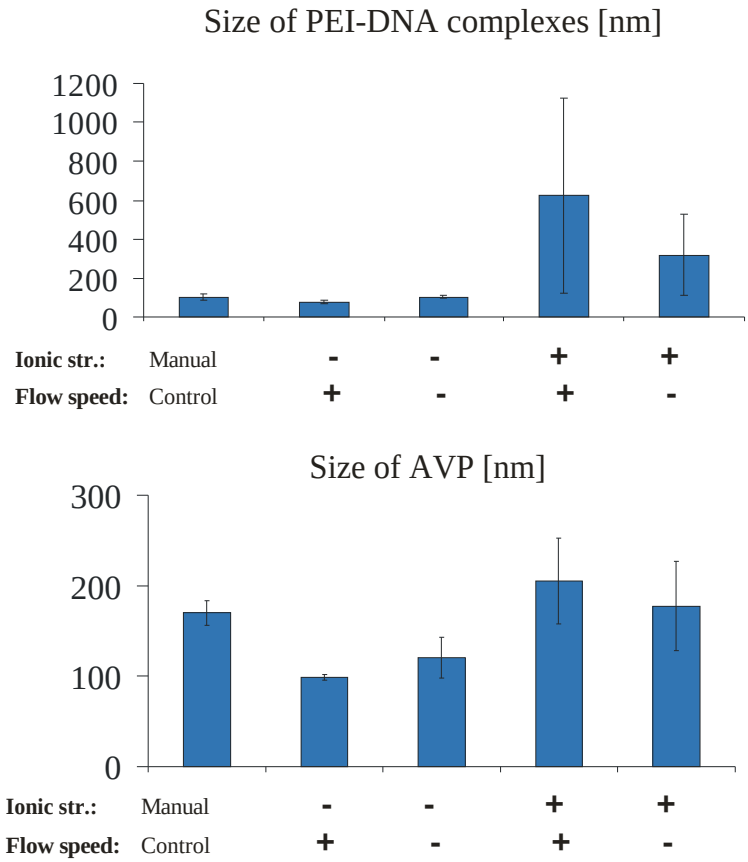

Figure 3.29 Size of PEI-DNA complexes and AVP prepared in the chipmixer statmix 6 under differing conditions. Preparations in low (5 mmol) and high (50 mmol) concentrated tris buffer using low (0.05 ml/min) and high (0.25 ml/min) flow speed were compared to particles prepared by manual pipetting. Error bars depict standard deviation of three independent mixing experiments.

The higher (50 mM) concentrated Tris buffer also possessing higher ionic strength led to bigger PEI-DNA condensates and in some experiments even to large aggregates which caused huge standard deviations in graphical display. The AVP resulting from them were a bit bigger than those derived from PEI-DNA complexes prepared at low ionic strength or manually but still smaller than the PEI-DNA complexes from which they derived.

Variation of flow speed of the liquids in the syringes did not show a consistent influence on particle size.

Transfection efficiency:

A plasmid coding for GFP was used as model DNA and allowed to evaluate the percentage of cells expressing the green fluorescenting protein by flow cytometry. So the biological effectiveness of the different AVP samples can be judged (see chapter 2.1.13 and 2.1.14). Transfection efficiency was measured 24 h after cell transfection with the freshly produced AVP prepared under differing conditions in the chip-mixer Statmix 6.

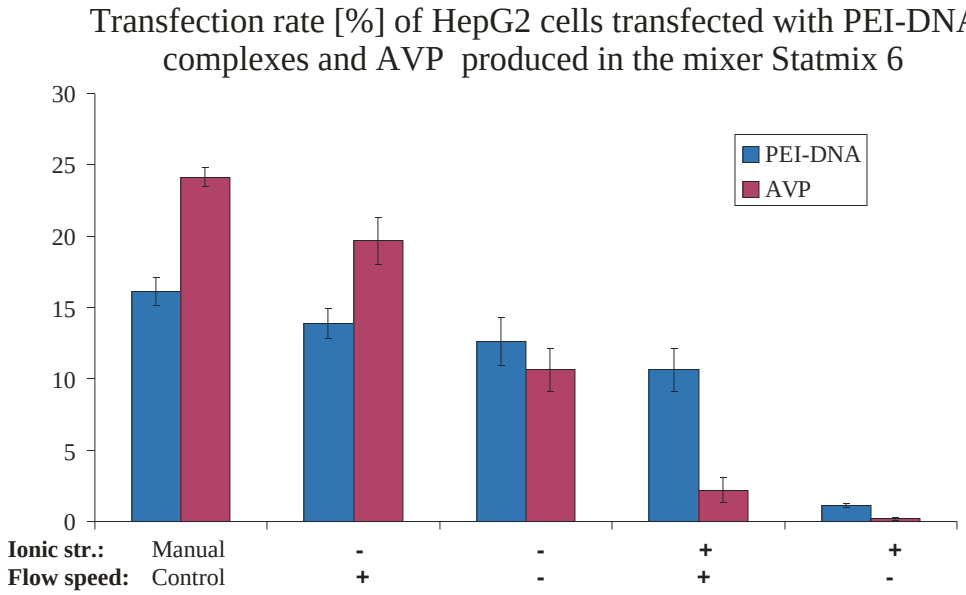

Figure 3.30: Percentage of HepG2 cells expressing green fluorescent protein (GFP) after transfection with PEI-DNA complexes and AVP produced in the mixer Statmix 6. Buffer of differing concentration (5 and 50 mmol) and thereby differing ionic strength was used and flow speed was varied (0.05 and 0.25 ml/min). AVP from production in buffer of low ionic strength and high flow speed reached transfection rates comparable to those of particles prepared by manual pipetting. Error bars depict standard deviation of three wells of transfected cells.

Working with a biological system leads to strong day to day fluctuations in transfection results. In this experiment already the core of the AVP, the PEI-DNA condensates showed an unusual high efficiency. Nevertheless, processing the PEI-DNA cores with the AVE-DOPE liposomes to AVP improved transfection efficiency for the manual control and in one of the AVP lots from the mixer.

Transfection efficiency of particles from the mixer did not reach the transfection rate of AVP prepared manually, even when it came close to it in the best AVP lot from the mixer. This lot

was prepared using low ionic strength buffer and low flow speed and also showed small defined particles in size measurement before (see figure 3.29).

Preparation in buffer of high ionic strength led to PEI-DNA complexes and AVP derived from them that were less successful in transfection than particles prepared in low ionic strength buffer. This could be explained by the increased particle size seen in PCS for particles prepared in the high ionic strength buffer (see figure 3.29) that might alter or inhibit normal uptake of the AVP. A trend that higher flow speed led to better transfecting particles could be supposed from the first experiment.

However, a repetition of the evaluation in cell culture with new lots (figure 3.31) showed no such relation. Again PEI-DNA complexes and AVP from the mixer were able to transfect cells and again transfection rate of particles produced in low salt buffer exceeded that of particles prepared in high salt buffer. Transfection success of particles from the mixer was lower than of those prepared by manual pipetting in this experiment. However, the main result was that the degree of transfection success of particles from the mixer was less reproducible than that of particles prepared manually.

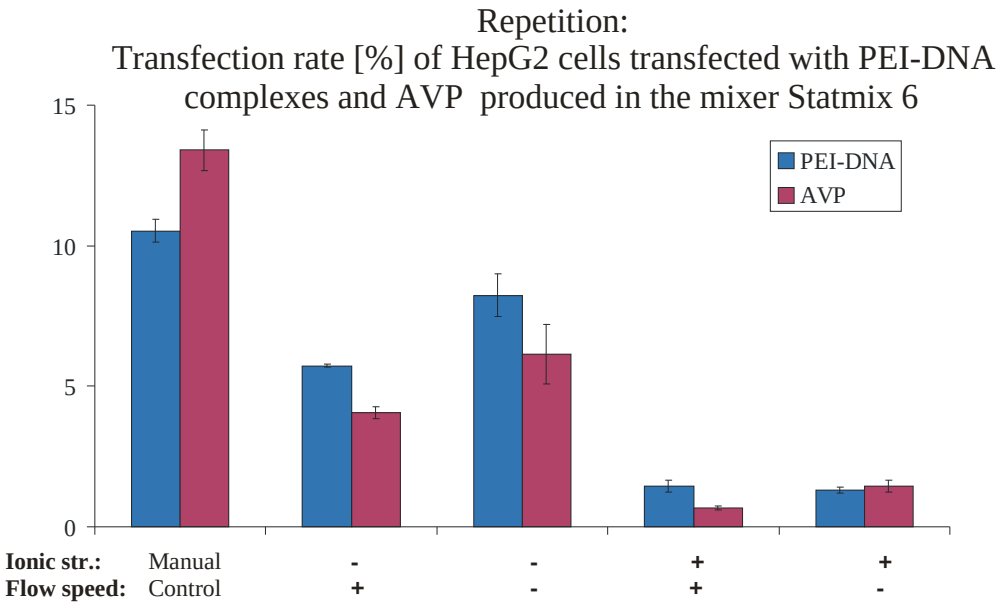

Figure 3.31: Repetition of the experiment described in figure 3.30. Again transfection rate in percentage of GFP expressing cells was evaluated for different samples prepared in the chipmixer Statmix 6. Samples were able to transfect cells, but the reproducibility of the trends seen before was low. Error bars depict standard deviation (n=3 for PEI-DNA and n=2 for AVP).

Summary:

The experiments prove that the setup of the chipmixer "Statmix 6" with syringe pumps was able to produce PEI-DNA complexes and AVP particles of repeatable size, that were biological active and able to transfect cells. Use of static mixers for the production of gene carrier vehicles has already been patented (Chen, 2003) and used and investigated successfully (Clement et al., 2005; Clement, 2005). However, in these recent works a one step preparation of anionic DNA with a cationic reagent was investigated, while we successfully prepared a complex vehicle consisting of DNA, cationic reagent and anionic liposomes in a two step production in a static chipmixer.

The AVP produced in the chipmixer Statmix 6 and their characterization confirmed the previously observed (see chapter 3.3.1) influence of concentration of the buffer and thereby its ionic strength on particle size primary of the PEI-DNA complexes and secondary also of the final AVP. In those experiments no linear influence of mixing speed on particle size was seen. The observed effect that PEI-DNA complexation under controlled conditions in buffer of low ionic strength led to small complexes, while the same procedure in high ionic strength buffer resulted in big particles with a tendency to aggregate is in accordance with the results of Ogris et al. who compared size of PEI-DNA complexes prepared in different media (Ogris et al., 1998).

Particles produced in the chipmixer were successfully used to transfect cells. Here as well PEI-DNA complexes as AVP produced in low ionic strength buffer showed increased transfection efficiency compared to particles produced in high ionic strength buffer. This result is consistent with increased particle size and a trend for aggregation seen for particles produced in high ionic strength buffer. Therefore, future experiments in the mixer were conducted in low concentrated buffer (5 mM Tris). A correlation between the production parameters mixing speed and transfection efficiency was not seen.

The fluctuation of transfection efficiency of particles from the mixer exceeded the normal cell culture dependant fluctuation rate. This became obvious as the control AVP produced by manual pipetting led to relatively stable transfection rates while in the same experiments transfection rate of particles from the mixer varied strongly.

3.3.3 Troubleshooting for AVP production in Statmix 6

Further experiments with the chip mixer were mainly focused on finding correlations between production parameters and transfection efficiency and finding a reason for the bad reproducibility of transfection efficiency of AVP from the mixer. The following areas were screened in experiments for critical parameters:

Type and shape of particle:

Particle size and form of AVP produced in the chipmixer in low concentrated buffer corresponded to that of particles produced by standard manual pipetting as seen by PCS measurements (figure 3.29) and the electron microscopy examinations of freeze fracture preparations in (figure 3.27).

Furthermore, AVP produced in the chipmixer were also examined by Cryo-TEM.

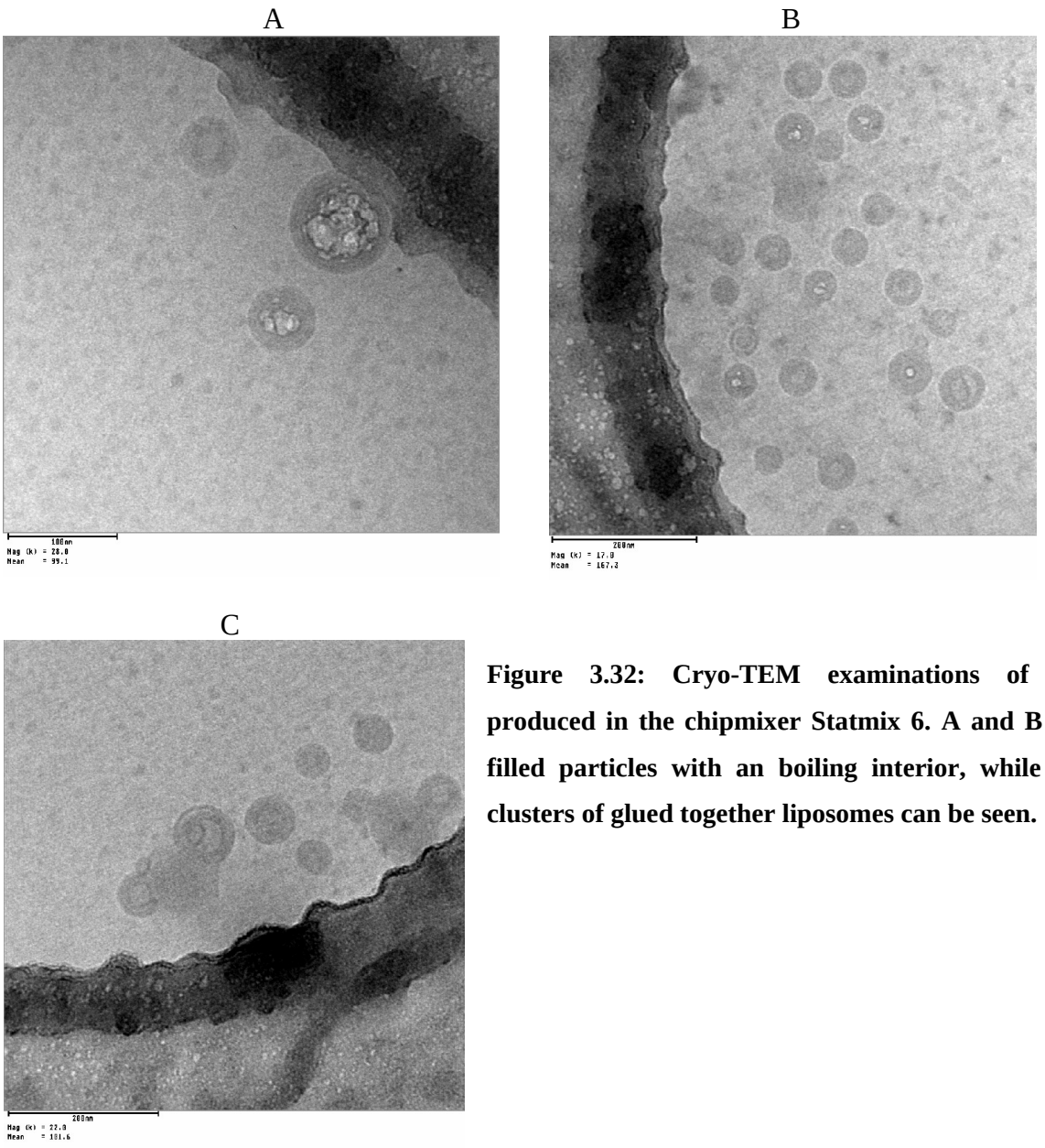

Figure 3.32: Cryo-TEM examinations of AVP produced in the chipmixer Statmix 6. A and B show filled particles with an boiling interior, while in C clusters of glued together liposomes can be seen.

Examination of AVE-act derived AVP produced in the chipmixer Statmix 6 in Cryo TEM showed filled AVP (figure 3.32 A and B), empty liposomes and free PEI-DNA complexes partially aggregated with liposomes (figure 3.32 C). Basically the same mixture as seen in earlier Cryo-TEM examinations of manually prepared AVP before (see chapter 3.1.2) was observed.

Particle size and form of particles produced in the chip-mixer and of manually prepared particles were the same and indicated successful formation of AVP in the chip-mixer. So a failure of AVP formation or the formation of completely different particle species could be excluded as source of the lowered reproducibility of transfection success of AVP produced in the mixer.

Shear forces during the second step of AVP preparation

In those experiments the focus was on the role of shear forces in the second step of AVP preparation. The combination of the PEI-DNA condensates with the anionic AVE liposomes was supposed to be shear force dependent according to the practical experience of co-workers in this field. To guarantee similar starting conditions, a common lot of PEI-DNA particles was freshly prepared in the mixer for each set of experiments. Afterwards this common stock was processed to AVP with liposomes applying differing shear forces.

- Flow speed of the second step of preparation in the mixer, the combination of PEI-DNA complexes was varied again. Now flow speeds between 0.05 ml/min and 1.0 ml/min per syringe were used to determine an influence of shear forces.
- The reagents were passed through the mixer and mixed not only one time, but also three and 10 times to test if one passage through the mixing chamber is not sufficient for proper AVP formation.
- To compensate an eventual lack of shear forces, AVP samples that had already been mixed in the chipmixer, were additionally mixed by normal pipetting according to the standard manual procedure after effluence from the chipmixer.

Cell culture dependant effects

- AVP from the mixer were compared to AVP from standard manual procedure on different cell lines (HepG2, L929, HEK293 and HUVEC) to exclude cell specific effects.
- Dose (amount of AVP per well in cell culture) dependent transfection efficiency of AVP prepared by mixer was compared to that of AVP prepared manually.

Adsorption to construction material of the mixer

A possible adsorption of AVP to the mixer, tube or syringe material was assumed early as a potential problem, so different experiments were performed to quantify and solve adsorption processes:

- Different types of liposomes (AVE, AVE-DOPE, AVE-act (see chapter 3.4.2) were used for AVP preparation to exclude liposome type specific interactions with surfaces.
- Zetapotential of AVP derived from the mixer was compared to that of AVP prepared manually.
- A surplus of the reagents PEI and liposomes was added either during the mixing process or after mixing to compensate a possible adsorption of those reagents to syringes, tubes or the mixing chamber itself.
- The AVP produced in the mixer were divided in an early fraction and a late fraction. Both fractions were tested separately in cell culture. Possible adsorption effects were expected to be more distinct in the first fraction. Here the surface of the mixer was unsaturated. The adsorbed material should gradually saturate the surfaces of the mixer and thereby lead to less apparent effects for the later fraction.
- Prevention of adsorption by saturation of surfaces in the mixer. Therefore, the mixer and tubes were rinsed through with PEI solution or a mix of PEI and liposomes (forms mock particles similar to AVP as seen in chapter 3.1.2).
- Use of the mixer planned and produced by ourselves (Mark II) that consisted of polyacrylate to produce particles for transfection as a control. They were able to transfect cells, but also showed lowered efficiency compared to manually produced AVP.
- Measurements of DNA content in samples prepared by different methods.

The strong variation in transfection efficiency of AVP produced in the mixer made recognition of critical parameters difficult. Transfection efficiency in cell culture is always variable, as cell culture as a biological system leads to variations itself. But the variations of particles from the mixer were too high to be regarded as normal. Even when only successful transfection experiments in which AVP produced by manual pipetting achieved constant high transfection rates were compared, a strong fluctuation of the transfection rate of particles produced in the chipmixer was evident.

As an example of the situation three transfection experiments in which the AVP sample prepared by manual pipetting led to high and comparable transfection efficiencies showing that cell culture and transfection procedure were successful and comparable were picked and are shown in Figure 3.33:

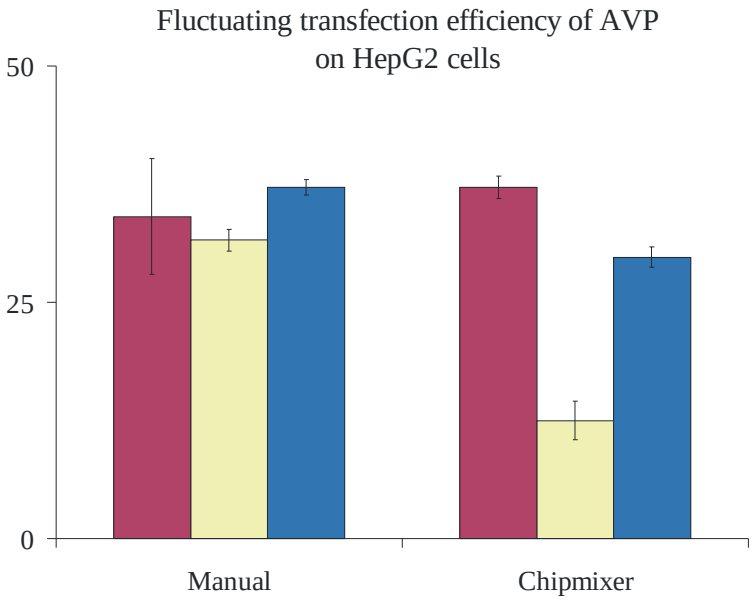

Figure 3.33: Comparison of the transfection rate of AVP prepared in the chipmixer to AVP from manual preparation in three successful transfection experiments. All AVP were derived from AVE-act liposomes.
Error bars depict standard deviation.

In contrast to the manually prepared AVP, the AVP derived from the mixer showed highly variable transfection results, even when the protocol and flow speed (0.5 ml/min per syringe) were kept the same. Therefore, most of the control experiments and variations mentioned above were performed in repetition.
Some of the variations mentioned before seemed to show an improvement of transfection rate and led to temporary believe in correlations between the changed parameters and biological efficiency. But none of them was able to reproduce good transfection results. The overall tendency was that AVP from the mixer led to stronger fluctuating and generally lower transfection results compared to those prepared by manual pipetting.

DNA content of AVP samples and consequences on transfection:

As reason for the fluctuating transfection results, adsorption effects were assumed. So DNA content of PEI-DNA complexes and AVP produced manually and in the chipmxier were measured and compared. To be able to measure the DNA content of the PEI-DNA and AVP samples, a standard procedure had to be adapted for AVP. An established sensitive method for the determination of DNA content is measurement of the fluorescence of the complex of the intercalating dye PicoGreen® with DNA (see chapter 2.1.17).

But condensation of DNA to PEI-DNA complexes leads to an extinction of that fluorescence, as the intercalating fluorescence dye is “squeezed” out of the complex with the nucleic acid. This extinction of fluorescence is actually used as proof of complete complexation of the nucleic acids for gene transfer vehicles such as AVP (Welz, 2000).

So the DNA has to be freed from AVP or PEI-DNA complexes before it can be measured. Moret et al. (Moret et al., 2001) showed the possibility to decomplex PEI-DNA complexes by either adding the polyanion heparin or raising the pH which leads to a decreased number of protonated and therefore positively charged N groups in PEI.

In initial experiments the addition of heparin and increasing the pH to decomplex the PEI-DNA particles were tested. By raising the pH to levels of 11.7 to 12 the fluorescence could be increased significantly, indicating liberated DNA which confirmed the results of Moret. Also complete breakdown of fluorescence when raising the pH above 13, as described by Moret, was observed. Using heparin as decomplexation agent did not lead to reconstitution of fluorescence to the same extent in our experiments. So an assay was established (see 2.1.17) that decomplexed DNA at pH 12 and measured the fluorescence of the DNA-PicoGreen® complex in a 96 well plate reader to determine the DNA content of AVP samples. Operating at this pH and also having additional chemicals (like PEI and liposomes) as part of the sample is beyond the specifications of PicoGreen®. Nevertheless, our method resulted in a linear calibration curve as well for pure DNA as for AVP (figure 3.34).

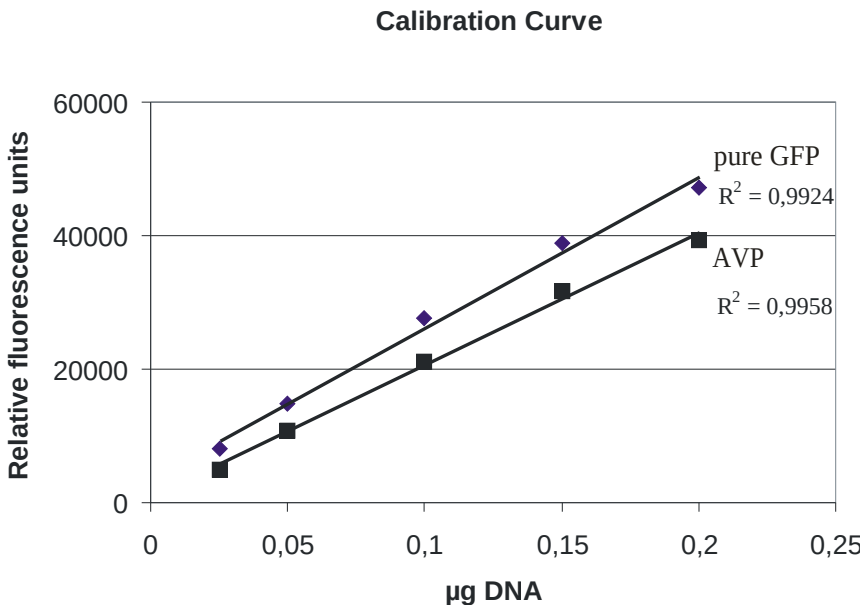

Figure 3.34: Calibration curves of amount of DNA versus fluorescence of the picogreen DNA complex. Measurements were done according to a modified routine that decomplexed DNA from AVP. Curves depict dilution series of free DNA (GFP plasmid) and of DNA (GFP plasmid) complexed to AVP.

The calibration curves for the non-complexed pure GFP plasmid and the AVP containing complexed plasmid differed from each other. A likely explanation is interference of the supplements (PEI, liposomes) included in AVP samples with the fluorescent complex. The calibration curve of the DNA freed from complexes was slightly lower than the curve of the pure DNA, an effect also seen for PEI-DNA complexes in the work of Moret et al (Moret et al., 2001). So the AVP calibration curves were used for calculation of DNA content in AVP samples.

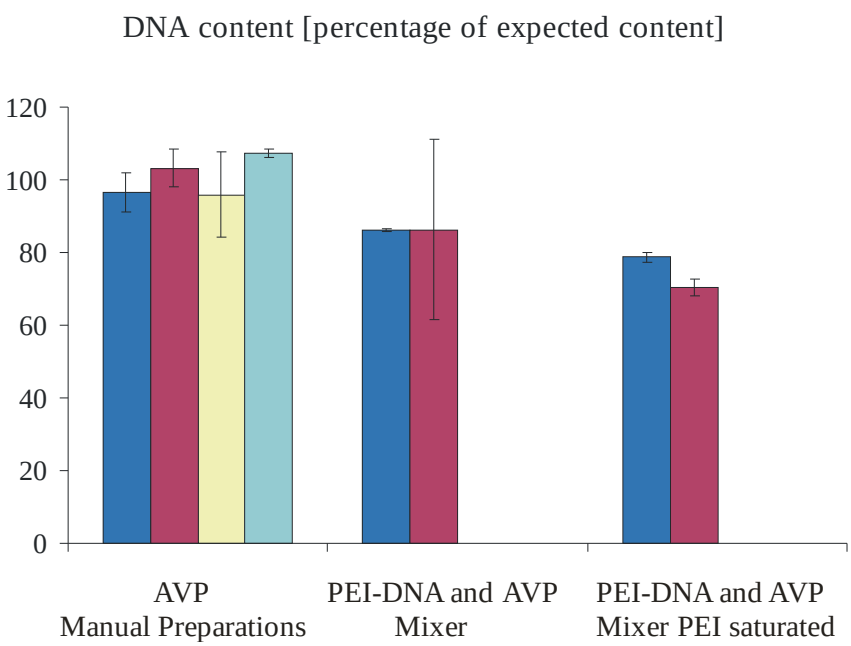

Figure 3.35: DNA content as percentage of the expexted content.
AVP produced manually were compared to PEI-DNA complexes and AVP produced in the mixer. Also samples from a mixer that was pre-treated with PEI to saturate its surfaces were included.
Error bars depict standard deviation

Measurements of DNA content in samples from the mixer showed a reduced DNA content (figure 3.35) as well for PEI-DNA complexes and AVP derived from the mixer. Rinsing the mixer with PEI did not decrease the loss of DNA. In comparision several manually prepared AVP samples showed a nearly constant DNA content that corresponded well to the calculated and expected content.

The AVP samples, for which DNA content was measured here, were used in parallel for transfecting HepG2 cells. AVP samples from the mixer, which showed a lowered DNA content, also showed lowered transfection efficiency compared to manually prepared AVP samples.

From the DNA content measurements (figure 3.35) and transfection rates of the same samples (figure 3.36) a connection between transfection efficiency and lowered DNA content was visible. So the lowered transfection efficiency from particles from the mixer can be explained as adsorption problem.

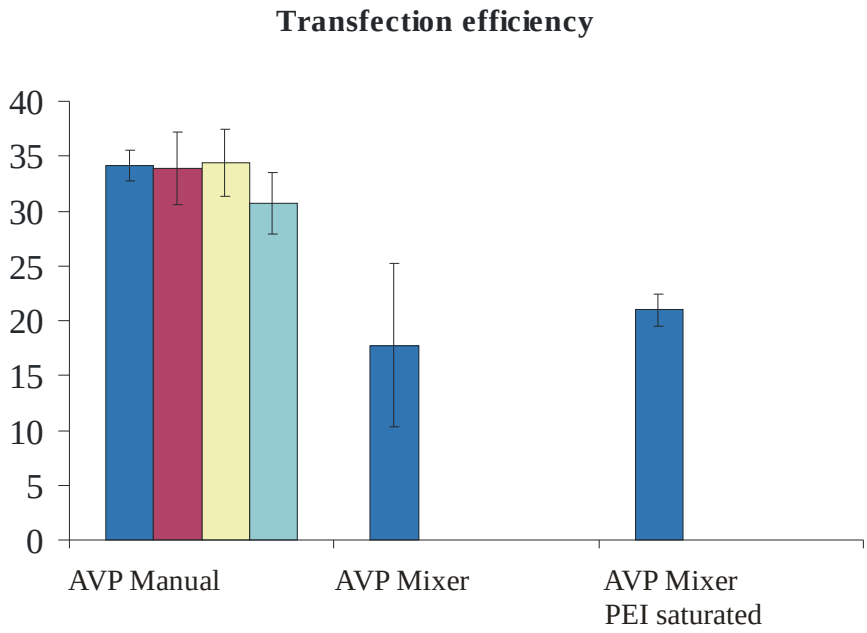

Figure 3.36: Transfection efficiency [% transfected cells] of AVP samples produced manually and in the mixer with determined DNA content. Error bars depict standard deviation.

Further increase of the dose normally decreases transfection efficiency. As a lowered content of the AVP samples from the mixer was expected also twice the dose of AVP (4 µg DNA per well) was tested parallel to the normal dose of 2 µg. As expected doubling the dose decreased the percentage of transfected cells for the manually prepared AVP as the optimum amount was surpassed. In contrast doubling the dose of AVP samples from the chipmixer increased transfection efficiency (figure 3.37). This pointed again to a lowered sample content, differing from the expected content for the samples from the chipmixer.

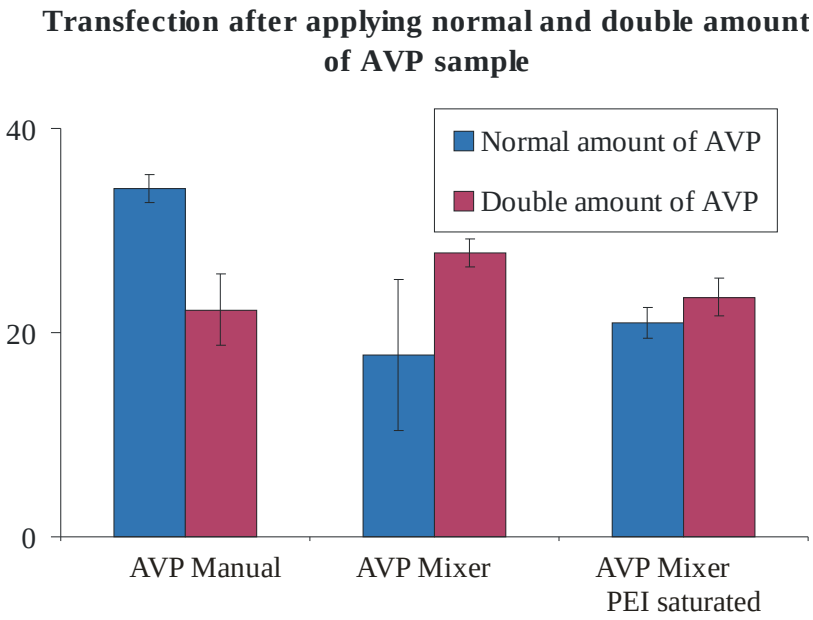

Figure 3.37: Transfection of HepG2 cells using normal amount of AVP (2µg DNA) and double amount (4 µg DNA). Doubling the dose led to a decline of transfection rate for manually prepared AVP as the optimum amount was surpassed. In contrast to that the transfection rate of AVP from the mixer profited from it. Error bars depict standard deviation

However, even with a doubled dose of AVP still the transfection rate did not reach the values of the manually prepared sample. Presumably the optimum was already surpassed or other effects like a surplus of PEI and liposomes interfered here.

Zetapotential of the AVP from the mixer examined here was + 20.9 mV (+/- 4.42) and thereby much lower than the +53.2 mV (+/- 1.58) of the parallel measured manually produced AVP. This lowered zetapotential can not be explained by an adsorption of the negatively charged DNA alone, but could derive from adsorption of positively charged PEI-DNA complexes to silica surfaces of the mixer. However, not in all experiments zetapotential of AVP from the mixer was lowered which also supports a theory of badly reproducible adsorption effects.

Summary:

The troubleshooting experiments showed that particle size and form of AVP prepared in the chipmixer as measured by PCS and visualized by TEM matched those prepared manually by pipetting. Transfection rate of AVP prepared in the mixer reached the rate of AVP prepared manually. But it varied despite various changes in the experimental setup. Our experiments suggest, that the reason for that is a loss of part of the samples prepared in the mixer, most likely by adsorption at either the teflon tubes, the glass syringes or at the Si-Glass-Si material of the chip mixer. As our educt-polymer polyethylenimine is known to adsorb to a variety of materials, also silica (Meszaros et al., 2002), and is also technically used to increase adhesion of materials (BASF, 1996) certain adsorption phenomena had to be expected.

Jule Clement also describes discrepancies between recovery rates and theoretically contained content for DNA and lipid in her studies on lipoplexes produced in a static mixer (Clement, 2005). Parallel studies of Wagner and Köhler showed adsorption effects during the synthesis of gold nanoparticles in the chipmixer/reactor Statmix 6, which was also used in our studies (Wagner, Koehler, 2005). They were able to reduce adsorption by hydrophobization of the mixer surfaces by silanization. It seems that large scale production of AVP in a static mixer is possible, if adsorption processes can be avoided, e.g. by altering the surface of the mixer.

Furthermore, no dependency of the quality of particles from applied forces was observed in the experiments performed with varying shear forces in the second step of AVP preparation in the chip mixer. Therefore, the initial assumption that high shear forces are necessary for proper AVP formation was doubted. This led to the systematic studies on shear force dependency of AVP formation (see chapter 3.4.3).

3.4 AVP variations and impact on structure and biological efficiency

3.4.1 Role of condensation agent

Protamine sulfate as DNA condensation agent

The AVP described in publications (A.Fahr and K.Müller, 2001; Muller et al., 2001; Nahde et al., 2001; Toenges et al., 2006), and in the other chapters of this work are based on the synthetic polymer polyethylenimin (PEI) with MW 5000 g/mol as cationic complexation agent for DNA. It was used in an amount resulting in a surplus of positive charge of 1:4.6 for the PEI-DNA complexes. Here 15 µg DNA in complexes were processed with AVE liposomes corresponding to ~ 60 µg phospholipids.

Sorgi et al. showed the general suitability of protamine sulfate as complexation agent for gene delivery (Sorgi et al., 1997). Sabine Bucké described the use of protamine sulfate (PS) as alternative complexation agent instead of polyethylenimine for genetic material in AVP in a surplus of positive charge of 1:3.6 followed by a combination with the 4 fold amount of AVE liposomes. Those AVP were successfully used by Bucké to transfer Oligonucleotides (Bucké, 2001). Christian Welz followed PS based AVP containing oligonucleotides into cells by fluorescence microscopy by Christian Welz (Welz et al., 2000).

In this work protamine sulfate as complexation agent for AVP was investigated more closely. Firstly a model DNA (herring) and later plasmid DNA in the charge ratio optimized by Sabine Bucké (Bucké, 2001) were used. PS-DNA complexes were combined with the standard amount of AVE liposomes and parallel with the fourfold amount of liposomes as described by Bucké to AVP.

	Z-average [nm]	PDI	Zetapotential [mV]
PS-DNA complex	90.7 (+/- 1.23)	0.186(+/- 0.003)	**+** 34.37 (+/- 5.85)
AVP (PS)	195 (+/-9.14)	0.334 (+/- 0.028)	+ 24.4 (+/-1.2)
AVP (PS) 4* liposomes	195 (+/- 5.97)	0.356 (+/- 0.005)	**- 54.2 (+/-1.5)**

Figure 3.38: Size in PCS (Z-average), zetapotential and polydispersity index (PDI) of protamine sulfate DNA complexes and AVP derived from them. AVP were prepared from the complexes with the standard amount of AVE liposomes and parallel with the 4 fold amount of AVE liposomes as Sabine Bucké suggested.

Size of PS-DNA complexes in PCS of ~ 90 nm was similar to the size of PEI-DNA complexes (see chapter 3.1). The final AVP derived from the PS-DNA complexes showed a size of 195 nm as well for those containing the standard amount of liposomes, as for those containing the fourfold amount. That is larger than the Z-average of the PEI derived AVP (see chapter 3.1.1) but still in the range of size variations seen during several successful AVP preparations and also comparable to the size measurements of Sabine Bucké that resulted in ~230 nm for this type of AVP.

Zeta potential of the PS-DNA complexes was positive and with + 34.37 mV comparable to that of PEI-derived complexes. AVP produced from them with the standard amount of liposomes was also positive and with + 24.4 mV a bit lower than that of PEI derived AVP. This can be explained by the lower charge surplus of 1: 3.6 instead of 1:4.5 for the PS-DNA complexes.

Interestingly the AVP complexes containing the fourfold amount of liposomes showed a negative zetapotential of –54.2 mV, corresponding well to the -56.9 mV measured by Sabine Bucké. In a control experiment also PEI derived AVP were produced with a fourfold amount of liposomes, but still exhibited a positive charge.

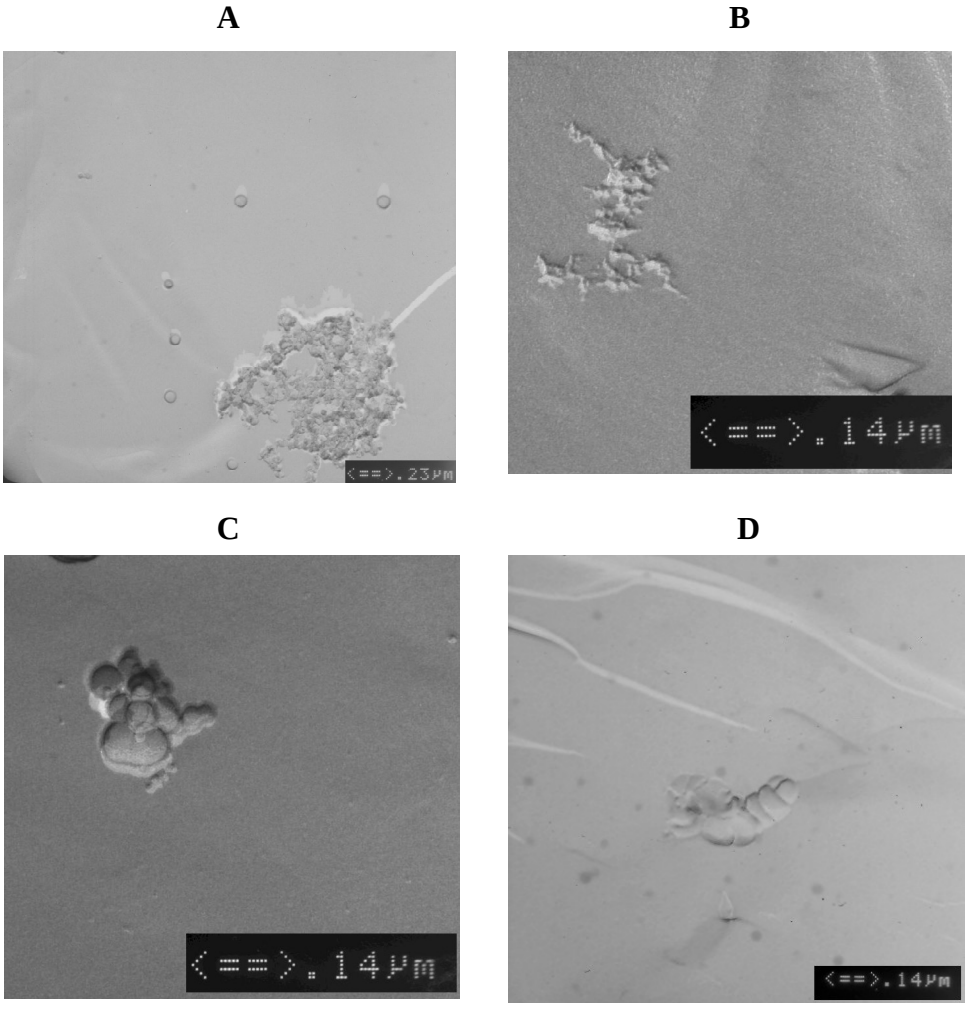

Figure 3.39: Protamine sulfate-DNA complexes (A, B) and AVP prepared with the normal (C) and increased (D) amount of liposomes.

Complexes derived from Protamine Sulfate were also prepared by freeze fracture and examined in TEM (figure 3.39).

Figure 3.39 A and B depict PS-DNA complexes. Small round defined particles, sized about 50 nm were found, but also some bigger aggregates (both figure 3.39 A). Wiry structure that could be sign of partially incomplete DNA complexation were found too (figure 3.39 B).

In the AVP samples containing the normal (figure 3.39 C) and increased (figure 3.39 D) liposome content small aggregations of PS-DNA complexes and liposomes could be seen. They were similar to the "glued together" deformed liposomes found in PEI derived AVP in freeze fracture and Cryo-TEM examinations (see chapter 3.1.2).

Transfection:

Plasmid DNA coding for the green fluorescent protein (GFP) was complexed with protamine sulfate. Part of the complexes was processed with the standard amount and part with the fourfold amount of AVE-liposomes to AVP.

The different AVP were used to transfect HepG2 cells. Their transfection efficiency was compared to "normal" PEI derived AVP.

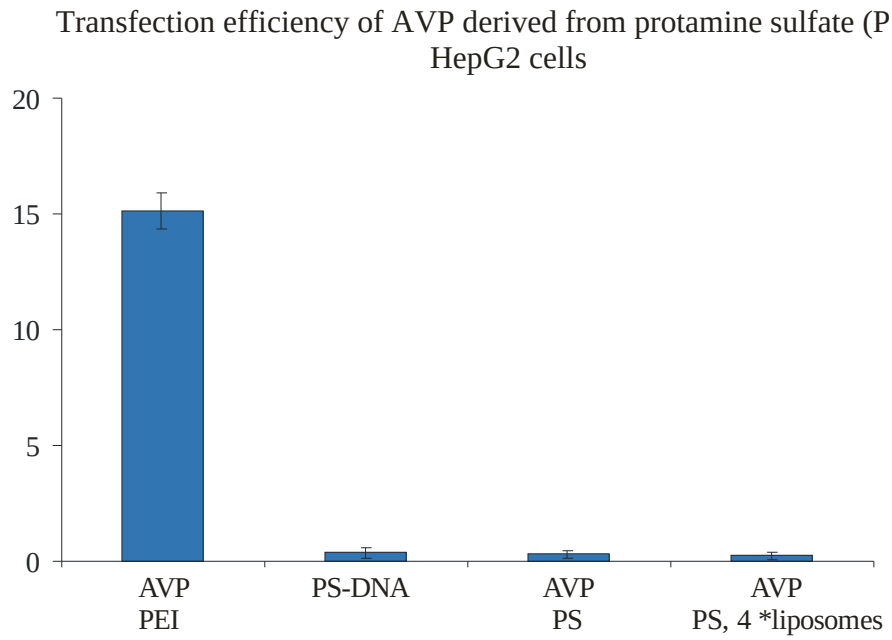

Figure 3.40: Comparison of transfection rate [% transfected cells] of protamine sulfate derived PS-DNA complexes and AVP to normal PEI derived AVP.

As seen in figure 3.40 all the protamine sulfate derived particles were unable to transfect cells with the plasmid coding for the green fluorescent protein. In the same experiment AVP derived from the same plasmid and the same AVE-liposomes but PEI instead of PS as complexation agent were able to transfect cells.

Poly-L-lysine as condensation agent

Poly-L-lysine (PLL) is also investigated as cationic complexation reagent for gene therapy. As Ruponen et al. reported PLL-DNA complexes to be stable against the influence of anionic glycosaminglycans (Ruponen et al., 1999; Ruponen et al., 2001), they were tested as DNA complexation reagent for AVP.

The main focus here was the formation of small defined PLL-DNA complexes as potential cores for the AVP to avoid the formation of bigger AVP aggregates.

PLL-DNA complexes:

Therefore, size of PLL-DNA complexes based on PLL with a molecular weight of 15.000 g/mol and 150.000 g/mol were produced. Charge ratios 2:1 and 4:1 excess positive charge were selected as they were successfully used by Ruponen et al (Ruponen et al., 2001).

MW PLL [g/mol]	Surplus of pos. Charge	Zave [nm] PDI	Zave [nm] PDI Stored overnight
15.000	2:1	102 (+/- 1.15) 0.283 (+/- 0.014)	114 (+/- 0.596) 0.200 (+/- 0.01)
15.000	4:1	84.1 (+/- 8.56) 0.346 (+/- 0.065)	76 (+/- 0.884) 0.359 (+/-0.022)
150.000	**2:1**	**95.8 (+/-0.584)** **0.236 (+/- 0.020)**	**96.4 (+/-0.441)** **0.254 (+/- 0.010)**
150.000	4:1	78.7 (+/- 2.45) 0.346 (+/-0.037)	75.8 (+/- 2.03) 0.388 (+/- 0.040)

Figure 3.41: Size (Z-average) and size distribution (PDI) of PLL-DNA complexes derived from PLL with MW 15.000 and 150.000 g/mol and excess of pos. charge ratio 2:1 and 4:1. Size measurements were performed immediately after production and after overnight storage.

Particle size was measured by PCS directly after preparation and after overnight storage. All formulations resulted in small complexes sized below 120 nm (figure 3.41). The formulation containing PLL MW 150.000 g/mol in charge ratio 2:1 was chosen for further processing to AVP as here particles size and PDI were low and stayed low during overnight storage.

AVP based on PLL-DNA complexes

Freshly prepared PLL-DNA complexes (PLL MW 150.000 g/mol, excess pos. charge 2:1) were processed with AVE-liposomes to AVP. Their size and zeta potential were measured by PCS. The measurement resulted in a Z-average of 225 nm (+/-1.33) and a PDI of 0.201 (+/-0.013). Values comparable with the standard PEI derived AVP.

Interestingly zeta potential of these AVP was negative (-54.1 mV) and reached the negative potential of the AVE liposomes. In contrast to the use of protamine sulfate, already the normal amount of liposomes led to a negative charge. This could be explained by the lower excess of positive charge (only 2:1) in the PLL-DNA complexes. Another explanation would be that free negatively charged liposomes may have influenced the measurement.

PLL-DNA complexes and AVP based on them were also examined by Cryo TEM.

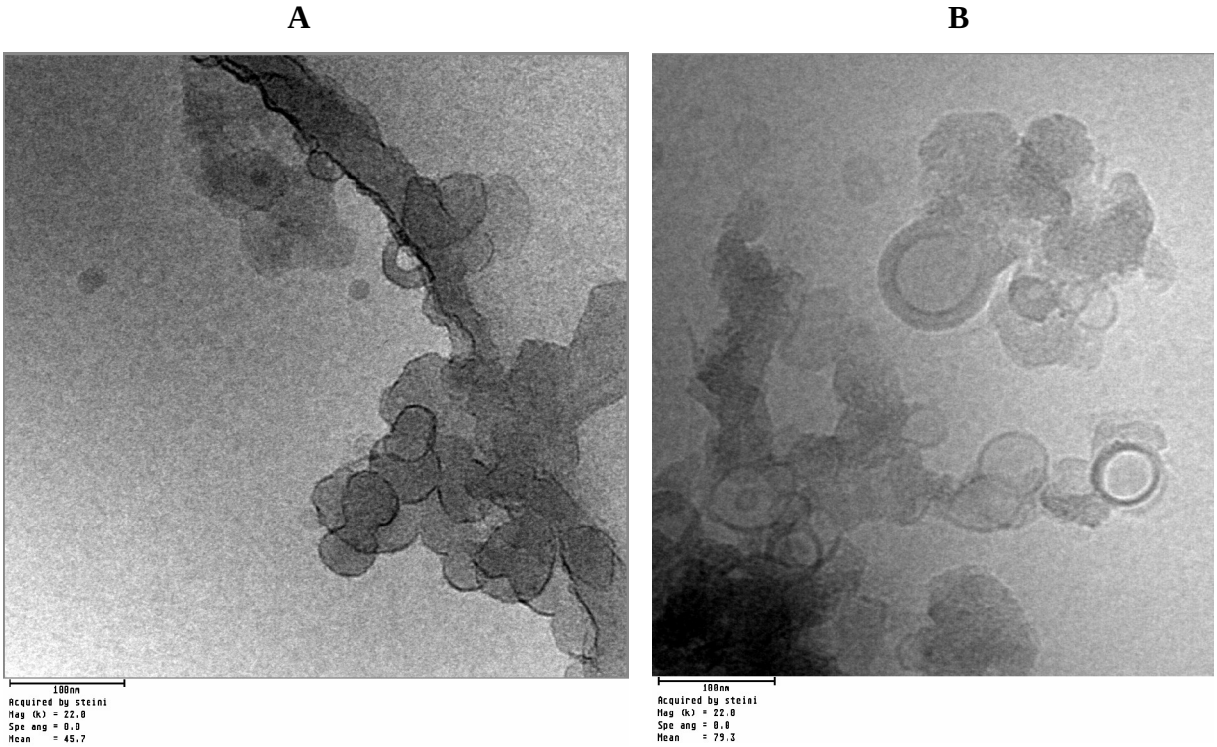

Figure 3.42: PLL derived PLL-DNA complexes (A) and AVP (B) in Cryo-TEM.

PLL-DNA complexes (figure 3.42 A) appeared in Cryo-TEM as small round particles sized about 60 nm clustered at the edge of the examination grid. The AVP (figure 3.42 B) sample based on PLL-DNA complexes contained liposomes, seemingly partially coated and aggregated to small clusters with PLL-DNA. However, neither the filled particles known from PEI derived AVP nor the glued together clusters of deformed liposomes or bigger aggregates were visible. In the PLL-DNA mass attached to the liposomes kind of a fingerprint structure, described by Labat-Moleur (Labat-Moleur et al., 1996) as sign of complexed DNA, could be found.

Transfection efficiency:

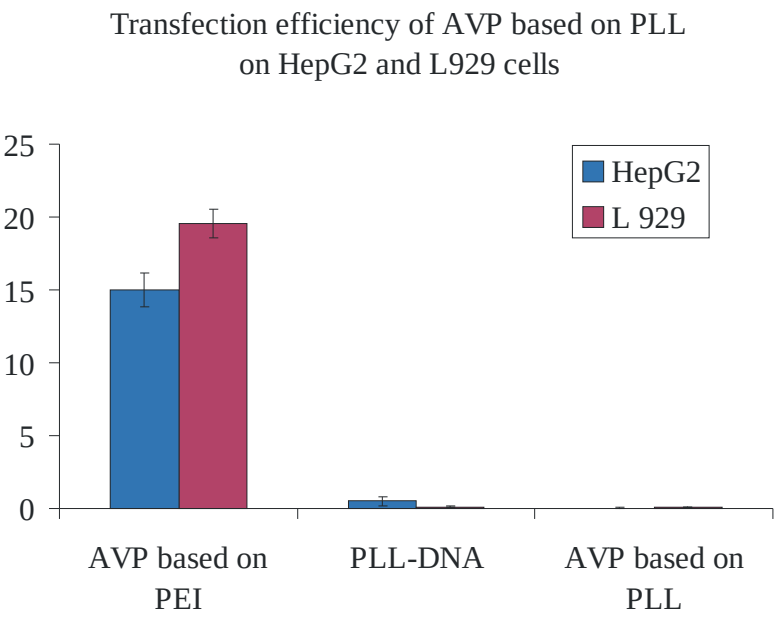

Figure 3.43: Transfection rate [% transfected cells] of HepG2 and L929 cells after transfection with PLL-DNA complexes and PLL based AVP in parallel to PEI derived AVP.
Error bars depict standard deviation

Transfection efficiency of the described PLL based DNA complexes and AVP was tested in cell culture on the cell lines HepG2 and L929 mouse fibroblast using plasmid coding for green fluorescent protein. In contrast to a parallel tested PEI derived AVP sample they showed nearly no ability to transfect either line.

jetPEI ® as DNA condensation agent

jetPEI ® is a commercial transfection reagent based on “linear polyethylenimine” (Polyplus, 2002). So the polymer does not principally differ from the PEI MW 5000 g/mol that was used as standard transfection reagent in this work. But degree of branching and molecular weight still can differ and influence transfection efficiency. Also the used PEI MW 5000 g/mol is intended as cheap standard chemical while jetPEI® is specially intended and sold as reagent for transfection. So jetPEI®-DNA complexes were shortly investigated as a potential educt for AVP mainly in respect to a possible improvement of transfection efficiency.

An examination of AVP derived from jetPEI ® after negative staining preparation showed particles similar to the ones seen in PEI MW 5000 g/mol based AVP samples (see 3.1.2).
Round particles sized ~ 150 nm and interpreted as the filled structures derived from liposomes were found. Next to them and sometimes also attached to them also smaller particles sized about 50 nm were visible and interpreted as PEI-DNA complexes.

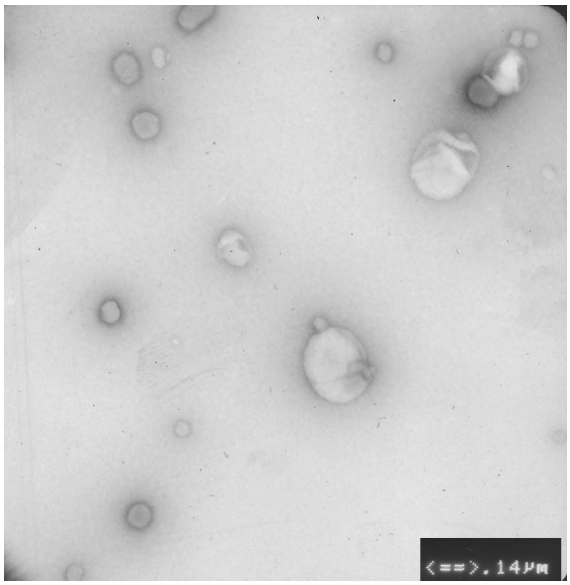

Figure 3.44: Electron microscopy of jetPEI based AVP after negative staining preparation. Seemingly filled particles sized about 150 nm are found next to smaller about 50 nm sized particles interpreted as PEI-DNA.

Transfection:

JetPEI was used to complex GFP plasmid and process the complexes with AVE-liposomes to AVP according to the standard procedure, but with a N/P ratio of 7 as recommended by the manufacturer. Those jetPEI derived AVP prove successful in first orientation transfection experiments. In a direct comparison of jetPEI derived AVP to AVP derived from standard PEI MW 5000 g/mol, AVP derived from jetPEI showed superior transfection rates on HepG2 cells as seen in figure 3.45. Moreover, they reached high transfection rate already with a dose corresponding to 1 µg plasmid per well (as recommended by jetPEI´s manufacturer) instead of the 2 µg plasmid per well established as optimum for standard AVP.

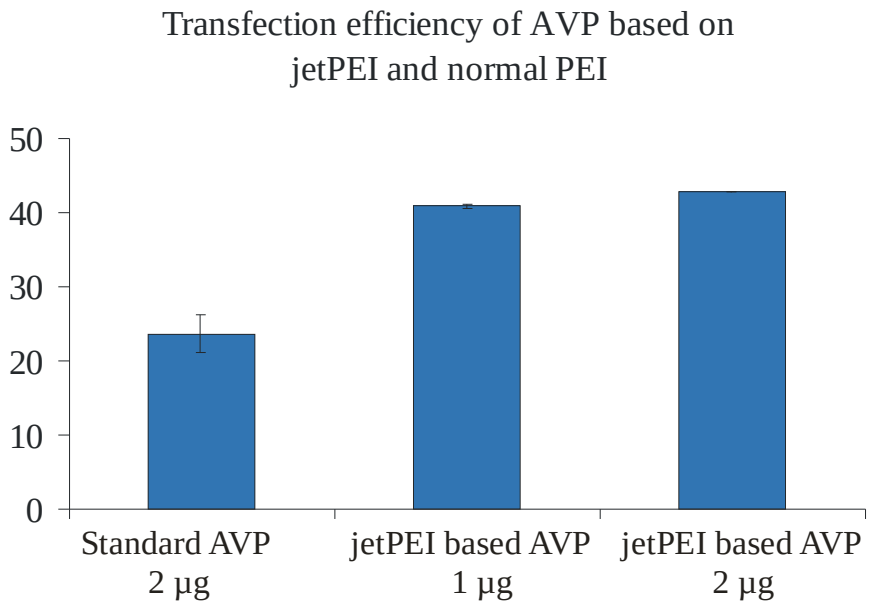

Figure 3.45: Transfection efficiency as percentage of GFP expressing HepG2 cells after transfection with AVP based on PEI MW 5000 g/mol (Standard AVP) and jetPEI. Standard AVP were tested in a dose of 2 µg (n=3) and jetPEI AVP in a dose of 1 µg (n=2) and 2 µg (n=1).

Summary:

The differing cationic reagents protamine sulfate, poly-L-lysine and jetPEI were all able to complex DNA. But their complexes and the derived AVP showed different properties on closer examination.

Protamine sulfate as complexation agent led to DNA complexes and AVP that were comparable to PEI derived AVP in their size and form as depicted in freeze fracture. Their zetapotential after processing with the normal amount of AVE was positive. A surplus of AVE liposomes led to a negative zetapotential which is in accordance with the earlier investigations of Bucké (Bucké, 2001). This constitutes an interesting point with regard to a possible *in vivo* application, as less interaction with positively charged plasma components can be expected from a negatively charged gene transfer vehicle. Sabine Bucké and Christian Welz (Welz et al., 2000) had already shown great effectiveness of protamine sulfate derived AVP in the transport of oligonucleotides. However, in our experiments PS derived AVP were unable to transfect HepG2 cells with GFP-plasmid. As we had chosen GFP expression in cell culture as reference test system for the biological effectiveness we focused on PEI derived AVP in further experiments.

PLL-DNA complexes prove to be compact as shown in PCS measurements and Cryo-TEM. The AVP derived from them appeared to have the same size in PCS, but their structure in Cryo-TEM differed greatly from the structures observed for AVP based on PEI or protamine sulfate. Furthermore, they were not able to transfect plasmid GFP in our *in vitro* experiments. This result matches the result of experiments of Ruponen et al. where PLL-DNA complexes were inferior to PEI in respect to their ability to transfect cells (Ruponen et al., 2001).

JetPEI derived AVP sample appeared similar to standard AVP derived from PEI MW 5000 g/mol in PCS and electron microscopy examination. This is logical as principally the same polymer was used. Transfection efficiency of those particles was visibly increased in first trials on the cell line HepG2 and also the “dose” of DNA processed to AVP needed to obtain this result was lower. So this AVP variation promised to be a valuable tool to increase transfection rate, which was confirmed in later cell culture experiments. However, those later investigations (see chapter 3.5.2) showed that transfection efficiency did not profit on all cell lines.

3.4.2 Variation of lipid composition in AVE liposomes

The blueprint for the layout of AVP with a core of condensed DNA and an anionic lipid hull was adopted from natural enveloped viruses. Also the composition of the original AVE (artifcial viral envelope) liposomes of DLPE, DOPS and Chol was inspired by the lipid composition of a virus, to be specific from the HIV virus (Chander and Schreier, 1992). While already AVP derived from the original AVE were successful there were indications that AVE could be improved further to obtain higher transfection efficiency.
In the work of Christian Rothkopf on transfection of pulmonary epithelial cells by AVP the exchange of DLPE for DOPE led to increased transfection success.
Peter Hölig showed in binding studies of AVE liposomes to HUVEC cells (Hölig, 2007), that AVE liposomes containing an activated N-glut-PE anchor as preparation for an intended coupling to antibodies already showed increased unspecific binding to cells.

Modified AVE-liposomes and resulting AVP

Both directions were followed in order to improve AVP. Therefore, two variations of the original AVE liposomes (composition DLPE:DOPS:Chol, molar ratio 1:1:1) were produced:

- AVE-DOPE: here the DLPE was replaced by DOPE, resulting in a composition of DOPE, DOPS and Chol 1:1:1 molar ratio
- AVE-act, into which an additional N-glut-DOPE lipid was introduced, which led to a composition of 3/10 DLPE, 3/10 DOPS, 3/10 Chol and 1/10 N-glut-DOPE molar ratio. These liposomes also went through the activation process for the N-glut DOPE anchor (see chapter 2.1.1).

No apparent changes in the physical parameters size and zeta potential of the modified liposomes were observed. The different AVE liposomes were sized about 90 nm and had strong negative zeta potential.

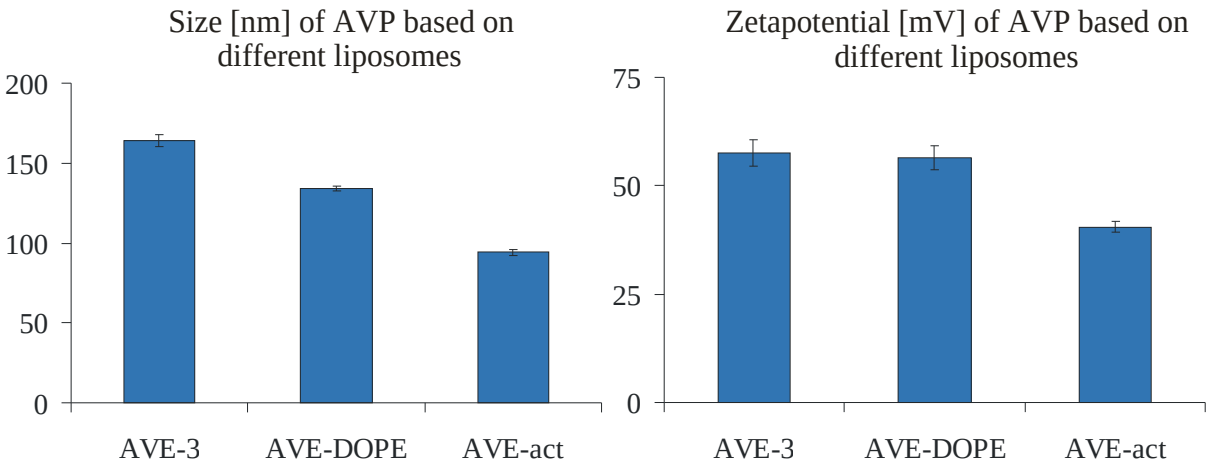

Figure 4.46: Size (Z-average) in PCS and zetapotential of AVP derived from different types of AVE liposomes. Error bars depict standard deviation.

The AVP derived from the different kind of AVE liposomes were comparable in regard to their size and zeta potential but showed small variations as seen in (Fig 4.46). In this measurement AVP derived from AVE-act liposomes led to smaller and a bit less charged particles.

Influence of modified liposome composition on transfection efficiency:

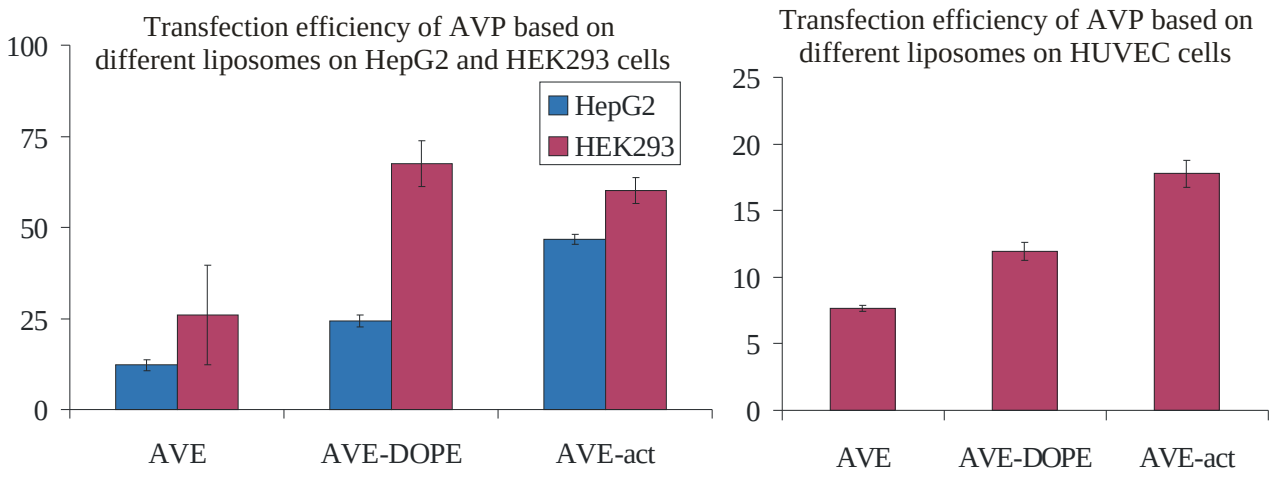

Figure 3.47: Two typical transfection experiments in which the transfection efficiency [% transfected cells] of AVP derived from different types of liposomes was compared with n = 3 for the experiment on HepG2 and HEK 293 cells and n=2 for the experiment on HUVEC cells.

Aim of the modification of the AVE-liposomes was to improve the ability to transfect cells of the AVP. Verification in cell culture showed an improvement by both methods on different types of cells. On HepG2 und HUVEC cells, AVP derived from AVE-act liposomes showed highest transfection efficiency, followed by AVP derived from AVE-DOPE. On HEK 293, AVE-act and AVE-DOPE led to similarly increased transfection efficiencies with a slight plus for AVE-DOPE.

While AVE-DOPE are prepared exactly in the same way as standard AVE, AVE-act preparation includes incubation with the carbodiimid EDC (see chapter 2.1.1) and purification on a gel bead column. To certify that the improved transfection rate is due to the activated anchor, control experiments were performed:

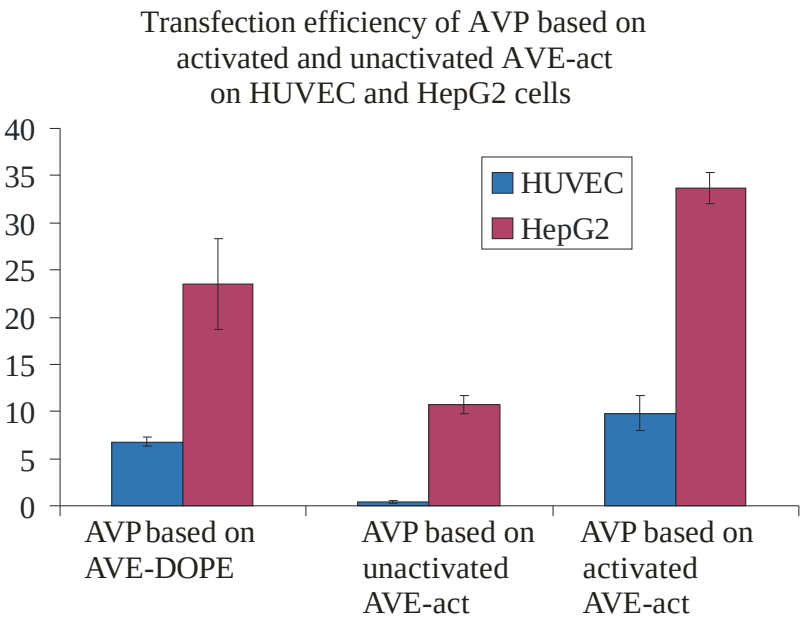

Figure 3.48: Transfection efficiency [% GFP expressing cells] after transfection with AVP based on AVE-act liposomes before and after activation compared to AVP based on AVE-DOPE liposomes as standard. Error bars depict standard deviation.

AVE liposomes having the composition of AVE-act (1/10 N-glut-DOPE) were prepared with and without going through the activation process and used for AVP preparation. The activated AVE-act liposomes increased transfection efficiency strongly (figure 3.48). AVP produced from them surpassed transfection efficiency of AVE-DOPE based AVP as well on HepG2 as on HUVEC cells. Liposomes with the same composition that were not activated did not show this improvement.

In another experiment standard AVE-3 without anchor lipid went through the complete activation process but did not lead to improved transfection compared to untreated AVE-3. So neither the components of the liposomes nor the activation process itself but only the combination is responsible for the increased transfection success.

Toxicity of AVE-act and AVP-act

As EDC is a reactive and toxic chemical and the toxicity of the activated anchor itself was not known, a cell toxicity assay was performed.

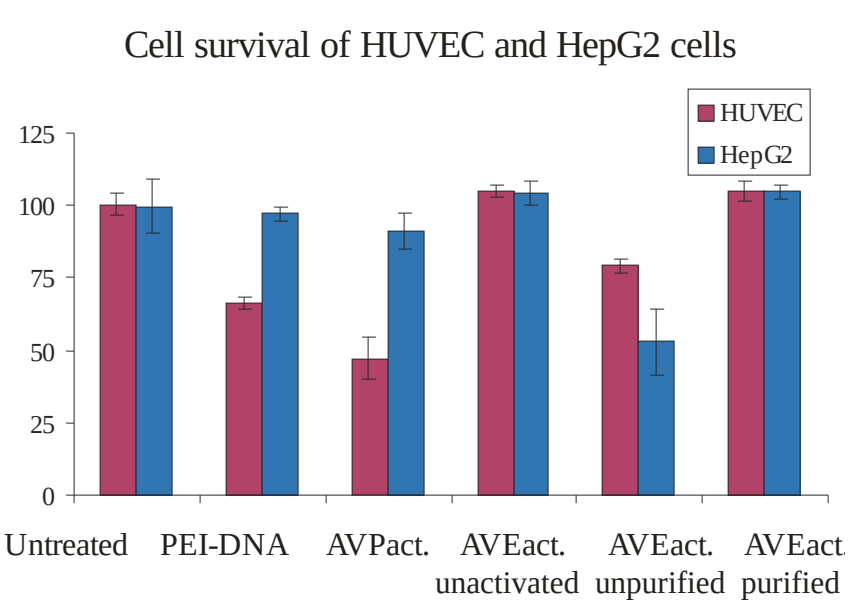

Figure 3.49: Survival of HepG2 and HUVEC cells [% of untreated control] treated with AVP-act or its components PEI-DNA complex and AVE-act liposomes (unactivated, activated but unpurified, and purified). Error bars depict coefficient of variation, the experiment was performed with n = 3.

Cells were treated with PEI-DNA complexes and AVP-act derived from those PEI-DNA complexes. Additionally pure AVE-act liposomes before activation, activated but unpurified and activated and purified were tested. The amount of reagent per well was the same as added during normal transfection. Also treatment of the cells (6 h incubation with reagent followed by media change and 18 h rest before measurement) was identical to a standard transfection.

In the Sulforhodamine B (SRB) assay (see 2.1.15) cell viability is estimated by measuring total protein of attached cells, assuming that dead cells detach and get washed away. This examination (figure 3.49) showed a toxic effect of the PEI-DNA complexes and the AVP-act derived from them on the sensitive primary HUVEC cells, while the more robust HepG2 cells were nearly unaffected. The pure AVE-act liposomes themselves were not toxic as long as they were either purified from excess EDC or not activated at all, while the activated unpurified sample containing excess EDC showed toxicity on both cell lines.

Summary:

As expected the different variations of AVE liposomes were of comparable size and zetapotential as they still contained comparable amounts of anionic lipid (phosphatidylserine) and were prepared by the same routine. Consequently also the AVP derived from them showed similar physical properties.

Both liposome variations successfully increased transfection efficiency of AVP based on them.

The improvement found by including the phospholipid DOPE in our system is in accordance with earlier investigations that showed a positive effect of the "helper" lipid DOPE on transfection efficiency for gene transfer vehicles based on cationic lipids (Felgner et al., 1994; Hafez et al., 2001; Hui et al., 1996). Fahrhood et al. explained this increased transfection efficiency by the membrane destabilizing properties of DOPE caused by its ability to form hexagonal structures (Farhood et al., 1995).

The AVE-act liposomes also led to a better transfection and the improvement could be located to be the activated anchor itself. This is in accordance to the work of Peter Hölig (Hölig, 2007), who had shown an increased unspecific binding of liposomes containing this activated carbodiimid anchor to cells. The AVE-act liposomes themselves prove to be non-toxic when purified from excess EDC as it was done in routine procedure.

So both methods were valuable in increasing transfection efficiency. The unspecific binding of AVE-act to cell surfaces is an effect that influences transfection positive in cell culture. Here it can play an important role in improving transfection efficiency for research assays, as it did in research on an overexpressed protein (see chapter 3.5.2). But it would not be applicable in *in vivo* experiments, as here specific targeted binding to certain cells is aspired.

3.4.3 Dependence of AVP formation from shear forces

The AVP preparations in the chipmixer (see chapter 3.3.) did not show a dependence of particle size or transfection efficiency from mixing speed. Therefore, the initial theory that the successful combination of PEI-DNA complexes with AVE liposomes to AVP depends on strong shear forces was doubted. Occurring adsorption processes interfered in experiments using the chipmixer and made conclusions hard. Therefore, a new set of experiments to determine the influence of shear forces for each preparation steps was started. Here just the surfaces also present in standard manual preparation by pipetting were used. To avoid effects caused by interactions with differing surface areas and materials all preparations were done in eppendorf tubes that were also used in manual preparation.

Shear forces during the two step preparation of AVP were varied in four manually prepared samples. The manual pipetting steps of the standard preparation with tip attached to the bottom of the eppendorf tube were replaced systematically by soft inversion of the eppendorf cup for 10 times minimizing the occurring shear forces.

- Sample I was prepared by manual pipetting with attached tip as well in the complexation of PEI with DNA as in the processing with AVE liposomes. This procedure corresponds to the classical preparation as described in chapter 2.1.3
- Sample II was prepared by manual pipetting only in the complexation of PEI-DNA followed by mixing with AVE liposomes by gentle inversion.
- Sample III was prepared by soft inversion mixing for both steps.
- Sample IV was prepared by adding PEI and liposomes to the DNA in one step and mixing by inversion. Thereby also the ripening time normally included between complexation and combination with liposomes was omitted.

Plasmid coding for GFP was used as model DNA and allowed testing transfection efficiency in cell culture besides physical characterisation by PCS and zetapotential measurements.
The experiments were carried out with AVP derived from three different types of liposomes and tested on HepG2 and HEK 293 cells. This was done to verify that possible resulting size and zetapotential variations or uniformities of AVP are not restricted to one type of AVE liposomes nor possible impacts on cell culture influenced by one type of test cells,

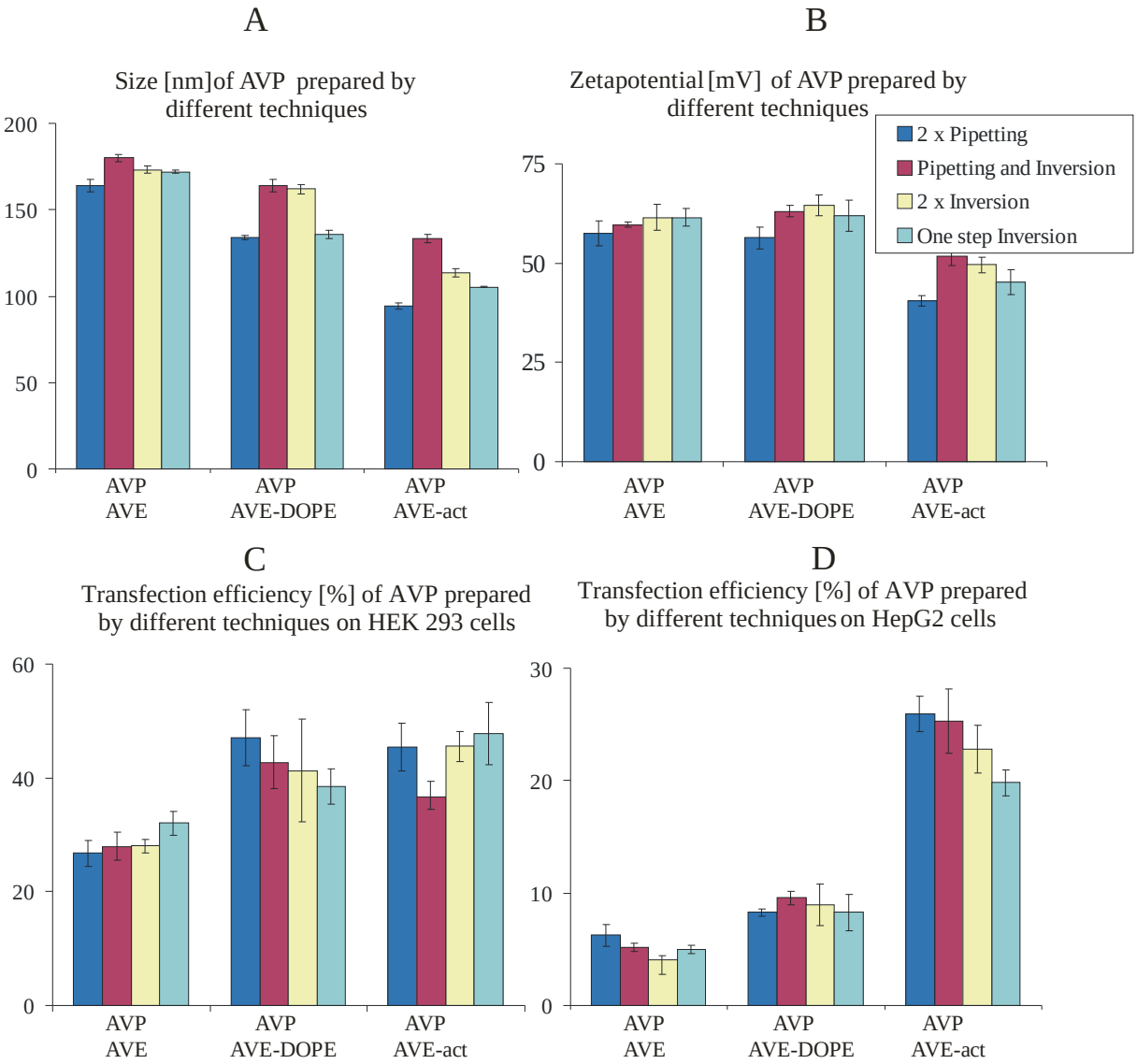

Figure 3.50: AVP produced by different techniques characterized by size (Z-average) in PCS, zetapotential and transfection efficiency (percentage of GFP expressing cells) on HEK 293 and HepG2 cells. Error bars depict standard deviation.

Neither size, zetapotential nor transfection efficiency of the samples prepared with differing shear forces showed big differences as seen in Figure 3.50. A trend that AVP prepared by manual pipetting were smaller than those prepared by inversion could be interpreted from the data but the size differences are only minor.

In general transfection was more successful on HEK 293 cells, while on HepG2 cells transfection rate of AVE-3 and AVE-DOPE derived AVP was low. The overall picture of differently prepared AVP tested on both cell lines showed no superiority for one of the preparation techniques. All variations in the preparation process resulted in particles that were equally small, equally charged and equally successful in transfection as those prepared by standard pipetting.

Another sample of AVP based on AVE-act was prepared by the two step preparation with soft inversion and resulting low shear forces in both steps and examined in Cryo-TEM.

A **B**

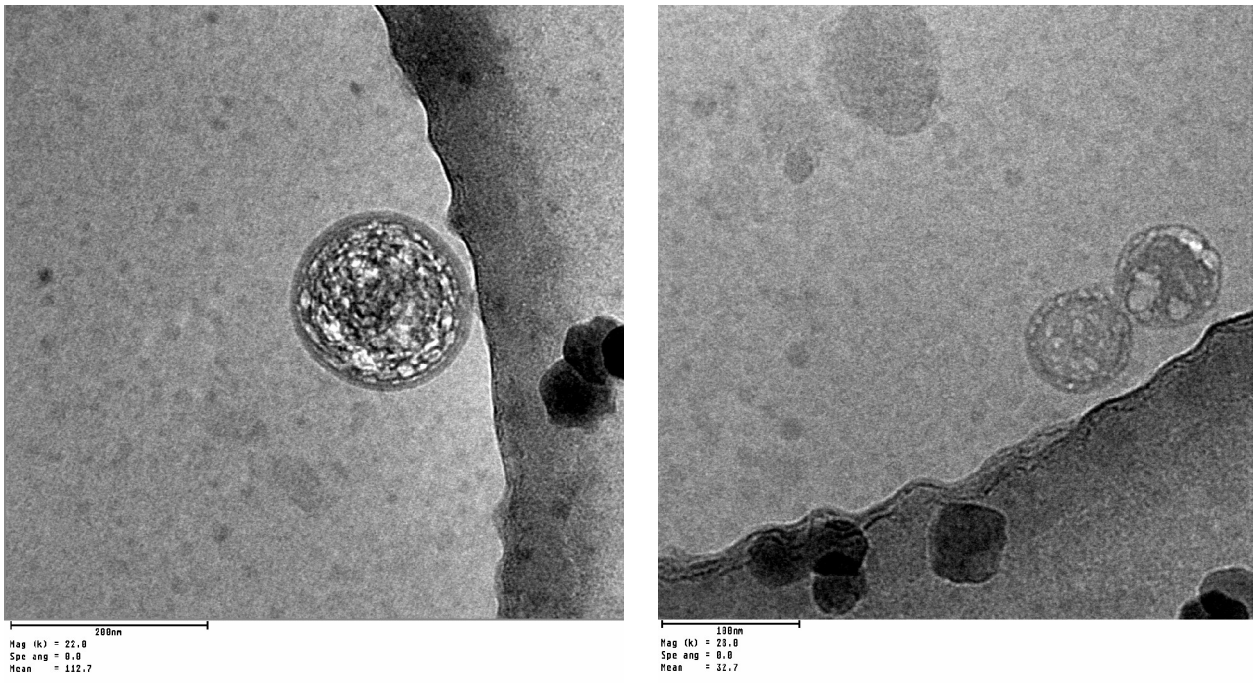

Figure 3.51: AVP derived from AVE-act liposomes prepared by a two step preparation using only soft inversion to avoid strong shear forces examined in Cryo-TEM. Size bar corresponds to 200 nm in A and to 100 nm in B.

Here the filled particles enclosed by a smooth liposomal membrane were found again (figure 3.51 A) next to small separate particles, interpreted as PEI-DNA complexes (3.51 B). So the appearance of the sample in Cryo-TEM was similar to the AVP prepared by standard manual pipetting (see chapter.3.1.2).

Summary:

All variations in the preparation procedure led to small and well transfecting particles that did not differ in size, zeta potential or transfection efficiency. The sample prepared by soft inversion in both steps contained similar filled particles and free PEI-DNA aggregates as seen in samples prepared by pipetting. Even omitting the two step preparation and the ripening period for the PEI-DNA complexes did not change the final particles. So the theory that in AVP preparation high shear forces are needed to obtain filled particles and good transfection rates did not prove to be true. In contrast the results indicate that AVP are generated by a self formation of oppositely charged structures for which only mixing and not applying force is necessary.

3.5. Employing AVP for novel cell culture applications

Parallel to the determination of the properties of AVP and their formation process, these particles were also applied for new applications in co-operations with other work groups.

3.5.1 Competitiveness of AVP for siRNA transfection

Short interfering RNA (siRNA) is a new promising approach to gene therapy. Shortly siRNA allows the effective inactivation of specific mRNA and thereby suppression of genes (Elbashir et al., 2001).
In a co-operation with Dr. Lars Tönges from the group of Dr. Paul Lingor from the medical faculty of the University of Göttingen, AVP were used to transfect siRNA into primary neuronal cells, which was a new challenge for AVP.

Design of AVP for siRNA transfection

AVP had not been used for transfection of siRNA before and primary cells are known to be very sensitive to transfection vectors (Lingor et al., 2004).
Unlike in plasmid transfection where the DNA has to reach the nucleus, siRNA only has to reach the cytoplasm in order to show its effect. That is true also for antisense oligonucleotides that Sabine Bucké had already successfully transfected into cells using AVP (Bucké, 2001). In her experiments AVP based on protamine sulfate with an increased amount of AVE liposomes were superior to the other formulations.
At the time of the planning of the siRNA experiments the AVP based on AVE liposomes containing DOPE were the most successful variety in transfecting GFP plasmid in cell culture.
Based on those thoughts preparation of several AVP variations was arranged:

- PEI based AVP containing AVE liposomes
- PEI based AVP containing AVE-DOPE lipsomes
- Protamine sulfate based AVP containing AVE liposomes
- Protamine sulfate based AVP containing the fourfold amount of AVE-3 liposomes

Together with Lars Tönges Cy-3 fluorescence labelled siRNA was processed to the different types of AVP and used to transfect primary hippocampal neuronal cells with a dose of AVP

corresponding to 100 ng siRNA per well. This dose corresponds to 1/20 of the dose used in plasmid transfection before. Parallel also another novel transfection reagent: stearylated octaarginin (Futaki et al., 2001) and the commercial transfection reagent Lipofectamin ® were tested.

In this evaluation AVP, and also the two other reagents, succeeded in transporting the fluorescence marked siRNA into the cells, visible as accumulation of fluorescence in the cells. The PEI based AVP containing AVE-DOPE liposomes led to the highest accumulation of fluorescence of the different AVP samples. Therefore, it was chosen as representative AVP variation for the experiments to come.

Lars Tönges successfully used these AVP for further si-RNA transfection experiments, now transferring not only fluorescence marked model siRNA, but siRNA targeted on mRNA coding for a target protein. Usage of AVP for this task led to specific knockdown of the protein combined with low toxicity and is depicted in detail in the joint publication (Toenges et al., 2006).

3.5.2 Using AVP to explore the role of the enzyme Thiopurine-S-methyltransferase (TPMT) in stable transfected cells

In a co-operation with the groups of Prof. Dr. Julijana Kristl and Prof. Dr. Irena Mlinaric-Rascan (both faculty of pharmacy, Ljubljana, Slovenia) during a one year research period in Slovenia AVP were used to investigate the role of the enzyme Thiopurine-S-methyltransferase (TPMT).

The enzyme TPMT is of pharmaceutical relevance as it catalyzes the inactivation of thiopurine drugs such as 6-mercaptopurine (6-MP) and 6-thioguanine (6-TG). Genetic polymorphisms of this enzyme occurs and can lead to lowered enzyme activity (Tai et al., 1999; Milek et al., 2006) and consequently to increased toxicity during standard dose therapy with thiopurine drugs (Weinshilboum, 2001; Krynetski et al., 1996).

The joint project was aimed at clarifying the endogenous role of TPMT and at usage and optimization of AVP as versatile transfection reagent for this task. In detail: AVP were optimized for the transfection of target cell lines and used to transfect those cells with a plasmid coding for a fusion protein between TPMT and green fluorescenting protein (EGFP) designed by Miha Milek who is investigating the enzyme (Milek et al., 2006). Furthermore, cells that stably overexpress the recombinant protein and reference cells that stably overexpress the pure GFP protein were established and characterized.

The results of this successful project that demonstrated the potential of AVP in cell biology studies and provided a valuable beginning of futher research on the enzyme TPMT were published in a joint publication (Egle et al., 2007) and are therefore summarized only shortly below:

Optimization of artificial viral particles for target cells

Target cells were HEK 293 kidney cells and HepG2 liver carcinoma cells, that both had been successfully transfected by AVP before (see chapter 3.4.2), and the T-lymphoma cell line Jurkat that is particularly difficult to transfect (Schakowski et al., 2004).

So the knowledge gained in researching different AVP formulations (see chapter 3.4) was used and AVP were varied by:

- use of different types of AVE liposomes
- different mixing ratios of PEI-DNA
- replacement of the normally used PEI MW 5000 g/mol for jetPEI®

in order to find an AVP formulation suitable for the transfection of Jurkat cells.

Jurkat cells were successfully transfected and best transfection results were achieved using AVP based on AVE-act (see chapter 3.4.2) and containing PEI MW 5000 in the standard charge ratio (see chapter 2.1.3).

Establishment of stable EGFP-TPMT protein expressing cell lines

To facilitate research on the expressed recombinant protein AVP were used to establish cell lines expressing the recombinant protein not only transiently, but stably over several generations, which constituted a new challenge for AVP.

So Jurkat, HEK 293 and HepG2 cells were transfected with plasmids coding for the recombinant EGFP-TPMT fusion protein and for EGFP as reference. Resistance to the antibiotic G418®, normally toxic also for eukaryotic cells, was also encoded in the used plasmids. Therefore, stable transfected cells could be identified and selected by the addition of G418® to the cell culture media.

The degree of expression of the recombinant protein in the selected clones was determined by measuring the intensity of the green fluorescence of the EGFP protein using flow cytometry. Cell populations showing high fluorescence intensity and monoclonal characteristics were successfully established and the populations showing highest fluorescence were chosen (see figure 3.52).

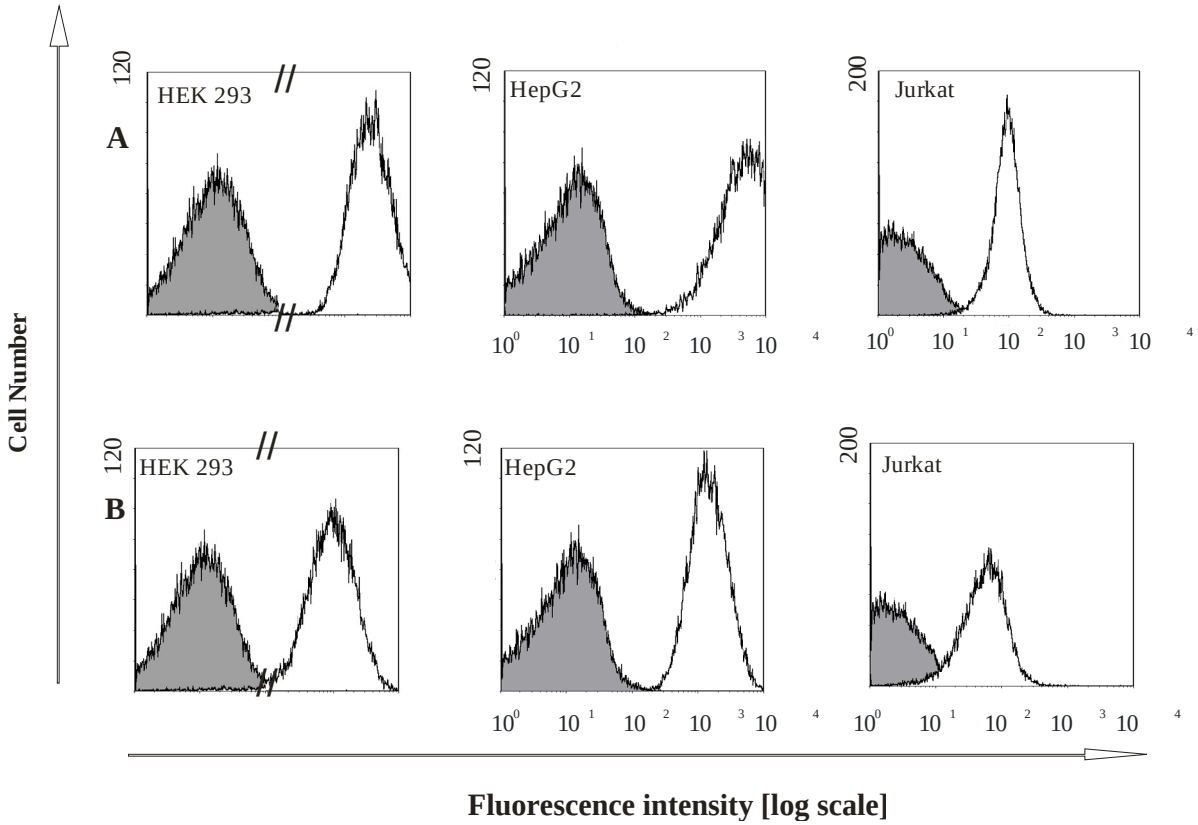

Figure 3.52: Selection of stably expressing clones

Flow cytometry histogramms of green fluorescence of selected stable clones expressing either green fluorescent protein EGFP (A), or recombinant EGFP-TPMT protein (B). The selected stable clones show homogenous populations of cells with increased fluorescence compared to the autofluorescence of untransfected cells (grey). Fluorescence intensity of transfected HEK 293 clones exceeded the average detection range. Therefore, intensity profiles of HEK 293 are depicted on a fractured log scale (Egle et al., 2007).

Parallel, expression of the recombinant fusion EGFP-TPMT protein was also detected in the selected stable transfected cell populations by immunoblotting with anti-TPMT antibodies after separation of the cell proteins by gel electrophoresis (Egle et al., 2007).

Further characterization of cells expressing the recombinant protein

After detection of the recombinant fusion protein in the stable transfected cells by flow cytometry and immunoblotting those cell poplulations were characterized further. In a toxicity assay a modified sensitivity to thiopurine drug, sign of an active enzyme (Coulthard et al., 2002; Dervieux et al., 2001), was shown for HEK293 cells stable expressing EGFP-TPMT.

And in fluorescence microscopy the recombinant protein could be detected distributed evenly across all cellular compartments (Egle et al., 2007).

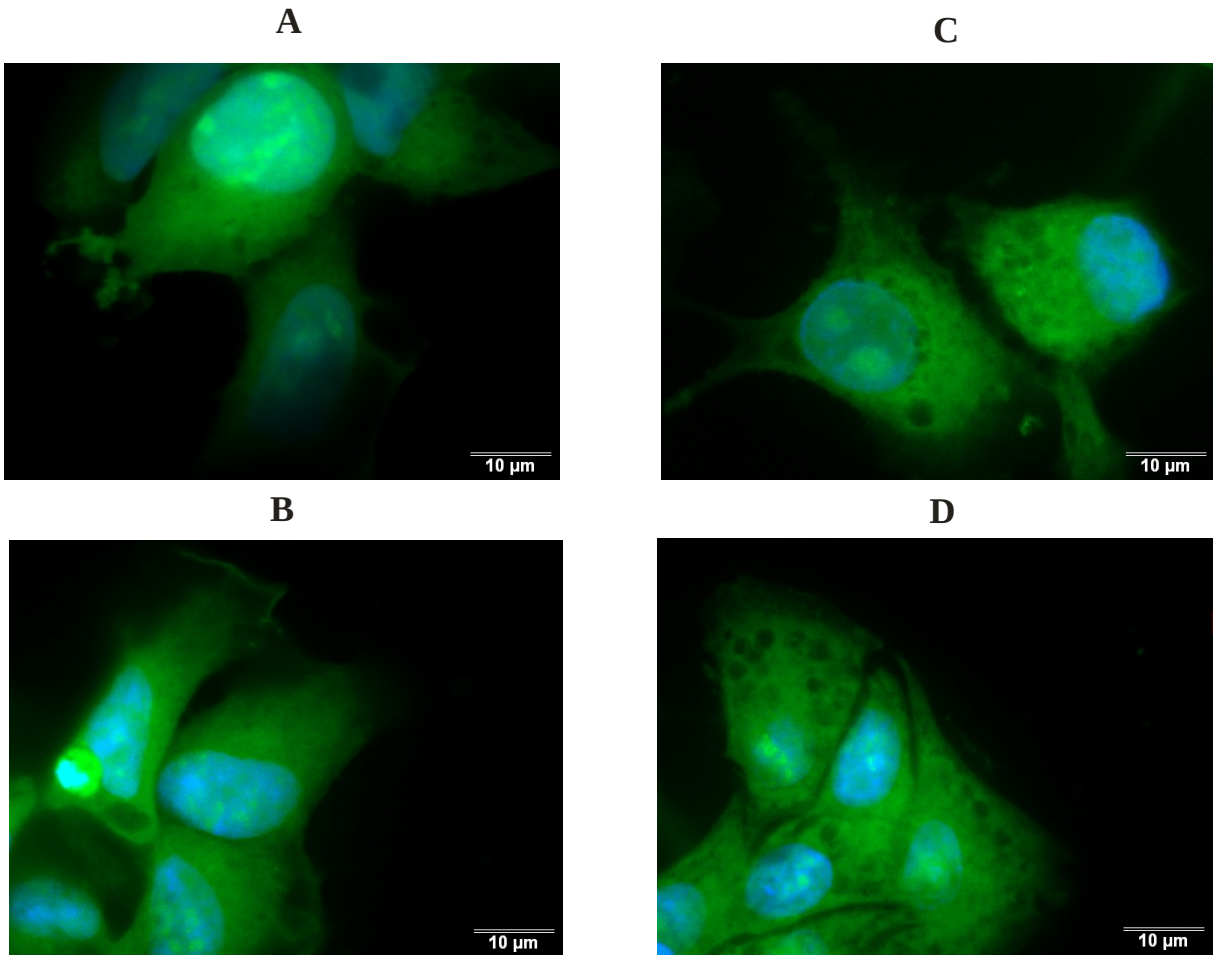

Figure 3.53 Indetermined expression of EGFP-TPMT protein in fluorescence microscopy. Green fluorescence of HEK 293 clones stably expressing EGFP (A) or the recombinant EGFP-TPMT (B) and HepG2 clones also stable expressing EGFP (C) or EGFP-TPMT (D) observed with 60 -fold objective in fluorescence microscopy. Nuclei were additionally stained blue (Egle et al., 2007).

3.6 Observations and comments on testing AVP *in vitro*

Biological success of our systems was estimated by transfecting cells in cell culture with a plasmid coding for green fluorescent protein and determining the percentage of cells expressing that protein in flow cytometry (see chapter 2.1.13 and 2.1.14).
Transfection *in vitro* can be an aim in itself e.g. to clarify processes in the cell (see overexpression of an enzyme in chapter 3.5.2). But in research on gene delivery vectors it is mostly used as model for the effectiveness of the vectors to actually transfect cells in respect to a later *in vivo* application.
Therefore, the model conditions have to be selected carefully to obtain results that are evaluable, comparable and lead to reproducible results.

Influence of media on transfection efficiency

One important parameter in *in vitro* transfection experiments is the cell culture medium used during the transfection. Different media are used that can range from pure buffer to full cell culture media that allows growth and proliferation. One important factor is the presence of serum in the media, which is beneficial for cells and an approximation to natural condition. But serum ingredients can interact with the gene transfer vectors itself and reduce their effectiveness (Tros de Ilarduya, Duzgunes, 2000).
Transfection procedure established by advanced co-workers was changing normal cell growth media to media 199 (M199) containing 10 % FCS before transfection. After transfection cells were incubated for six hours with the transfection reagent, followed by media change back to normal growth medium. As new cell lines were employed transfection in normal cell growth media was tested vs. the suggested M199 containing 10 % FCS. Media was changed back to normal media six hours after transfection for both assays.

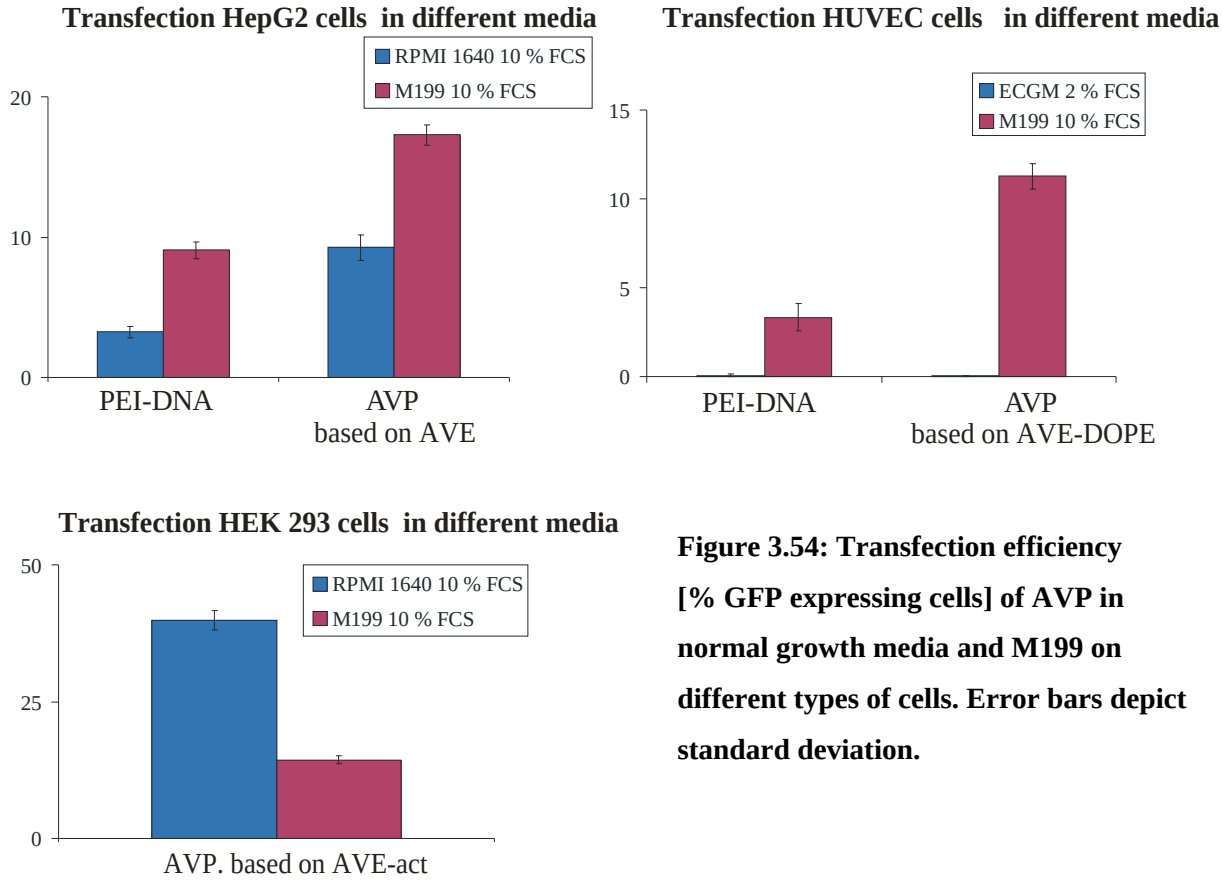

Figure 3.54: Transfection efficiency [% GFP expressing cells] of AVP in normal growth media and M199 on different types of cells. Error bars depict standard deviation.

Change of normal growth media to M199 including 10 % fetal calf serum (FCS) led to a strong improvement of the number of transfected cells for HepG2 and HUVEC cells. In contrast to that transfection of HEK 293 cells was superior in native growth medium RPMI1640 without media change prior to transfection. Here it could also have played a role that HEK 293 cells are only weakly attached to the well surface and two media changes in less than 8 hours might led to a partially detachment of the cells.

Influence of serum containing media on particle size

AVP were able to transfect cells in 10 % FCS containing media, so a short investigation of their behaviour in the 10 % containing FCS M199 was done:

PEI-DNA complexes and two lots of AVP, both derived from a production in the chipmixer Statmix 6, were diluted as routinely done for PCS measurements in Tris buffer 10 mM. Parallel they were diluted in the media used in the transfection step in cell culture: M199 containing 10 % FCS. After 30 minutes incubation size and zetapotential were compared.

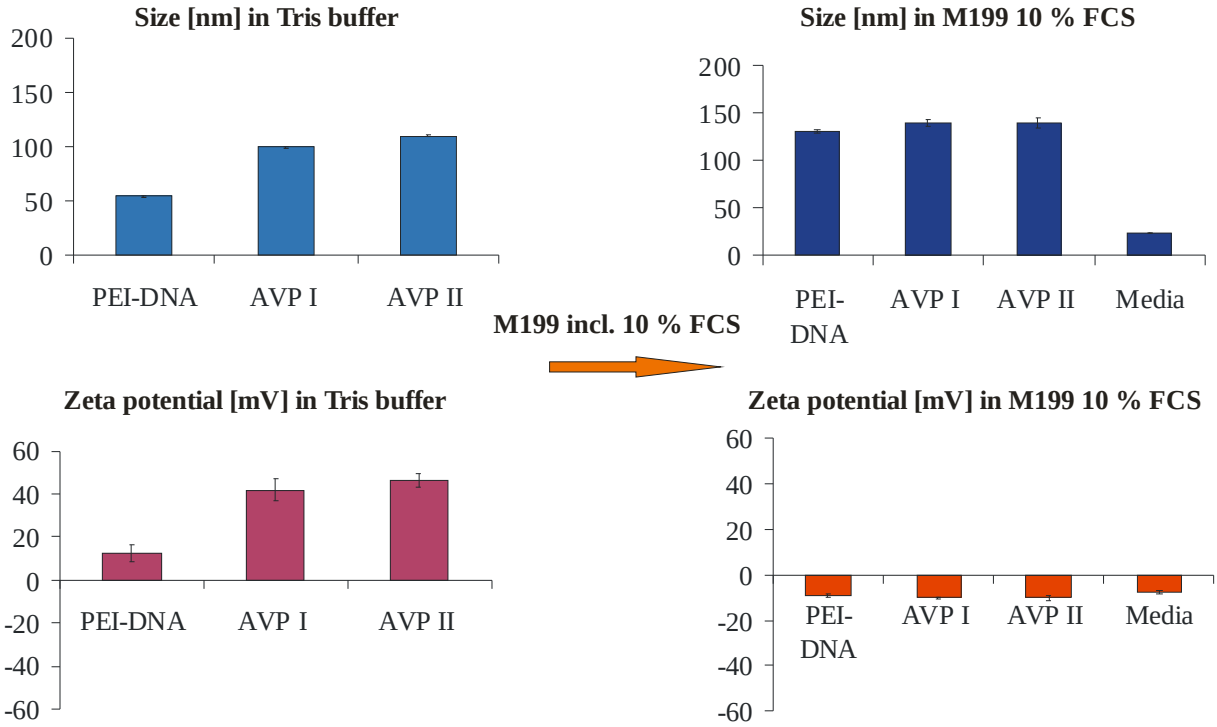

Figure 3.55: Size [Z-average in PCS] and Zetapotential of PEI-DNA complexes and two lots of AVP (AVP I and II) after 30 min incubation in Tris buffer or M199 containing 10 % FCS. Error bars depict standard deviation.

Size of all samples increased, while zetapotential switched from positive to negative values of about – 10 mV (figure 3.55). The salts and the serum contained in M199 incl 10 % FCS led to increased ionic strength compared to the pure tris buffer. This might have had an influence on the extent of the zetapotential but it can not explain the complete switch of the charge.
A parallel examined control of pure media (M199 incl. 10 % FCS) showed small particles with a Z-average of 23.75 nm and a negative zetapotential of –7.59 mV. Nearly exactly the potential the formerly positive samples changed to after contact with the serum containing media. A conclusion could be that negative serum ingredients attached to the surfaces of the positively charged PEI-DNA and AVP samples. This could explain the new generally negative zetapotential and the increase of size.

Summary and comments:

The presented experiments demonstrate that the media used for the transfection process has a strong influence on the number of successfully transfected cells. This influence could not be attributed to the presence of serum, as both the normal growth media and the alternatively used M199 contained 10 % fetal calf serum. Furthermore, the differences were cell line

dependent. While HEK 293 cells reached highest transfection rates in normal cell growth medium, transfection rates on HepG2 and HUVEC cells profited from a change to M199.
PEI-DNA complexes and AVP were able to transfect cells in serum-containing media. In contact with serum containing media they showed moderate increase in size and their zetapotential seemed to switch to the negative potential of serum ingredients. These results promise a moderate interaction with blood ingredients for an eventual *in vivo* application as only moderate size increase and no big aggregates were observed.
Already these orientation experiments showed that small changes in cell culture and in transfection procedure can strongly influence transfection results. Moreover, those changes do not have to show the same influence on different cell lines.

Even bigger differences can be anticipated when the artificial simplified system cell culture is compared to the complex *in vivo* system in a living being.
Just one example: unspecific binding of particles to cells, caused e.g. by an attraction of cationic charged particles (De Smedt et al., 2000) to the anionic membrane of cells might increase transfection in cell culture, while after an injection in the blood circuit it might be highly contra-productive as here it might lead to an early inactivation of the particles by binding to anionic blood ingredients.
So transfection experiments in cell culture represent a valuable model to gain knowledge about interaction of particles with living cells and new understandings of the way transfection vehicles work can be won from this model. But it has to be kept in mind that the results normally are not directly transferable to *in vivo* applications.
In this work the step from *in vitro* to *in vivo* was not done as animal test facilities were not present and the necessary regulatory procedures would have gone beyond the frame of this work. However, as first orientation experiment AVP were included into an experiment on rats of another group. AVP including plasmid coding for GFP were injected into the tail vein of a rat. The rat did not show signs of discomfort and was sacrificed after 48 hours. Green fluorescence was found in fluorescence microscopic examination of slices of the liver. This green fluorescence and the fact that the rat was not negatively affected by the AVP injection are promising, even when this was just an orientation experiment and no systematic investigation.

4. Concluding summary and outlook

In this work the non-viral gene transfer vehicle artificial viral particles (AVP) was characterized in greater detail, improved and used for new cell culture applications.

Size characterization by photon correlation spectroscopy showed that AVP and its educts polyethylenimine-DNA (PEI-DNA) complexes and artificial viral envelope (AVE) liposomes are in the nano-range below 300 nm. Zetapotential measurements resulted in a negative surface charge for the AVE liposomes, while as well the PEI-DNA complexes as the final product AVP showed a positive potential. Those results were in accordance with former descriptions of AVP.

Visualization in transmission electron microscopy using negative staining, freeze-fracture and Cryo preparation showed a variety of particles in AVP samples: Filled particles with a liposomal hull size about 150 nm as described before were found next to empty liposomes, small PEI-DNA condensates and aggregates of deformed liposomes.

Ultracentrifugation allowed separating defined particles that appeared filled and sized about 150 nm in electron microscopy from the bigger aggregates. However, these defined particles were not able to transfect cells in cell culture.

Lowered centrifugation speed still separated the bigger aggregates from the fraction of defined particles. Here also 50 nm small particles interpreted as pure PEI-DNA complexes were found along the 150 nm sized particles in the fraction of the defined particles. This mix was able to transfect cells in cell culture, thus suggesting that the mix of defined particles is necessary for transfection success.

To trace AVP into cells by electron microscopy the plasmid was marked with 10 nm gold particles. Ultrathin slices of HepG2 cells transfected with AVP containing marked plasmid were examined in TEM. Here gold-marked AVP could be seen outside the cells and freshly taken up in endosomes that were clearly separated from cytosol. But also free gold-marked AVP were found in cytosol. They appeared next to ruptured lipid membranes. So AVP can escape from endosomes which supports the proton sponge theory for PEI based gene transfer vehicles.

Tracing AVP with green fluorescent marked PEI and red marked liposomes on their way into cells with confocal laser scanning microscopy resulted in green stained nuclei. In conclusion AVP or part of it successfully reached the nucleus. The red fluorescence and green fluorescence were separated after passing the cell membrane, suggesting that AVP might be separated into its components again.

AVP creation was transferred successfully from manual pipetting to a user independent production in a static mixer supplied by syringe pumps. This excluded influences of manual dexterity and day to day performance of the operator in systematic studies and showed the possibility of production upscale. A mini static mixer with low dead volume was constructed from perspex and used for first experiments. Advanced experiments were performed on a Si-glass-Si chipmixer obtained from the group of Prof. Dr. Michael Köhler (TU Ilmenau). AVP produced in the chipmixer were similar in size, structure and ability to transfect cells to manually produced AVP. Results showed also that adsorption in the mixer occurred and was the reason for repeatability problems.

The components of AVP and the applied shear forces were screened for their influence on AVP structure and biological efficiency. Change of the cationic reagent used to complex the DNA from polyethylenimine (MW 5000 g/mol) to PEI specially manufactured for transfection resulted in increased transfection efficiency and unchanged structure of AVP. Usage of protamine sulfate (PS) or poly-L-lysin (PLL) for this task led to a dramatic decrease of transfection efficiency. The structure of AVP derived from PS did not differ from the structures seen before in PEI derived AVP, while PLL derived AVP contained no filled particles. Variation of the lipid composition of AVE liposomes led to increased transfection efficiency. The inclusion of the helper lipid DOPE or of an activated N-glut-PE group, that is normally used to couple targeting motifs and increases unspecific binding, increased transfection efficiency.

Shear forces were varied during complexation of DNA and processing of PEI-DNA complexes with AVE liposomes. For both steps no dependence of either size, zetapotential, structure or biological efficiency of the produced AVP from the applied forces was detected. In conclusion, the complexation of DNA with PEI as well as the processing of PEI-DNA complexes with AVE liposomes to AVP are rather self aggregations caused by ionic interactions of differing charges than shear force dependent processes.

In co-operation with Dr. Lars Tönges (University of Göttingen) AVP were compared with other commercial and non-commercial transfection reagents. It could be shown that they are suitable and competitive to transfect siRNA into sensitive primary neuronal cells.

In co-operation with Miha Milek and under supervision of Prof. Dr. Julijana Kristl and Prof. Dr. Irena Mlinaric-Rascan (all University of Ljubljana, Slovenia) AVP were successfully adapted and used to transfect target cells with a recombinant protein consisting of an EGFP part and an enzyme part. Here, selection of stable transfected cells was achieved and allowed further studies on that enzyme.

Conclusion and outlook:

The former conception of AVP as filled particle with a liposomal hull was expanded. The described filled particles with a smooth liposomal hull are contained in AVP but they are not the only particle species. Ultracentrifugation in combination with cell culture experiments showed that a mix of those filled liposome derived particles with small PEI-DNA particles is responsible for transfection success. AVP could be traced on their way into the cell by electron microscopy and confocal laser scanning microscopy. Their production was transferred from manual pipetting to a chipmixer system allowing upscale. Additional to the former positive reports AVP prove that they are a successful transfection system also suitable for new applications such as siRNA transfection and stable expression of a recombinant protein. They have a potential as they can be optimized for their specific task by selection of the proper condensation agent and type of AVE liposomes. However, AVP in their presently characterized form will have their main field of application in cell culture.

References

Reference List

A.Fahr and K.Müller, T. Nahde R. Müller S. Brüsselbach, 2001. A New Liposomal Vector In Gene Therapy For Targetting Tumor Endothelial Cells. Arch Pharm Pharm Med Chem 334 Suppl 2 21 .

Alfredsson, Viveka, 2005. Cryo-TEM studies of DNA and DNA-lipid structures. Current Opinion in Colloid & Interface Science 10, 269-273.

Bally, M. B., Harvie, P., Wong, F. M. P., Kong, S., Wasan, E. K., and Reimer, D. L., 1999. Biological barriers to cellular delivery of lipid-based DNA carriers. Advanced Drug Delivery Reviews 38, 291-315.

Bartsch, Martin, Weeke-Klimp, Alida H., Hoenselaar, Evelien P. D., Stuart, Marc C. A., Meijer, Dirk K. F., Scherphof, Gerrit L., and Kamps, Jan A. A. M., 2004. Stabilized Lipid Coated Lipoplexes for the Delivery of Antisense Oligonucleotides to Liver Endothelial Cells In Vitro and In Vivo. Journal of Drug Targeting 12, 613-621.

BASF, 1996. Lupasol Product Range, technical information.

Baum, Christopher, Dullmann, Jochen, Li, Zhixiong, Fehse, Boris, Meyer, Johann, Williams, David A., and von Kalle, Christof, 2003. Side effects of retroviral gene transfer into hematopoietic stem cells. Blood 101, 2099-2114.

Behr, J.-P., 1989. Efficient gene transfer into mammalian primary endocrine cells with lipopolyamine-coated DNA. Cell Biology 86, 6982-6986.

Behr, Jean Paul, 1997. The proton sponge. A trick to enter cells the viruses did not exploit. Chimia 51, 34-36.

Belguise-Valladier, Pascale and Behr, Jean Paul, 2001. Nonviral gene delivery: Towards artificial viruses. Cytotechnology 35, 197-201.

Blaese, R. Michael, Culver, Kenneth W., Miller, A. Dusty, Carter, Charles S., Fleisher, Thomas, Clerici, Mario, Shearer, Gene, Chang, Lauren, and Chiang, Yawen, 1995. T Lymphocyte-directed gene therapy for ADA- SCID: initial trial results after 4 years. Science (Washington, D.C.) 270, 475-480.

References

Boussif, Otmane, Lezoualc'h, Frank, Zanta, Maria Antonietta, Mergny, Mojgan Djavaheri, Scherman, Daniel, Demeneix, Barbara, and Behr, Jean Paul, 1995. A versatile vector for gene and oligonucleotide transfer into cells in culture and in vivo: polyethylenimine. Proceedings of the National Academy of Sciences of the United States of America 92, 7297-7301.

Brown, M. D., Schatzlein, A. G., and Uchegbu, I. F., 2001. Gene delivery with synthetic (non viral) carriers. International Journal of Pharmaceutics 229, 1-21.

Bruesselbach, Sabine, Mueller, Kristina, and Fahr, Alfred., 7-12-2000. Neue liposomale Vektorkomplexe und deren Verwendung für die Gentherapie, Int. Patent WO 2000074646.

Bucké, Sabine, Biophysikalische und in vitro Charakterisierung liposomaler Hybridvektoren zur antiangiogenen Gentherapie von Tumorerkrankungen, 2001,Phillips-Universität Marburg

Chander, R. and Schreier, H., 1992. Artificial viral envelopes containing recombinant human immunodeficiency virus (HIV) gp160. Life Sci 50, 481-489.

Chen, C. and Okayama, H., 1987. High-efficiency transformation of mammalian cells by plasmid DNA. Mol Cell Biol 7, 2745-2752.

Chen, Xian, 25-3-2003. Concurrent flow mixing methods and apparatus for the preparation of gene therapy vectors, US-Patent 653713, March 03.

Cho, Yong Woo, Kim, Jong Duk, and Park, Kinam, 2003. Polycation gene delivery systems: Escape from endosomes to cytosol. Journal of Pharmacy and Pharmacology 55, 721-734.

Choosakoonkriang, Sirirat, Lobo, Brian A., Koe, Gary S., Koe, Janet G., and Middaugh, C. Russell, 2003. Biophysical characterization of PEI/DNA complexes. Journal of Pharmaceutical Sciences 92, 1710-1722.

Clement, Jule, Methoden zur Charakterisisierung von großtechnisch hergestellten Lipoplexen zum Gentransfer, 2005,Albert Ludwig Universität Freiburg i. Br.

Clement, Jule, Kiefer, Karin, Kimpfler, Andrea, Garidel, Patrick, and Peschka-Suess, Regine, 2005. Large-scale production of lipoplexes with long shelf-life. European Journal of Pharmaceutics and Biopharmaceutics 59, 35-43.

Conner, Sean D. and Schmid, Sandra L., 2003. Regulated portals of entry into the cell. Nature (London, United Kingdom) 422, 37-44.

References

Cormack, Brendan P., Valdivia, Raphael H., and Falkow, Stanley, 1996. FACS-optimized mutants of the green fluorescent protein (GFP). Gene 173, 33-38.

Cotten, Matt, Wagner, Ernst, Zatloukal, Kurt, Phillips, Stephen, Curiel, David T., and Birnstiel, Max L., 1992. High-efficiency receptor-mediated delivery of small and large (48 kilobase) gene constructs using the endosome-disruption activity of defective or chemically inactivated adenovirus particles. Proceedings of the National Academy of Sciences of the United States of America 89, 6094-6098.

Coulthard, Sally A., Hogarth, Linda A., Little, Margaret, Matheson, Elizabeth C., Redfern, Christopher P. F., Minto, Lynne, and Hall, Andrew G., 2002. The effect of thiopurine methyltransferase expression on sensitivity to thiopurine drugs. Molecular Pharmacology 62, 102-109.

D'Souza, M. Patricia, Ambudkar, Suresh V., August, J. Thomas, and Maloney, Peter C., 1987. Reconstitution of the lysosomal proton pump. Proceedings of the National Academy of Sciences of the United States of America 84, 6980-6984.

Davis, H. L., Whalen, R. G., and Demeneix, B. A., 1993. Direct gene transfer into skeletal muscle in vivo: factors affecting efficiency of transfer and stability of expression. Hum Gene Ther 4, 151-159.

de Jonge, Jorgen, Leenhouts, Johanna M., Holtrop, Marijke, Schoen, Pieter, Scherrer, Peter, Cullis, Pieter R., Wilschut, Jan, and Huckriede, Anke, 2007. Cellular gene transfer mediated by influenza virosomes with encapsulated plasmid DNA. Biochemical Journal 405, 41-49.

De Smedt, Stefaan C., Demeester, Joseph, and Hennink, Wim E., 2000. Cationic polymer based gene delivery systems. Pharmaceutical Research 17, 113-126.

Dervieux, Thierry, Blanco, Javier G., Krynetski, Eugene Y., Vanin, Elio F., Roussel, Martine F., and Relling, Mary V., 2001. Differing contribution of thiopurine methyltransferase to mercaptopurine versus thioguanine effects in human leukemic cells. Cancer Research 61, 5810-5816.

Duguid, John G., Li, Cynthia, Shi, Mei, Logan, Mark J., Alila, Hector, Rolland, Alain, Tomlinson, Eric, Sparrow, James T., and Smith, Louis C., 1998. A physicochemical approach for predicting the effectiveness of peptide-based gene delivery systems for use in plasmid-based gene therapy. Biophysical Journal 74, 2802-2814.

References

Egle,R., Milek,M., Mlinaric-Rascan,I., Fahr,A., Kristl,J., 2007. A novel gene delivery system for stable transfection of thiopurine-S-methyltransferase gene in versatile cell types. European Journal of Pharmaceutics and Biopharmaceutics accepted for publication 04.10.2007.

Elbashir, Sayda M., Harborth, Jens, Lendeckel, Winfried, Yalcin, Abdullah, Weber, Klaus, and Tuschl, Thomas, 2001. Duplexes of 21-nucleotide RNAs mediate RNA interference in cultured mammalian cells. Nature (London, United Kingdom) 411, 494-498.

Escriou, V., Ciolina, C., Helbling-Leclerc, A., Wils, P., and Scherman, D., 1998. Cationic lipid-mediated gene transfer: analysis of cellular uptake and nuclear import of plasmid DNA. Cell Biology and Toxicology 14, 95-104.

Farhood, Hassan, Serbina, Natalya, and Huang, Leaf, 1995. The role of dioleoyl phosphatidylethanolamine in cationic liposome mediated gene transfer. Biochimica et Biophysica Acta, Biomembranes 1235, 289-295.

Farrell, Laura Lee, Pepin, Joel, Kucharski, Cezary, Lin, Xiaoyue, Xu, Zhenghe, and Uludag, Hasan, 2007. A comparison of the effectiveness of cationic polymers poly-L-lysine (PLL) and polyethylenimine (PEI) for non-viral delivery of plasmid DNA to bone marrow stromal cells (BMSC). European Journal of Pharmaceutics and Biopharmaceutics 65, 388-397.

Felgner, Jiin H., Kumar, Raj, Sridhar, C. N., Wheeler, Carl J., Tsai, Yali J., Border, Richard, Ramsey, Phillip, Martin, Michael, and Felgner, Philip L., 1994. Enhanced gene delivery and mechanism studies with a novel series of cationic lipid formulations. Journal of Biological Chemistry 269, 2550-2561.

Felgner, Philip L., Gadek, Thomas R., Holm, Marilyn, Roman, Richard, Chan, Hardy W., Wenz, Michael, Northrop, Jeffrey P., Ringold, Gordon M., and Danielsen, Mark, 1987. Lipofection: a highly efficient, lipid-mediated DNA-transfection procedure. Proceedings of the National Academy of Sciences of the United States of America 84, 7413-7417.

Filion, Mario C. and Phillips, Nigel C., 1998. Major limitations in the use of cationic liposomes for DNA delivery. International Journal of Pharmaceutics 162, 159-170.

Fischer, Alain, 2001. Gene therapy: some results, many problems to solve. Cellular and Molecular Biology (Paris, France, Printed) 47, 1269-1275.

References

Fritze, Andreas, Hens, Felicitas, Kimpfler, Andrea, Schubert, Rolf, and Peschka-Suess, Regine, 2006. Remote loading of doxorubicin into liposomes driven by a transmembrane phosphate gradient. Biochimica et Biophysica Acta, Biomembranes 1758, 1633-1640.

Funhoff, Arjen M., van Nostrum, Cornelus F., Koning, Gerben A., Schuurmans-Nieuwenbroek, Nancy M. E., Crommelin, Daan J. A., and Hennink, Wim E., 2004. Endosomal Escape of Polymeric Gene Delivery Complexes Is Not Always Enhanced by Polymers Buffering at Low pH. Biomacromolecules 5, 32-39.

Futaki, Shiroh, Ohashi, Wakana, Suzuki, Tomoki, Niwa, Miki, Tanaka, Seigo, Ueda, Kunihiro, Harashima, Hideyoshi, and Sugiura, Yukio, 2001. Stearylated Arginine-Rich Peptides: A New Class of Transfection Systems. Bioconjugate Chemistry 12, 1005-1011.

Gao, X. and Huang, L., 1996. Potentiation of cationic liposome-mediated gene delivery by polycations. Biochemistry 35, 1027-1036.

Gardlik, Roman, Palffy, Roland, Hodosy, Julius, Lukacs, Jan, Turna, Jan, and Celec, Peter, 2005. Vectors and delivery systems in gene therapy. Medical Science Monitor 11, RA110-RA121.

Gehl, J., 2003. Electroporation: Theory and methods, perspectives for drug delivery, gene therapy and research. Acta Physiologica Scandinavica 177, 437-447.

Germershaus, Oliver, Merdan, Thomas, Bakowsky, Udo, Behe, Martin, and Kissel, Thomas, 2006. Trastuzumab-Polyethylenimine-Polyethylene Glycol Conjugates for Targeting Her2-Expressing Tumors. Bioconjugate Chemistry 17, 1190-1199.

Gershon, Hezi, Ghirlando, Rodolfo, Guttman, Susan B., and Minsky, Abraham, 1993. Mode of formation and structural features of DNA-cationic liposome complexes used for transfection. Biochemistry 32, 7143-7151.

Godbey, W. T., Wu, K. K., and Mikos, A. G., 1999a. Tracking the intracellular path of PEI/DNA complexes for gene delivery. Proceedings of the International Symposium on Controlled Release of Bioactive Materials 26th, 220-221.

Godbey, W. T., Wu, Kenneth K., and Mikos, Antonios G., 1999b. Size matters: molecular weight affects the efficiency of poly(ethylenimine) as a gene delivery vehicle. Journal of Biomedical Materials Research 45, 268-275.

References

Guo, Jerry and Xin, Hao, 2006. Chinese gene therapy. Splicing out the West? Science 314, 1232-1235.

Hafez, I. M., Maurer, N., and Cullis, P. R., 2001. On the mechanism whereby cationic lipids promote intracellular delivery of polynucleic acids. Gene Therapy 8, 1188-1196.

Hahn, William C., 2002. Immortalization and transformation of human cells. Molecules and Cells 13, 351-361.

Hirsch-Lerner, Danielle, Zhang, Ming, Eliyahu, Hagit, Ferrari, Marylin E., Wheeler, Carl J., and Barenholz, Yechezkel, 2005. Effect of \"helper lipid\" on lipoplex electrostatics. Biochimica et Biophysica Acta, Biomembranes 1714, 71-84.

Hölig, Peter, Erzeugung und Characterisierung zielgerichteter liposomaler Trägersysteme für die Tumortherapie, 2007, Phillips Universität Marburg

Hui, Sek Wen, Langner, Marek, Zhao, Ya Li, Ross, Patrick, Hurley, Edward, and Chan, Karen, 1996. The role of helper lipids in cationic liposome-mediated gene transfer. Biophysical Journal 71, 590-599.

Jaaskelainen, Ilpo, Sternberg, Brigitte, Monkkonen, Jukka, and Urtti, Arto, 1998. Physicochemical and morphological properties of complexes made of cationic liposomes and oligonucleotides. International Journal of Pharmaceutics 167, 191-203.

Kettering, M., Winter, J., Zeisberger, M., Bremer-Streck, S., Oehring, H., Bergemann, C., Alexiou, C., Hergt, R., Halbhuber, K. J., Kaiser, W. A., and Hilger, I., 2007. Magnetic nanoparticles as bimodal tools in magnetically induced labelling and magnetic heating of tumour cells: an in vitro study. Nanotechnology 18, 175101-1-175101/9.

Kirner, T., Albert, J., Gunther, M., Mayer, G., Reinhackel, K., and Kohler, J. M., 2004. Static micromixers for modular chip reactor arrangements in two-step reactions and photochemical activated processes. Chemical Engineering Journal (Amsterdam, Netherlands) 101, 65-74.

Krynetski, Eugene Y., Tai, Hung Liang, Yates, Charles R., Fessing, Michael Y., Loennechen, Thrina, Schuetz, John D., Relling, Mary V., and Evans, William E., 1996. Genetic polymorphism of thiopurine S-methyltransferase: clinical importance and molecular mechanisms. Pharmacogenetics 6, 279-290.

References

Kunath, Klaus, von Harpe, Anke, Fischer, Dagmar, Petersen, Holger, Bickel, Ulrich, Voigt, Karlheinz, and Kissel, Thomas, 2003. Low-molecular-weight polyethylenimine as a nonviral vector for DNA delivery: comparison of physicochemical properties, transfection efficiency and in vivo distribution with high-molecular-weight polyethylenimine. Journal of Controlled Release 89, 113-125.

Labat-Moleur, F., Steffan, A.-M., Brisson, C., Perron, H., Feugeas, O., Furstenberger, P., Oberling, F., Brambilla, E., and Behr, J.-P., 1996. An electron microscopy study into the mechanism of gene transfer with lipopolyamines. Gene Therapy 3, 1010-1017.

Lee, Robert J. and Huang, Leaf, 1996. Folate-targeted, anionic liposome-entrapped polylysine-condensed DNA for tumor cell-specific gene transfer. Journal of Biological Chemistry 271, 8481-8487.

Lehrman, Sally, 1999. Virus treatment questioned after gene therapy death. Nature (London) 401, 517-518.

Li, S. and Huang, L., 2000. Nonviral gene therapy: promises and challenges. Gene Therapy 7, 31-34.

Lingor, Paul, Michel, Uwe, Scholl, Ulrike, Bahr, Mathias, and Kugler, Sebastian, 2004. Transfection of \"naked\" siRNA results in endosomal uptake and metabolic impairment in cultured neurons. Biochemical and Biophysical Research Communications 315, 1126-1133.

Liu, Ge, Li, DeShan, Pasumarthy, Murali K., Kowalczyk, Tomasz H., Gedeon, Christopher R., Hyatt, Susannah L., Payne, Jennifer M., Miller, Timothy J., Brunovskis, Peter, Fink, Tamara L., Muhammad, Osman, Moen, Robert C., Hanson, Richard W., and Cooper, Mark J., 2003. Nanoparticles of Compacted DNA Transfect Postmitotic Cells. Journal of Biological Chemistry 278, 32578-32586.

Lv, Hongtao, Zhang, Shubiao, Wang, Bing, Cui, Shaohui, and Yan, Jie, 2006. Toxicity of cationic lipids and cationic polymers in gene delivery. Journal of Controlled Release 114, 100-109.

Markova, Svetlana V., Golz, Stefan, Frank, Ludmila A., Kalthof, Bernd, and Vysotski, Eugene S., 2004. Cloning and Expression of cDNA for a Luciferase from the Marine Copepod Metridia longa: A novel secreted bioluminescent reporter enzyme. Journal of Biological Chemistry 279, 3212-3217.

References

Mehier-Humbert, Sophie and Guy, Richard H., 2005. Physical methods for gene transfer: Improving the kinetics of gene delivery into cells. Advanced Drug Delivery Reviews 57, 733-753.

Merdan, Thomas, Kunath, Klaus, Fischer, Dagmar, Kopecek, Jindrich, and Kissel, Thomas, 2002. Intracellular processing of poly(ethylene imine)/ribozyme complexes can be observed in living cells by using confocal laser scanning microscopy and inhibitor experiments. Pharmaceutical Research 19, 140-146.

Meszaros, Robert, Thompson, Laurie, Bos, Martin, and de Groot, Peter, 2002. Adsorption and Electrokinetic Properties of Polyethylenimine on Silica Surfaces. Langmuir 18, 6164-6169.

Milek, M., Murn, J., Jaksic, Z., Lukac Bajalo, J., Jazbec, J., and Mlinaric Rascan, I., 2006. Thiopurine S-Methyltransferase Pharmacogenetics: Genotype to Phenotype Correlation in the Slovenian Population. Pharmacology 77, 105-114.

Moret, I., Esteban Peris, J., Guillem, V. M., Benet, M., Revert, F., Dasi, F., Crespo, A., and Alino, S. F., 2001. Stability of PEI-DNA and DOTAP-DNA complexes: effect of alkaline pH, heparin and serum. Journal of Controlled Release 76, 169-181.

Mortimer, I., Tam, P., MacLachlan, I., Graham, R. W., Saravolac, E. G., and Joshi, P. B., 1999. Cationic lipid-mediated transfection of cells in culture requires mitotic activity. Gene Therapy 6, 403-411.

Muller, Kristina, Nahde, Thomas, Fahr, Alfred, Muller, Rolf, and Brusselbach, Sabine, 2001. Highly efficient transduction of endothelial cells by targeted artificial virus-like particles. Cancer Gene Therapy 8, 107-117.

Müller, Rainer H, Zetapotential und Partikelladung in der Laborpraxis, 1996,Wissenschaftliche Verlagsgesellschaft mbH Stuttgart

Müller, Rainer H., Schumann, Raimund, and Thode, Kai, Teilchengrößenmessung in der Laborpraxis, 1996,Wissenschaftliche Verlagsgesellschaft mbH Stuttgart

Nabel, Gary J., Nabel, Elizabeth G., Yang, Zhi Yong, Fox, Bernard A., Plautz, Gregory E., Gao, Xiang, Huang, Leaf, Shu, Suyu, Gordon, David, and Chang, Alfred E., 1993. Direct gene transfer with DNA-liposome complexes in melanoma: Expression, biologic activity, and

lack of toxicity in humans. Proceedings of the National Academy of Sciences of the United States of America 90, 11307-11311.

Nahde, T., Muller, K., Fahr, A., Muller, R., and Brusselbach, S., 2001. Combined transductional and transcriptional targeting of melanoma cells by artificial virus-like particles. The journal of gene medicine 3, 353-361.

Neu, Michael, Sitterberg, Johannes, Bakowsky, Udo, and Kissel, Thomas, 2006. Stabilized Nanocarriers for Plasmids Based Upon Cross-linked Poly(ethylene imine). Biomacromolecules 7, 3428-3438.

Ogris, M., Steinlein, P., Kursa, M., Mechtler, K., Kircheis, R., and Wagner, E., 1998. The size of DNA/transferrin-PEI complexes is an important factor for gene expression in cultured cells. Gene Therapy 5, 1425-1433.

Ott, Marion G., Schmidt, Manfred, Schwarzwaelder, Kerstin, Stein, Stefan, Siler, Ulrich, Koehl, Ulrike, Glimm, Hanno, Kuehlcke, Klaus, Schilz, Andrea, Kunkel, Hana, Naundorf, Sonja, Brinkmann, Andrea, Deichmann, Annette, Fischer, Marlene, Ball, Claudia, Pilz, Ingo, Dunbar, Cynthia, Du, Yang, Jenkins, Nancy A., Copeland, Neal G., Luethi, Ursula, Hassan, Moustapha, Thrasher, Adrian J., Hoelzer, Dieter, von Kalle, Christof, Seger, Reinhard, and Grez, Manuel, 2006. Correction of X-linked chronic granulomatous disease by gene therapy, augmented by insertional activation of MDS1-EVI1, PRDM16 or SETBP1. Nature Medicine (New York, NY, United States) 12, 401-409.

Papazisis, K. T., Geromichalos, G. D., Dimitriadis, K. A., and Kortsaris, A. H., 1997. Optimization of the sulforhodamine B colorimetric assay. Journal of Immunological Methods 208, 151-158.

Park, Tae Gwan, Jeong, Ji Hoon, and Kim, Sung Wan, 2006. Current status of polymeric gene delivery systems. Advanced Drug Delivery Reviews 58, 467-486.

Pearson, Sue, Jia, Hepeng, and Kandachi, Keiko, 2004. China approves first gene therapy. Nat Biotechnol 22, 3-4.

Peng, Zhaohui, 2005. Current status of gendicine in China: recombinant human Ad-p53 agent for treatment of cancers. Hum Gene Ther 16, 1016-1027.

References

Pitard, Bruno, Oudrhiri, Noufissa, Vigneron, Jean Pierre, Hauchecorne, Michelle, Aguerre, Olivier, Toury, Renee, Airiau, Marc, Ramasawmy, Rajen, Scherman, Daniel, Crouzet, Joel, Lehn, Jean Marie, and Lehn, Pierre, 1999. Structural characteristics of supramolecular assemblies formed by guanidinium-cholesterol reagents for gene transfection. Proceedings of the National Academy of Sciences of the United States of America 96, 2621-2626.

Pollard, Helene, Remy, Jean Serge, Loussouarn, Gildas, Demolombe, Sophie, Behr, Jean Paul, and Escande, Denis, 1998. Polyethylenimine but not cationic lipids promotes transgene delivery to the nucleus in mammalian cells. Journal of Biological Chemistry 273, 7507-7511.

Polyplus, 2-2-2002. jetPEI Material Safety Data sheet.

Rabino, Isaac, 2003. Gene therapy: ethical issues. Theor Med Bioeth 24, 31-58.

Rainer H.Müller, Zetapotential und Partikelladung in der Laborpraxis, 1996,Wissenschaftliche Verlagsgesellschaft mbH Stuttgart

Rainer H.Müller, Raimund Schuhmann, and Kai Thode, Teilchengrößenmessung in der Laborpraxis, 1996,Wissenschaftliche Verlagsgesellschaft mbH Stuttgart

Rieseberg, Marco, Kasper, Cornelia, Reardon, Kenneth F., and Scheper, Thomas, 2001. Flow cytometry in biotechnology. Applied Microbiology and Biotechnology 56, 350-360.

Roerdink, Frits, Wassef, Nabila M., Richardson, Earl C., and Alving, Carl R., 1983. Effects of negatively charged lipids on phagocytosis of liposomes opsonized by complement. Biochimica et Biophysica Acta, Biomembranes 734, 33-39.

Rubin, Harry, 2002. The disparity between human cell senescence in vitro and lifelong replication in vivo. Nature Biotechnology 20, 675-681.

Ruponen, Marika, Ronkko, Seppo, Honkakoski, Paavo, Pelkonen, Jukka, Tammi, Markku, and Urtti, Arto, 2001. Extracellular glycosaminoglycans modify cellular trafficking of lipoplexes and polyplexes. Journal of Biological Chemistry 276, 33875-33880.

Ruponen, Marika, Yla-Herttuala, Seppo, and Urtti, Arto, 1999. Interactions of polymeric and liposomal gene delivery systems with extracellular glycosaminoglycans: physicochemical and transfection studies. Biochimica et Biophysica Acta, Biomembranes 1415, 331-341.

References

Sakurai, Haruna, Sakurai, Fuminori, Kawabata, Kenji, Sasaki, Tomomi, Koizumi, Naoya, Huang, Haiying, Tashiro, Katsuhisa, Kurachi, Shinnosuke, Nakagawa, Shinsaku, and Mizuguchi, Hiroyuki, 2007. Comparison of gene expression efficiency and innate immune response induced by Ad vector and lipoplex. Journal of Controlled Release 117, 430-437.

Schakowski, Frank, Buttgereit, Peter, Mazur, Martin, Maerten, Angela, Schoettker, Bjoern, Gorschlueter, Marcus, and Schmidt-Wolf, Ingo G. H., 2004. Novel non-viral method for transfection of primary leukemia cells and cell lines. Genetic Vaccines and Therapy 2, No.

Shoji, Jun'ichi, Tanihara, Yuko, Uchiyama, Tsuneo, and Kawai, Akihiko, 2004. Preparation of virosomes coated with the vesicular stomatitis virus glycoprotein as efficient gene transfer vehicles for animal cells. Microbiology and Immunology 48, 163-174.

Smith, Lynn and Byers, Jacqueline Fowler, 2002. Gene therapy in the post-Gelsinger era. JONAS Healthc Law Ethics Regul 4, 104-110.

Sorgi, Frank L., Bhattacharya, Soumendu, and Huang, Leaf, 1997. Protamine sulfate enhances lipid-mediated gene transfer. Proceedings of the International Symposium on Controlled Release of Bioactive Materials 24th, 37-38.

Sternberg, Brigitte, Hong, Keelung, Zheng, Weiwen, and Papahadjopoulos, Demetrios, 1998. Ultrastructural characterization of cationic liposome-DNA complexes showing enhanced stability in serum and high transfection activity in vivo. Biochimica et Biophysica Acta, Biomembranes 1375, 23-35.

Tabatt, Kerstin, Kneuer, Carsten, Sameti, Mohammad, Olbrich, Carsten, Muller, Rainer H., Lehr, Claus Michael, and Bakowsky, Udo, 2004. Transfection with different colloidal systems: comparison of solid lipid nanoparticles and liposomes. Journal of Controlled Release 97, 321-332.

Tagawa, T., Manvell, M., Brown, N., Keller, M., Perouzel, E., Murray, K. D., Harbottle, R. P., Tecle, M., Booy, F., Brahimi-Horn, M. C., Coutelle, C., Lemoine, N. R., Alton, E. W. F. W., and Miller, A. D., 2002. Characterisation of LMD virus-like nanoparticles self-assembled from cationic liposomes, adenovirus core peptide mu and plasmid DNA. Gene Therapy 9, 564-576.

Tai, H. L., Fessing, M. Y., Bonten, E. J., Yanishevsky, Y., d'Azzo, A., Krynetski, E. Y., and Evans, W. E., 1999. Enhanced proteasomal degradation of mutant human thiopurine S-

methyltransferase (TPMT) in mammalian cells: mechanism for TPMT protein deficiency inherited by TPMT*2, TPMT*3A, TPMT*3B or TPMT*3C. Pharmacogenetics 9, 641-650.

Teichler Zallen, D., 2000. US gene therapy in crisis. Trends in Genetics 16, 272-275.

The Journal of Gene Medicine, 2007. Gene Therapy Clinical Trials Worldwide. The Journal of Gene Medicine .

Thomas, M. and Klibanov, A. M., 2003. Non-viral gene therapy: polycation-mediated DNA delivery. Applied Microbiology and Biotechnology 62, 27-34.

Thompson, L., 2000. Human gene therapy. Harsh lessons, high hopes. FDA Consum 34, 19-24.

Toenges, Lars, Lingor, Paul, Egle, Roman, Dietz, Gunnar P. H., Fahr, Alfred, and Baehr, Mathias, 2006. Stearylated octaarginine and artificial virus-like particles for transfection of siRNA into primary rat neurons. RNA 12, 1431-1438.

Torchilin, Vladimir and Weissig, Volkmar, 2003. Liposomes, Second Edition: A Practical Approach. 396.

Tros de Ilarduya, C. and Duzgunes, N., 2000. Efficient gene transfer by transferrin lipoplexes in the presence of serum. Biochimica et Biophysica Acta, Biomembranes 1463, 333-342.

Tsien, R. Y., 1998. The green fluorescent protein. Annu Rev Biochem 67, 509-544.

Tsuchiya, Yuri, Ishii, Tsuyoshi, Okahata, Yoshio, and Sato, Toshinori, 2006. Characterization of protamine as a transfection accelerator for gene delivery. Journal of Bioactive and Compatible Polymers 21, 519-537.

Van Meel, F. C. M. and Pearson, P. L., 1979. Do human spermatozoa reactivate in the cytoplasm of somatic cells? Journal of Cell Science 35, 105-122.

Voigt, Rudolf and Fahr, Alfred, Pharmazeutische Technologie. Für Studium und Beruf, 2007,Deutscher Apotheker Verlag

Wagner, Ernst, Cotten, Matt, Foisner, Roland, and Birnstiel, Max L., 1991. Transferrin-polycation-DNA complexes: the effect of polycations on the structure of the complex and

References

DNA delivery to cells. Proceedings of the National Academy of Sciences of the United States of America 88, 4255-4259.

Wagner, J. and Koehler, J. M., 2005. Continuous Synthesis of Gold Nanoparticles in a Microreactor. Nano Letters 5, 685-691.

Weinshilboum, Richard, 2001. Thiopurine pharmacogenetics: clinical and molecular studies of thiopurine methyltransferase. Drug Metabolism and Disposition 29, 601-605.

Welz, C., Neuhuber, W., Schreier, H., Metzler, M., Repp, R., Rascher, W., and Fahr, A., 2000. Nuclear transport of oligonucleotides in HepG2-cells mediated by protamine sulfate and negatively charged liposomes. Pharmaceutical Research 17, 1206-1211.

Welz, Christian, Biophysikalische Untersuchungen für die Entwicklung nichtviraler Gentherapeutika, Kondensation von Nukleinsäuren und Transfektion von Leberzellen mit nichtviralen Trägersystemen, 2000,Philips-Universität Marburg

Wiethoff, Christopher M. and Middaugh, C. Russell, 2003. Barriers to nonviral gene delivery. Journal of Pharmaceutical Sciences 92, 203-217.

Yamauchi, Masahiro, Kusano, Hiroko, Saito, Etsuko, Iwata, Takeshi, Nakakura, Masashi, Kato, Yasuki, and Aoki, Noboru, 2006. Development of wrapped liposomes: Novel liposomes comprised of polyanion drug and cationic lipid complexes wrapped with neutral lipids. Biochimica et biophysica acta 1758, 90-97.

Yan, X., Poelstra, K., Scherphof, G. L., and Kamps, J. A. A. M., 2004. A role for scavenger receptor B-I in selective transfer of rhodamine-PE from liposomes to cells. Biochem Biophys Res Commun 325, 908-914.

Zabner, Joseph, Fasbender, Al J., Moninger, Tom, Poellinger, Kristi A., and Welsh, Michael J., 1995. Cellular and molecular barriers to gene transfer by a cationic lipid. Journal of Biological Chemistry 270, 18997-19007.

Zhang, Y. P., Sekirov, L., Saravolac, E. G., Wheeler, J. J., Tardi, P., Clow, K., Leng, E., Sun, R., Cullis, P. R., and Scherrer, P., 1999. Stabilized plasmid-lipid particles for regional gene therapy: formulation and transfection properties. Gene therapy 6, 1438-1449.

References

Zhang, Yuan, Xian, Rong Qi, Gao, Yan, Wei, Lai, Maitani, Yoshie, and Nagai, Tsuneji, 2007. Mechanisms of co-modified liver-targeting liposomes as gene delivery carriers based on cellular uptake and antigens inhibition effect. Journal of Controlled Release 117, 281-290.

Zinkant, Katrin, 27-4-2006. Tod nach Heilung. Zeit online .

List of abbreviations:

6-MP	6-mercaptopurine
6-TG	6-thioguanine
AVE	Artificial viral envelope liposomes
AVE-act	AVE liposomes containing an activated anchor
AVE-DOPE	AVE liposomes containing DOPE
AVP	Artificial viral particles
AVP-act	Artificial viral particles based on AVE-act liposomes
AVP-DOPE	AVP based on AVE-DOPE liposomes
Chol	Cholesterol
Cryo-TEM	Cryo-transmission elektron microscopy
DiI	1-1'-Dioctadecyl-3,3,3',3'-tetramethylindocarbocyanine
DLPE	1,2-Dilauroyl-sn-glycero-3-phosphoethanolamine
DNA	Desoxyribonucleic acid
DOPE	1,2-Dioleoyl-sn-glycero-3-phosphoethanolamine
DOPS	1,2-Dioleoyl-sn-glycero-3-phospho-l-serine
ECGM	Endothelial cell growth media
EDC	N-(3-dimethylaminopropyl)-N'-ethylcarbodiimide hydrochloride
EGFP	Enhanced green fluorescent protein
FCS	Fetal calf serum
GFP	Green fluorescent protein, used synonymously to EGFP
HEK293	Human embryonic kidney 293 cells
HepG2	HepG2 hepatocellular carcinoma cells
HUVEC	Human umbilical vein endothelial cells
M199	Media 199
mRNA	Messenger ribonucleic acid
MW	Molecular weight
N-glut-DOPE	1,2-Dioleoyl-sn-glycero-3-Phosphoethanolamine-N(glutaryl)
PCS	Photon correlation spectroscopy
PDI	Polydispersity index
PEI	Polyethylenimine
PLL	Poly-L-lysine

Abbreviations

PS	Protamine Sulfate
RCF	Radial centrifugal force
Rh-PE	1,2-Dioleoyl-sn-glycero-3-Phosphoethanolamine-N-(Lissamine Rhodamine B Sulfonyl)
RNA	Ribonucleic acid
RPM	Rounds per minute
si-RNA	Short interfering ribonucleic acid
SRB	Sulforhodamine B
TEM	Transmission electron microscopy
TPMT	Thiopurine-S-methyltransferase

Characterization and optimization of the non-viral gene transfer vehicle “Artificial viral particles” (AVP)

Hauptaussagen der Dissertation von
Roman Egle, Doktorand der PharmazeutischenTechnologie
Oktober 2007

Ziel der Arbeit:

Die Erstellung von Darreichungsformen für Nukleinsäuren ist eine neue technologische Herausforderung. Verschiedene nicht-virale Überträger wurden bereits, und werden momentan, als mögliche Alternativen zur Verwendung von viralen Überträgern entwickelt und untersucht. Zusammensetzung und Aufbau dieser Überträger ist essentiell für Erfolg und Toleranz in biologischen Systemen. Ein vielversprechender Ansatz für die nicht-virale Gentherapie ist das Überträgersystem “artificial viral particles” (AVP), also „künstliche virenähnliche Partikel“. Sie imitieren grundsätzlich den Aufbau von umhüllten Viren mit einem kompakten Kern und einer Lipidhülle. Sie bestehen aus dem kationischen Polymer Polyethylenimin (PEI), um die Nukleinsäuren zu kompaktieren, kombiniert mit anionischen Liposomen, um die virale Hülle zu imitieren. Trotz anfänglicher Arbeiten, die durchgeführt wurden, als das System etabliert wurde, sind noch Fragen bezüglich der AVP selbst und ihrer Eignung für Anwendungen im Bereich der Medizin und der Grundlagenforschung offen.

Ziel dieser Arbeit war daher die genaue Charakterisierung von AVP und die Optimierung ihrer Zusammensetzung und ihrer Herstellung. Weiterhin sollten sie für neue Anwendungen angepasst und verwendet werden.
Folglich wurden mehrere Aufgabenstellungen in dieser Arbeit angegangen:

- Charakterisierung der AVP Struktur durch Elektronenmikroskopie und Ladungs- und Größenmessungen. Suchen eines Zusammenhangs zwischen biologischer Aktivität und Struktur nach Trennung von verschiedenen Partikeltypen durch Ultrazentrifugation.
- Verfolgung der Aufnahme und des weiteren Schicksals von AVP in Zellen unter Verwendung von Fluoreszenzmarkern und elektronenmikroskopischen Untersuchungen von Ultradünnschnitten transfizierter Zellen.

- Übertragung der AVP Herstellung von manuellem Pipettieren zu einem Verfahren in einem statischen Mischer, das benutzerunabhängig ist und dessen Maßstab sich leicht vergrößern lässt.
- Untersuchung der Einflüsse einer veränderten AVP Zusammensetzung und der während der Herstellung aufgewendeten Kräfte, auf Struktur und biologische Effizienz der AVP. Verwendung der gewonnen Erkenntnisse um zur Verbesserung der AVP. In Zusammenarbeiten wurden AVP auch als innovatives Reagenz für den Transfer von siRNA und für eine dauerhafte Expression eines rekombinanten Proteins getestet.

Zusammenfassung und Schlussfolgerungen:

In dieser Arbeit wurde das nicht-virale Genüberträgersystem “artificial viral particles (AVP)” genauer untersucht, verbessert und für neue Anwendungen in der Zellkultur verwendet.

- Das frühere Konzept von AVP als gefüllte Partikel mit einer liposomalen Hülle wurde erweitert. Die beschriebenen gefüllten Partikel mit einer glatten liposomalen Hülle sind in AVP enthalten, aber sie sind nicht die einzige Partikelart. Durch Ultrazentrifugation in Kombination mit Zellkulturversuchen, wurde gezeigt, dass ein Gemisch dieser gefüllten Partikel mit kleinen PEI-DNA Partikeln für den Transfektionserfolg verantwortlich ist.
- AVP konnten auf ihrem Weg in die Zelle mittels Elektronenmikroskopie und konfokaler Laser Rastermikroskopie verfolgt werden. Die Ergebnisse wiesen darauf hin, dass AVP sich aus Endosomen befreien können, und unterstützen die „Protonenschwamm“ Theorie.
- Die Übertragung der AVP Herstellung von manuellem Pipettieren auf einen Minimischer gelang, was eine Produktion im größeren Maßstab ermöglicht.
- Es wurde gezeigt, dass AVP ein erfolgreiches System zur Transfektion von Zellen sind, das auch für neue Anwendungsbereiche, wie siRNA Transfektion, oder die stabile Expression eines rekombinanten Proteins, geeignet ist. Sie haben Potential, da sie für spezielle Aufgaben optimiert werden können, indem das geeignete Polymer zur DNA Kompaktierung und die passenden AVE Liposomen gewählt werden. Allerdings werden AVP in ihrer momentan charakterisierten Form ihr Hauptanwendungsgebiet in der Zellkultur haben.

Persönliche Angaben:

Name:	Roman Egle
Geburtsdatum:	03.08.1975
Geburtsort:	München
Familienstand:	ledig

Ausbildung:

Schule:

08/1982 – 07/1986	**Grundschule** in Neumarkt i.d. OPf.
08/1986 – 07/1995	**Gymnasium** "Willibald-Gluck" Gymnasium in Neumarkt i.d. OPf. Abiturnote: 1,8 (gut)

Studium:

10/1996 – 04/2001	**Pharmaziestudium** in Regensburg, Gesamtnote 1,89 (gut)
09/2002	**Approbation als Apotheker**
seit 01/2003	**Promotion** am Lehrstuhl für Pharmazeutische Technologie der Friedrich-Schiller-Universität-Jena unter Leitung von Prof. Dr. A. Fahr

Berufserfahrung:

09/1995 – 09/1996	**Zivildienst** Seniorenheim "Martin-Schalling-Haus", Neumarkt i.d.OPf.
05/2001 – 10/2001	**Pharmaziepraktikum** in der "Delphin Apotheke", München
11/2001 – 04/2002	**Pharmaziepraktikum** bei "Hexal Pharmaforschung", Holzkirchen
07/2002 – 11/2002	**Apotheker in der Pharmazeutischen Entwicklung** bei "Hexal Pharmaforschung", Holzkirchen
01/2003 – 04/2006	**Wissenschaftlicher Mitarbeiter** am Lehrstuhl für Pharmazeutische Technologie der Friedrich-Schiller-Universität-Jena
05/2006 – 04/2007	**Young researcher training** am Lehrstuhl für Pharmazeutische Technologie der Universität Ljubljana, Slowenien
06/2007 – 09/2007	**Wissenschaftlicher Angestellter** am Lehrstuhl für Pharmazeutische Technologie der Friedrich-Schiller-Universität-Jena

Publications and Presentations:

Publications:

1.) “Stearylated octaarginine and artificial virus-like particles for transfection of siRNA into primary rat neurons”
Toenges,L., Lingor,P., Egle,R., Dietz,G.P.H., Fahr,A., & Baehr,M.
RNA 12[7] (2006) 1431-1438

2.) “A novel gene delivery system for stable transfection of thiopurine-S-methyltransferase gene in versatile cell types”
Roman Egle, Miha Milek, Irena Mlinarič-Raščan, Alfred Fahr, Julijana Kristl
Accepted for publication in the “European Journal of Pharmaceutics and Biopharmaceutics”

3.) “A static microchip-mixer in the production of a complex gene transfer vehicle (AVP)”
Roman Egle, J.M. Köhler, Alfred Fahr
Submitted to the “Journal of Biomedical Nanotechnology“

Oral presentations:

1) “Kolloidale Trägersysteme zur Gentherapie: Untersuchungen zur Struktur und Zellprozessierung mittels EM“
Kuratorium für Elektronenmikroskopie, July 2003, Jena, Germany
2.) „Electron microscopy of gene carrier systems“
2nd Ameland Liposome Workshop, September 8 –1 2 2003, Ameland, The Netherlands.

3.) “AVP green light for cells”
17th Mountain/Sea Liposome Workshop, April 4 – 8 2005, Oberjoch, Germany,

4.) “Von der Natur lernen, künstliche Viren als Gentransfervehikel“
Symp(h)atol Treffen, June 17 2005, Jena, Germany

Publications and Presentations:

5.) “AVP artificial viral particles green light for cells”
Mitteldeutsche Technologentage, November 4, 2005, Jena, Germany
6.) „Update to AVP: new insights into structure and mechanism of a nonviral gene transfer system“
Controlled Release Society, German Chapter Annual Meeting, February 24, 2006, Jena, Germany

7.) “AVP (a nonviral gene transfer system) as tool for protein function studies”Socrates intensive programme “Innovative therapeutics: from molecules to medicine” July 3 - 13, 2006, Athens, Greece

8.) „Strategies to investigate the role of the enzyme TPMT using the gene carrier system AVP”
Galenos 4th. Thematic workshop, September 7 - 9, 2006, Cagliari, Italy

Poster Presentations:

1) “AVP manufacturing in static mixer Statmix 6 in gene transfer experiments”
3. Workshop “ Microtechnology for Chemistry and Biology Laboratories“, February, 21 - 23, 2006, Ilmenau, Germany

2.) “Investigation of AVP for transfection of tpmt-gene into target cells”
Socrates Intensive Programme "Skin Barrier Function: Pharmaceutic and Cosmetic Applications", September 15 - 29, 2006, Lyon, France

3.) “Investigation of TPMT expression in different kind of cells using the complex gene transfer vehicle AVP”
Young Pharmaceutical Scientists Meet in Amsterdam - Pre-Satellite Meeting of the 3rd Pharmaceutical Sciences World Congress (PSWC 2007), April 20 - 21, 2007, Amsterdam, The Netherlands

Selbstständigkeitserklärung:

Hiermit erkläre ich Roman Egle, daß ich die vorliegende Arbeit selbständig und nur unter Verwendung der angegebenen Hilfsmittel und Literatur angefertigt habe.

Roman Egle

Jena, den 12.10.2007